Stable carbon, oxygen, and nitrogen isotope analysis of serially-sampled fossil tooth enamel from equid third molars from the Eemian site of Neumark-Nord 2, Germany.

Vink, Marissa

Stable carbon, oxygen, and nitrogen isotope analysis of serially-sampled fossil tooth enamel from equid third molars from the Eemian site of Neumark-Nord 2, Germany.

Marissa Vink

Front Cover Image: An equid third molar from Neumark-Nord 2, Germany, before (left) and after sampling (right). Photographs taken by author

Stable carbon, oxygen, and nitrogen isotope analysis of serially-sampled fossil tooth enamel from equid third molars from the Eemian site of Neumark-Nord 2, Germany.

Marissa Vink – s2191008

Research Master thesis – 1086THRSY

Supervisors: Dr. A. G. Henry & Dr. T. Lüdecke

Leiden University, Faculty of Archaeology

Arnhem, 08-06-2023, Final

Acknowledgements

There are many who I would like to thank for their support during my studies. Firstly, I want to thank both of my supervisors, Dr. Amanda Henry and Dr. Tina Lüdecke, who have been there for me throughout the entire process of this research. Dr. Henry helped me figure out what I want to do, not only for my thesis research, but also further in my academic career. She put me in touch with Dr Lüdecke, who provided me with a place to explore my interests in isotopes studies and with experience in the laboratory at the Max Planck Institute of Chemistry, Germany. I greatly enjoyed my time at the institute and cannot wait to return there to join Dr. Lüdecke's research group (HoMeCo) as a PhD student. Next, I want express my gratitude to the other two members of the HoMeCo group, Sven Brömme and Dr. Jennifer Leichliter, as well as the rest of the department at the MPIC, who helped me whenever I had questions (or needed to move between apartments), and made me feel right at home. Lastly, I want to thank my parents, partner, and best friend, who supported me throughout the writing process, as well as with moving to and from Germany. I would not have been able to do it without you.

Table of Contents

List of figures

List of tables

List of equations

Equation 1: $\delta^{H}X = (R_{sample}/R_{standard} - 1) * 1000$ *or* $\delta^{H}X = ((R_{sample} - R_{standard})/R_{standard}) * 1000$

Equation 2: $\delta^{18}O_{PO4} \approx 0.9 * \delta^{18}O_{bodywater} + 23$

Equation 3: $\delta^{18}O_{PO4} \approx 0.71 * \delta^{18}O_{bodywater} + 22.60$ *or* $\delta^{18}O_{bodywater} \approx (\delta^{18}O_{PO4} - 22.60) / 0.71$

Equation 4: $\delta^{18}O_{VSMOW} \approx 1.03092 * \delta^{18}O_{VPDB} + 30.92$

Equation 5: $\delta^{18}O_{PO4} + 1 \approx 0.9787 * (\delta^{18}O_{CO3} + 1) + 0.0142$

Equation 6: $\delta^{15}N_{sample} = (\delta^{15}N_{measured} - (f_{blank} * \delta^{15}N_{blank})) / f_{sample}$

Equation 7: $f_{blank} = N\ content_{blank} / N\ content_{measured}$

Equation 8: $f_{sample} = 1 - f_{blank}$

Equation 9: $\delta^{18}O_{PO4} \approx 0.98 * \delta^{18}O_{CO3} - 8,5$

Equation 10: $\delta^{18}O_{PO4} \approx 0.9787 * \delta^{18}O_{CO3} - 7.1$

List of appendices

1 Introduction

One of the most important drivers of (human) evolution is diet and therefore it is vital to understand diet and its changes in the past. As a result, over the past several decades, one of the main focusses of paleontological research has been the reconstruction of ancient diet and food webs. Both traditional stable isotope measurements in tooth enamel (e.g., carbon and oxygen) and trace element ratios in bioapatite (e.g., Sr/Ca and Ba/Ca) have been used to advance our knowledge and understanding of the dietary ecology of past organisms (e.g., Balter et al., 2002; Cerling & Harris, 1999). However, information on trophic level is rare. Recently, novel geochemical methods have been developed to explore trophic proxies (e.g., calcium and zinc isotopes) to further our understanding feeding behaviours of vertebrates and past ecosystems (e.g., Jaouen & Pons, 2016; Martin et al., 2017). Although these systems are very promising, data relating to variability in isotopic fractionation and baseline variation of these elements is limited.

In contrast, the nitrogen isotope ratio ($^{15}N/^{14}N$ ratio, expressed as $\delta^{15}N$) of organic material has been used for several decades already as a well-established proxy for trophic spacing of animals in both marine and terrestrial food webs (e.g., Ambrose & DeNiro, 1986; Caut et al., 2009; Schoeninger, 2014; Schoeninger & DeNiro, 1984). In addition, $\delta^{15}N$ values have been studied in a range of settings, both natural and experimental (e.g., DeNiro & Epstein, 1981; Sponheimer et al., 2003; Wolf et al., 2009). However, its application in the palaeontological record has been hampered by the poor preservation of organic matter, which contains nitrogen, during fossilization. The analysis of nitrogen isotopes in fossil vertebrates has thus been mainly limited to relatively young sites (generally <100 ka), with well-preserved collagen in bone or dentin (e.g., Bocherens & Drucker, 2003; Britton et al., 2012; DeNiro, 1985). Compared to these organic rich materials, enamel is much more diagenetically resistant than bone and dentin due to its highly mineralized matrix trapping the organic matter (e.g., Koch et al., 1997; Wang & Cerling, 1994; Zazzo et al., 2004). It therefore has a high potential to preserve its isotopic fingerprint much better over large time scales, and could provide trophic information in deep time. However, the organic matter in enamel has a low nitrogen content (e.g., Robinson et al., 1995; Teruel J. de et al., 2015) and traditional combustion methods used for nitrogen isotope analysis require too large sample sizes.

In 2021, Leichliter et al. published a paper based on feeding experiment data of rodents, detailing a new method to measure $\delta^{15}N$ in tooth enamel. This *oxidation-denitrification* method is an adaption of a method first developed for $\delta^{15}N$ analysis in sea- and freshwater samples, as well as corals, diatoms, and foraminifera (Sigman et al., 2001; Weigand et al., 2016). Two articles employing this method have been published since. One focusses on the first combination of carbon, nitrogen, and oxygen stable isotope analyses on the same tooth enamel from animals in a single well-

constrained modern African ecosystem (Lüdecke and Leichliter et al., 2022). The other study focusses on the combination of carbon and nitrogen isotope analysis in tooth enamel of both modern mammals from several habitats across Africa and fossil mammals from Laos, in southeast Asia (Leichliter and Lüdecke et al., 2023). These publications show that the method works in both modern and fossil fauna assemblages and provide a modern dataset to which future fossil data can be compared.

1.1 Research aim and questions

As mentioned, the *oxidation-denitrification* method has already been applied twice in African/savannah environments, and once in a tropical environment. However, it has not been applied in a European/temperate environment. The values of the isotopes measured in this study ($\delta^{13}C$, $\delta^{15}N$, and $\delta^{18}O$), are dependent on a wide range of factors, one of which is the local environment, which can provide a baseline from which the isotope values can vary to a certain degree. Savannah, tropical, and temperate environments are so vastly different from one another that the $\delta^{15}N$ baseline will differ as well and thus measured $\delta^{15}N_{enamel}$ values cannot be directly compared between these environments. This means that it is necessary for future studies analysing $\delta^{15}N$ in temperate environments to understand what factors influence nitrogen isotopic fractionation in such places.

As it is the first time it is possible to analyse $\delta^{15}N$ in tooth enamel using this new method, there is still quite some information missing on what mechanisms influence the isotopic fractionation of nitrogen in enamel. One of these factors is seasonality, in particular the winter-summer seasonality present in temperate environments. These patterns can be reconstructed by e.g., measuring $\delta^{15}N$ and $\delta^{18}O$ in serially-sampled tooth enamel and see if and how they are correlated. This is due to the fact that one application of $\delta^{18}O$ values is as a measure for temperature and by extent seasonality in serially-sampled enamel (e.g., Pederzani & Britton, 2019), because tooth enamel mineralizes in a specific direction over the span of several months to years depending on tooth type and taxon (e.g., Kohn & Cerling, 2002). Furthermore, in order to further validate the utility of the new method to measure $\delta^{15}N$ in tooth enamel, it is crucial to compare $\delta^{15}N$ values from other biological tissues, usually collagen in archaeological settings, with the $\delta^{15}N$ values of tooth enamel of the same taxa and/or individuals.

The palaeontological site “Neumark-Nord 2” presents a unique opportunity to tackle all of these issues. It is well-preserved 120,000-year-old Middle-Palaeolithic Neanderthal butcher site in Germany (e.g., Gaudzinski-Windheuser & Roebroeks, 2014). Fossil fauna from this site produced one of the oldest and largest $\delta^{15}N$ datasets measured in collagen (Britton et al., 2019), which can be compared to the $\delta^{15}N$ values in tooth enamel from the same fossil assemblage measured here. In addition, the very rich zooarchaeological material recovered from this site contains many mammalian

teeth, including teeth from the same taxa (bovids and equids) of which the collagen was analysed for $\delta^{13}C$ and $\delta^{15}N$. However, even though so much isotopic research has been done at this site, there is no serially-sampled data available as of yet.

In order to understand if and how $\delta^{15}N$ in tooth enamel in a temperate environment is affected by seasonality and further validate the *oxidation-denitrification* method by comparing the $\delta^{15}N$ of tooth enamel and $\delta^{15}N$ of collagen, I will try to answer the following research questions:

1. *To what extent does seasonality impact the $\delta^{15}N$ pattern in the tooth enamel of serially-sampled equid third molars from the Eemian site Neumark-Nord 2, Germany?*
    a. *How are the $\delta^{13}C$ and $\delta^{18}O$ values of the serially-sampled equid teeth correlated?*
    b. *How are the $\delta^{13}C$ and $\delta^{15}N$ values of the serially-sampled equid teeth correlated?*
    c. *How are the $\delta^{15}N$ and $\delta^{18}O$ values of the serially-sampled equid teeth correlated?*
    d. *How does the relationship between seasonality and $\delta^{15}N$ values influence bulk sampling approaches of tooth enamel from temperate environments in the future?*

2. *To what extent, and why, do the $\delta^{15}N$ values of collagen compared to tooth enamel of equids from Neumark-Nord 2 differ from one another?*

The results of this study will provide first insights into the $\delta^{15}N$ patterning in herbivore teeth from temperate environments, which will further the development and applications of this new method. In addition, the serially-sampled data will expand the isotopic dataset of Neumark-Nord 2 and enable us to, in contrast to bulk sampled data, reconstruct seasonality at this site.

1.2 Chapter guide

I will start this thesis with providing background information on the archaeological context of Neumark-Nord 2, Germany, the site where the samples were excavated, in chapter 2. In chapter 3, I will provide an introduction of the concepts and terms related to mammalian teeth and tooth enamel, with a focus on horse teeth. Chapter 4 is the last background chapter and there I will focus on the chemistry of isotopes and the application of the different isotopic systems that are analysed in this study (stable carbon, oxygen, and nitrogen). In chapter 5, I will explain the materials and methods applied in this study. The results will be presented in chapter 6. In chapter 7, I will discuss these findings, present my interpretations, and make suggestions for future research. Lastly, I will give a short summary of the most important findings in chapter 8, as well as the answers to the research questions.

2 Archaeological context

2.1 Introduction

Figure 2.1: Location of Neumark-Nord 2 (NN2). Neumark-Nord 1 (NN1) is also shown (after Pop et al, 2015).

The samples analysed in this thesis were recovered from the site of Neumark-Nord 2 (NMN2), which is located in Saxony-Anhalt, Germany (figure 2.1). Neumark-Nord 2 is situated next to the bigger and much more well-known site Neumark-Nord 1 (NMN1). Both are lake basins and were discovered by Dietrich Mania when an open cast lignite mine exposed them. Neumark-Nord 1 was uncovered in 1985 and was excavated and surveyed over the next eleven years. It was a relatively large and deep lake and covers about 24 ha. However, since there were mining activities going on at the site, only small portions were excavated systematically and under severe time pressure (Gaudzinski-Windheuser & Roebroeks, 2014). The mining ceased in 1995 and in 1996 Mania discovered the Neumark-Nord 2 basin a few hundred meters to the northeast of Neumark-Nord 1. NMN2 represents a small, shallow pool at the margin of the NMN1 lake and covers an area of 2 ha. It was excavated between 2003 and 2008 (Gaudzinski-Windheuser & Roebroeks, 2014). After this, the former lignite quarry, and thus both sites, was inundated and repurposed as a recreational lake called the Geiseltalsee.

NMN1 and NMN2 are contemporaneous and date to the Eemian or Marine Isotope Stage (MIS) 5e/5d transition, the last interglacial period, based on stratigraphic, paleomagnetic, multiple amino acid racemisation and pollen analysis, as well as thermoluminescence dating (Gaudzinski-Windheuser & Roebroeks, 2014; Sier et al., 2011; Strahl et al., 2010). Interglacials are, relatively short (10,000 to 30,000 years), warm temperate periods in between a cycle of glacials, which are relatively long (40,000 to 100,000 years), extremely cold periods. The Eemian is dated to around 125,000 years ago and has a duration of 11,000 to 12,000 years.

Due to the calcareous character of fine-grained sedimentary matrix, which was deposited rapidly, wet and anaerobic conditions, as well as the absence of soil formation, there is incredibly preservation and little reworking of (organic) archaeological finds (García-Moreno et al., 2016; Gaudzinski-Windheuser et al., 2014). The excavations at NMN2 yielded an archaeological assemblage of around 23,000 pieces of lithics and 125,000 faunal remains (Kindler et al., 2014; Pop, 2014).

In this chapter, the formation of NMN2 will be discussed, as well as the Eemian environment, Eemian fauna, and hominin influence at the site. Lastly, the NMN2 find context of the analysed samples will be briefly described.

2.2 Site formation

Before the basin of Neumark-Nord 2 was formed, (peri)glacial sediments were deposited. These sediments date to the late Saalian or MIS 6 (Sier et al., 2011; Strahl et al., 2010), which is the glacial period preceding the Eemian. During the very last part of the Saalian, the frozen lignite, underlying the newly deposited glacial till, started to melt and it formed two diapirs, one to the north and one to the west of NMN2 (Pop et al., 2015). A diapir is an intrusion of a more mobile, deformable material (here the lignite) into the overlying rock (the glacial deposition). The two diapirs around NMN2 resulted in the continuous subsidence of the NMN2 location and basin formation. The basin infill is overlain by Weichselian gravel and loess deposits (Sier et al., 2011). The Weichselian is the glacial period following the Eemian.

The basin of NMN2 is shallow and shows rapid, on a geological timescale, nearly continuous infilling, with barely any evidence for soil formation during non-depositional periods (Sier et al., 2011). The sequence of sediments in the basin infill were described by Sier et al. (2011) along an eleven-meter-high profile, Hauptprofil 7 (HP7), from the deeper section of the basin (figure 2.2). Most of the infill consists of calcareous silt loams, which were deposited in a calm sedimentary setting in near-still water. The infilling occurred nearly continuous, with only a couple of short (<1 decade) interruptions due to the drying up of the basin. The sequence consists of 19 units of which unit 4-19 document the Eemian interglacial. Unit 8 contains the main archaeological find horizon named NMN2/2b.

2.3 Environment

Due to the vast number of basins dating to the Eemian period, a comprehensive tree pollen sequence is established for Southern England and the North European plain (Turner, 2000), which shows a relative uniformity from east to west. The pollen sequences of both Neumark-Nord basins have been correlated with this established sequence. There are multiple different interpretations on what the environment looked like in Europe during the Eemian based on these tree pollen. There are researchers who point to a closed-canopy environment (Bradshaw & Mitchell, 1999; Mitchell, 2005), while others point to a mosaic of grassland and forests that were maintained by large herbivores (Vera, 1997, 2000), and yet others take up an intermediate position pointing to the presence of closed forest with localized open patches (Sandom et al., 2014; Svenning, 2002).

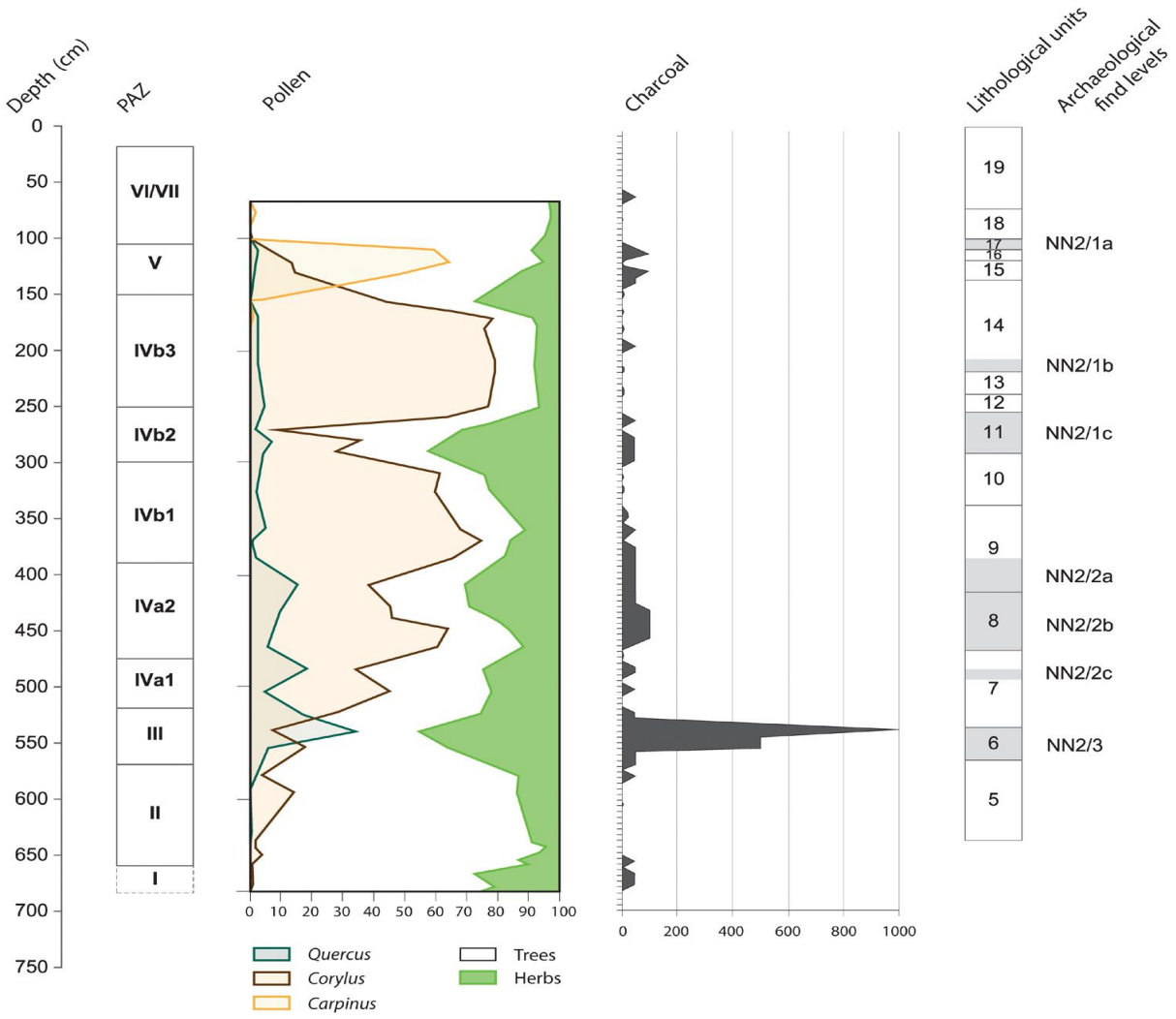

Figure 2.2: Environmental data of Hauptprofil 7, Neumark-Nord 2. Depth in cm, PAZ (pollen assemblage zones), percentage diagram of the composite pollen, the density of charcoal particles > 1 mm (particles/5 litres of sediment), lithological units, and archaeological find levels (Roebroeks et al, 2021, figure 2).

When zooming in on Neumark-Nord 2, it is clear from the stratigraphy and sedimentology that the water levels of this small, shallow basin fluctuated strongly with short periods of dry stands, as mentioned above (Pop et al., 2015; Sier et al., 2011). Based on pollen and non-pollen palynomorph (NPP) analysis, the pool started out as a freshwater pool, then held alternating fresh and brackish water, before reverting to a true freshwater pool at the end of the Eemian (Bakels, 2012). When looking at the main archaeological find layer, unit 8 in the stratigraphical sequence, it shows that there was a water body present at this time, which extended beyond the normal margin of the basin (Pop et al., 2015).

When turning to the environment surrounding the basin, the largest part of the sequence corresponds with the *Corylus* (hazel) pollen phase (figure 2.2). Pollen and NPP analyses show that the area around the pool must have been relatively open during the deposition of unit 6 – 11 (Bakels, 2012; Pop & Bakels, 2015). In addition, terrestrial molluscs, which are present in unit 6, 8/9, 11, and 14, are dominated by species adapted to open environments, while species that are adapted to forests

are nearly absent (Pop & Bakels, 2015). Almost all archaeological find layers are associated with dryer and more open environments based on these aforementioned proxies. Furthermore, oxygen isotope analysis shows that the climate at NMN2 during the early Eemian was generally comparable to the present climate, with similar mean annual temperatures and annual average rainfall $\delta^{18}O$ values (Britton et al., 2019).

2.4 Fauna

As mentioned above, more than 120,000 faunal remains have been excavated from NMN2. Most of them belong to large sized mammals like red and fallow deer, aurochs, and horses (Kindler et al., 2014). Some of the horse bones may belong to the wild ass, while there are also remains found from roe deer, a small cervid. Giant deer and wild boar are also present. Furthermore, megaherbivore remains, like those of rhinos and straight-tusked elephants, only occur in low frequency. This is in contrast to the faunal assemblage of NMN1, where elephants and fallow deer dominate and horses are absent (Gaudzinski-Windheuser et al., 2014; Kindler et al., 2020). For carnivores, foxes, wolfs, cave bears, and lions are represented at the site. Coprolites of hyenas have also been found. Furthermore, microfauna, fishes, molluscs, birds, and reptiles were also recorded. Overall, the faunal assemblage of NMN2 looks like a typical central European interglacial faunal community (Kindler et al., 2014).

2.5 Neanderthal presence

In the eighties and nineties of the last century, there existed a long debate about whether hominins were able to survive in the densely forested environment of the Eemian interglacial in north-western Europe (Roebroeks & Bakels, 2015). However, the discovery of an Eemian site at Caours in northern France put a stop to this debate and showed that Neanderthals were most definitely present in this period. Neumark-Nord 2 soon followed, with its clear pollen record, abundant flint artefacts and modified faunal remains, and was assigned as an Eemian Neanderthal site, even though no hominin remains were found (Kindler et al., 2020; Sier et al., 2011).

Almost 9,000 lithics from NMN2/2 were analysed by Pop (2014). Approximately 91 % of these are artefacts, which are lithics intentionally used or modified by hominins. Approximately 1.4 % of these artefacts were heated. It seems that intensive flint knapping took place at the site with a focus on high quantities of flakes. Neanderthals used small, well-prepared cores to make flakes, which were mostly directly used without any further modification. Retouch was probably only used to resharpen edges at on off-site location. Some opportunistic use of raw materials is also visible in the lithic assemblage.

Intense fragmentation of bone is apparent in the faunal assemblage. Surface mark analysis was performed on almost 2,200 bones from layer NMN2/2b. The results show that 11 % of all bone specimens show cut marks, with the number rising to 17 % when including possible cut marks (Kindler et al., 2014). Of the species present at NMN2, only elephant remains show an absence of cut marks. Some bones, from a range of species, were clearly used as tools. Break patterns of the bones were also analysed to determine if the bones were fresh or dry when broken. 50 % of the analysed long bones, showed fresh fractures associated with marrow extraction. Seasonality studies based on faunal remains indicate that Neanderthals were active at the site year-round (Kindler et al., 2020). Furthermore, surface marks made by carnivores are almost completely absent, which might indicate ongoing presence of Neanderthals, deterring competitors and scavengers from feeding at NMN2 (Kindler et al., 2020; Kindler et al., 2014).

During the excavation of NMN2, no hearth features were found. However, macroscopic charcoal remains and charred seeds were recovered from both the excavation and HP7 sediment samples. In addition, as mentioned above, some heated lithics and faunal remains were found during excavation. These fire proxies were investigated to determine if their origin was anthropogenic or natural (Pop et al., 2016). The flint artefacts and faunal remains point to temperature above 400 and 600°C respectively, and their spatial distribution is indicative of multiple, temporally distinct, fire events. The charcoal originates from deciduous tree species, and was probably produced within the watershed of the basin, since it co-occurs with charred seeds. The relatively high charcoal concentrations in layers with hominin presence and conversely, the relatively low concentrations in layers without hominin presence, seem to indicate a correlation between Neanderthal activity and fire activity at NMN2. The lack of hearth features can be explained by the higher water levels during periods of hominin presence (Pop & Bakels, 2015; Pop et al., 2015) and the presence of large herbivores (Pop et al., 2016).

As pointed out by Roebroeks et al. (2021), the first and biggest peak in charcoal concentrations, retrieved from HP7, falls in unit 6 (figure 2.2), which is also the unit where the first Neanderthal presence is documented. In addition, this also coincides with the start of a period with a semi-open environment surrounding NMN2, based on a reduction in the concentration of upland deciduous forest pollen and an increase in the concentration of upland herbs pollen. The higher levels of charcoal concentrations, although not as high as in unit 6, are sustained in the next 400-450 cm of HP7, which includes unit 8. Based on these proxies and comparisons with proxies from neighbouring Eemian lake basin sites, Roebroeks et al. (2021) suggest that Neanderthals continuously maintained open habitats at Neumark-Nord by their use of the landscape, which includes fire use, for roughly 2000 years.

2.6 Layer NMN2/2b

Thirteen of the fourteen teeth studied in this research come from the main find layer of Neumark-Nord 2, named NMN2/2b. The other tooth comes from the layer NMN2/2, but it is unknown what sublayer it was found in. Here I will only focus on the NMN2/2b layer. This layer contained more than 118,000 faunal remains and almost 20,000 lithic artefacts, and thus represents most of the material which was found at the NMN2 basin. Also present in this layer are thermally altered flint artefacts and bones, charred seeds, charcoal, and heated stone.

NMN2/2b corresponds to the sand and silt deposits of unit 8 (figure 2.2). Unit 8 is a finely laminated deposit, which is the result of afterflow (deposition by overland flow without the impact of raindrops; Pop et al., 2015). Based on the sedimentation rate of 0.11 cm per year calculated by Sier et al. (2011), find layer NMN2/2b was accumulated within 455 years (Kindler et al., 2014). Thermoluminescence dating of heated flints form this layer provide a weighted mean age of 121 ± 5 ka (Roebroeks et al., 2021). Based on both bone and lithic analysis, the finds in NMN2/2b seem to not have been heavily influenced by post-depositional processes and thus correspond relatively well with their original place of deposition (Kindler et al., 2014; Pop, 2014; Pop et al., 2015).

Based on pollen analysis, unit 8 correlates with the *Corylus*-phase or pollen zone IVa2 of the Eemian (Bakels, 2012; Sier et al., 2011). This pollen phase is dominated by *Corylus* or hazel trees. The analysis also showed that there were a wide variety of plants present at NMN2 during the IVa2 phase, including *Poaceae* (the grass family; Sier et al., 2011, Suppl. table S1 and figure S5). Appendix A shows a list of all plant genera and families present at NMN2 in unit 8. In addition, stable carbon and oxygen isotope analysis of freshwater molluscs (*Bithynia tentaculata*) from unit 8 show that this is the most humid phase in the sequence of Neumark-Nord 2 (Milano et al., 2020). The first half of this unit experienced high temperatures and humidity, whereas in the second part the temperature decreased and NMN2 experienced a dry event.

2.7 Conclusion

To summarise, Neumark-Nord 2 is an Eemian lake basin with a relatively typical Central European interglacial environment and an extremely rich archaeological record. The studies discussed above, point to NMN2 being a location where Neanderthals knapped flint, used fire, and processed hunted animals, and where they were able to maintain an open landscape surrounding the basin due to their use of the landscape for roughly 2000 years. Find layer NMN2/2b was accumulated within 455 years and is part of the *Corylus* pollen phase. In addition, it is the most humid phase with a semi-open environment and shows very little evidence for post-depositional processes.

3 Teeth and tooth enamel

3.1 Introduction

In this chapter, I will introduce the basic concepts and terms associated with teeth and enamel. This is important to understand since mammalian tooth enamel is analysed in this study. Firstly, I will focus on mammalian teeth in general, including the different components of a tooth and the composition of enamel. Then, I will zoom in on equid teeth and explain their morphology, growth and wear, with a specific focus on the third molar, which are the types of teeth (equid third molars) that were studied here.

3.2 Mammalian teeth

Nearly all mammalian species have teeth, which are relatively similar to each other in a range of aspects, including structure and development. Each tooth can be divided into three parts: the crown, which is the part of the tooth covered by enamel and usually exposed above the gum; the neck, which is the transition part between the crown and the root; and the root, which is the part of the tooth embedded in the socket in the jaw bone (e.g., Lacruz et al., 2017; figure 3.1). Located in the centre of each tooth is the pulp cavity, which has a very small opening at the apex of the root. Through this opening, blood vessels and nerves can enter the pulp cavity and supply the tooth with nutrients, so it continues growing. In most mammalian species, including equids, this aperture is closed at a certain age, so further growth ceases. These teeth are thus aptly named closed-rooted. Some species, including elephants, have open-rooted teeth, which means that the pulp cavity remains open and the teeth grow throughout life. The pulp cavity is surrounded by dentin. This material contains a large collagen component, like in bone, and forms the main mass of each tooth. The dentin is covered by enamel in the crown part and cementum in the root part of the tooth. Enamel is the hardest substance in the body of mammals and acts as a barrier to protect the tooth from outside forces. It borders the dentin along the dentin-enamel junction (DEJ or EDJ). Cementum surrounds the root of the tooth and 'cements' it to the jaw bone. For a more detailed overview of the structure of a mammalian tooth, see Lacruz et al. (2017).

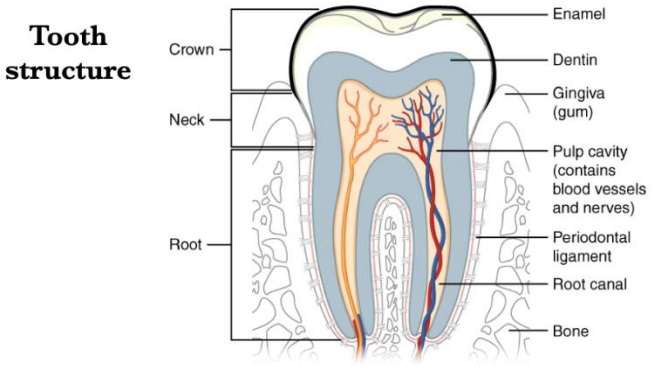

Figure 3.1: The structure of a human molar (Gorden Betts et al, 2013, p. 1103).

There are four different types of mammalian teeth: incisors,

canines, premolars, and molars. The function of each tooth type depends on the feeding and social habits of the species (e.g., Ungar & Lucas, 2010). In most herbivores, including horses, incisors are the front teeth and are mainly used to bite and cut food. The canines flank the incisors, and are long pointed teeth. They are mostly used for holding and tearing food. Premolars are transitionary teeth between the canines and molars. They have a flat surface and are used for chewing. Lastly there are molars. These have an even larger flat surface than premolars and are mostly used for grinding food. Both premolars and molars can vary quite a lot in morphology of the flat/biting surface and its cusps, due to differences in diet between species. For example, folivores (leaf eaters) have taller cusps and longer sheering blades in their (pre)molars, whereas grass eaters, like horses and gazelles, have very flat biting surfaces with ridges of enamel to grind their food (e.g., Ungar, 2015). It has to be noted that not all mammalian species possess all four tooth types, but most of them do.

The different sides of teeth are all termed differently (figure 3.2). The biting edge of incisors and canines is called the incisal surface, while the biting edge (or chewing surface) of premolars and molars is called the occlusal surface. The mesial side of the tooth is the side facing forward, touching the preceding tooth. The distal side on the other hand is the side facing backward, touching the succeeding tooth. For example, the mesial surface of the first molar faces the distal surface of the last premolar. The lingual side of a tooth faces the tongue. The side of incisors and canines that faces the lip is called labial, whereas the side of (pre)molars that faces the cheek is called buccal. To distinguish between teeth originating in the upper or lower jaw, upper jaw (maxilla) teeth are termed superior or maxillary teeth and lower jaw (mandible) teeth are termed inferior or mandibular teeth.

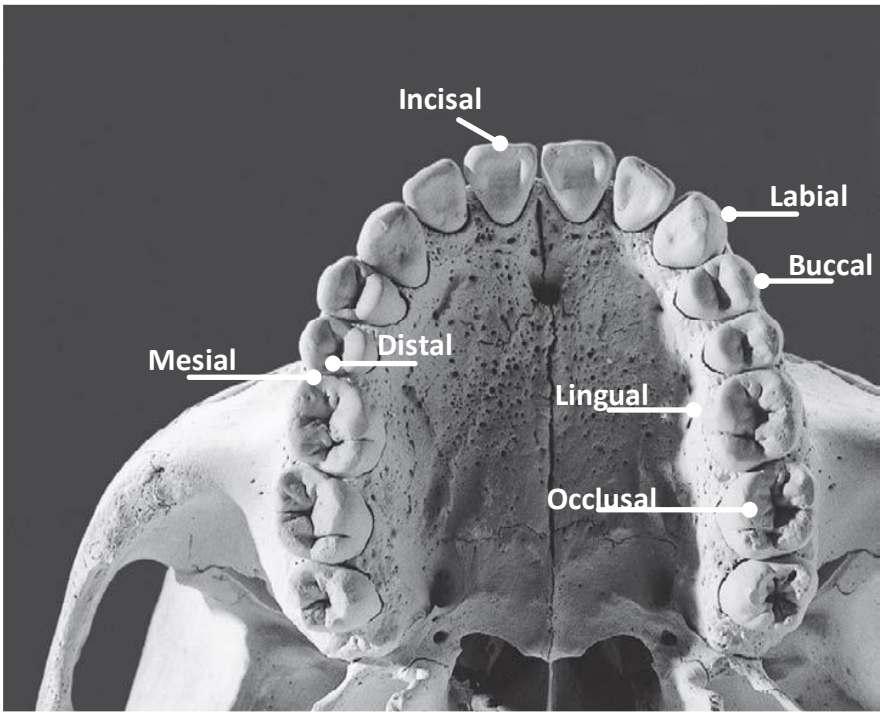

Figure 3.2: diagram of the directional terms of mammalian teeth, photograph of a human maxilla (after White and Folkens, 2005, p. 132).

Most mammal species, including horses, belong to the category of diphyodonts. This means that early in their life, individuals have a set of deciduous teeth (or milk teeth). This is later replaced by the permanent teeth. There are some species belonging to a different category of polyphyodonts, including the elephant, which means that their teeth are continuously replaced. Other species, like rats and mice, belong to the category of monophyodonts. This means that they have only a singular set of teeth, which is open-rooted and continuously grows throughout life (Lacruz et al., 2017).

As mentioned above, enamel is the hardest material in the body of mammals. It is a dense, highly mineralized material, consisting of 85 – 95 % wt. hydroxyapatite (depending on species) in mature enamel (Gil-Bona & Bidlack, 2020; Lacruz et al., 2017; Sakae et al., 1994; Teruel J. de et al., 2015). As hydroxyapatite is a mineral, it is inorganic and has a well-organized crystal matrix. This makes enamel exceptionally resistant to diagenetic alteration during fossilization when compared to bone and dentin, which are the other biological materials most often preserved in the fossil record (Koch et al., 1997; Kohn & Cerling, 2002; Lee-Thorp & Merwe, 1991; Sakae et al., 1994; Wang & Cerling, 1994; Zazzo et al., 2004). Bone and dentin are more poorly mineralized as they only contain between 60 – 70 % wt. hydroxyapatite. The chemical formula for pure hydroxyapatite is: $Ca_{10}(PO_4)_6(OH)_2$ (Elliott, 2002; Sakae et al., 1994). However, in enamel, hydroxyapatite contains ion substitutions/impurities, namely CO_3^{2-}, Mg^{2+}, and HPO_4^{2-}, which is why the hydroxyapatite in enamel, bone, and dentine is called carbonated hydroxyapatite or biological apatite. Tooth enamel contains less than 5 % wt. of structural carbonate (CO_3^{2-}; Lüdecke and Leichliter et al., 2022; Sakae et al., 1994), which is the part that is targeted for simultaneous stable carbon and oxygen isotope analysis. Oxygen isotopes can also be measured in the PO_4 component of enamel (Kohn & Cerling, 2002).

Nitrogen isotopes are commonly measured in the organic matter of bone and dentin, which consists of approximately 90 % wt. collagen. However, because bone and dentin are much more susceptible to diagenesis, nitrogen isotope analysis is restricted to relatively young (<100 kya) and well-preserved samples (Bocherens & Drucker, 2003; Britton et al., 2012; DeNiro, 1985; Jaouen et al., 2019). On the other hand, the organic matter in enamel (0.5 – 2 % wt. depending on taxon) is trapped within the crystalline structure of the hydroxyapatite and protected against diagenetic changes over long time-scales (Martínez-García et al., 2022; Robinson, 2014; Robinson et al., 1995; Savory & Brudevold, 1959; Teruel J. de et al., 2015). This organic matter consists mostly of enamel-specific proteins (namely amelogenin) and proteases (Castiblanco et al., 2015; Lacruz et al., 2017; Robinson et al., 1995; Welker et al., 2020), which contain nitrogen. Because most traditional analyses of nitrogen isotopes require a relatively large quantity of nitrogen, as mentioned in chapter 1, the low nitrogen content of enamel has meant that nitrogen isotopes in this tissue could not be measured routinely.

However, a recently developed method, *oxidation-denitrification*, described in more detail in chapter 5, requires much lower quantities of nitrogen for accurate measurement and thus allows us to analyse the nitrogen isotopic composition of (fossil) tooth enamel and explore this reservoir of information.

Enamel develops in two main stages: the secretory stage, which forms immature enamel, and the maturation stage, which forms mature and fully mineralized enamel (Gil-Bona & Bidlack, 2020; Lacruz et al., 2017; Robinson, 2014). During the first stage immature enamel is deposited along the enamel-dentine junction (EDJ) and grows outward (away from the dentin) and downwards (away from the crown, towards the root), until it reaches the full enamel thickness (figure 3.3). Immature enamel is softer than mature enamel, because it contains more organic material and water, and is much less mineralized, consisting of only roughly 30 % mineral wt. at the moment of secretion (Lacruz et al., 2017; Robinson et al., 1995). The first mineral crystals already form during this first stage. In the maturation stage, the mineral crystals grow in width and thickness and replace the organic matrix of immature enamel, providing it with its characteristic hardness. For a more detailed overview of enamel development see Lacruz et al. (2017), Passey and Cerling (2002), and Robinson et al. (1995). After full mineralization, enamel loses its capacity to regenerate and thus only preserves the individual's isotopic composition acquired during the early stages of life (i.e., infant to young-adult), because this is the time enamel forms. This sets it apart from other tissues (such as bone and dentin) that continuously remodel throughout life (e.g., Balasse et al., 1999; Kohn & Cerling, 2002; Passey & Cerling, 2002). To avoid the isotopic influence of the consumption of breast milk (Chinique de Armas et al., 2022; Dailey-Chwalibog et al., 2020; Fuller et al., 2006; Tsutaya & Yoneda, 2015), the last forming permanent teeth should be targeted (third molars in equids), because these start to develop only post-weaning.

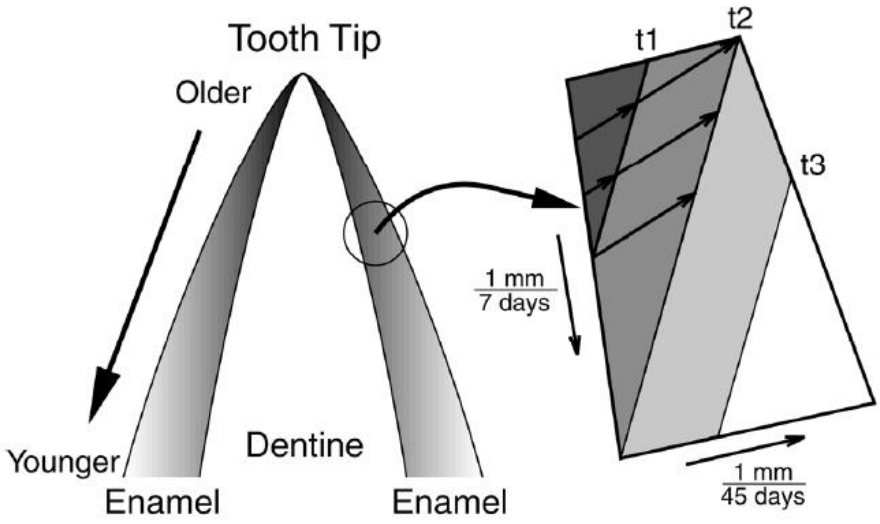

Figure 3.3: General diagram of how large herbivore teeth grow. The enamel grows downwards and outwards through time (Kohn and Cerling, 2002, figure 4, p. 464).

3.3 Equid teeth

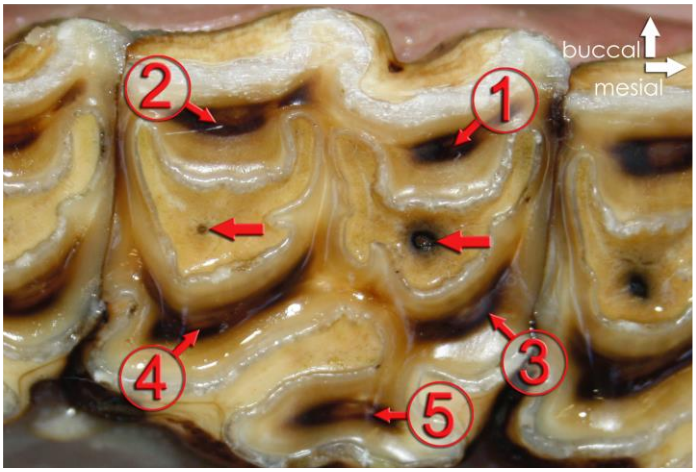

Figure 3.4: Occlusal surface of an equid maxillary cheek tooth. Red arrows show the canals for blood vessels. The yellowish-brown tissue is dentin. The enamel lophs are clearly visible as grey lines (after Staszyk et al 2015, p. 479).

Modern equids are diphyodonts, as mentioned above, and normally have 40 permanent teeth. In each quadrant of the mouth, they possess 3 incisors, 1 canine, 3 premolars, and 3 molars. Equids have hypsodont (high-crowned) teeth. This means that they feed on abrasive substances and their teeth are thus subject to considerable wear on the occlusal surface. To compensate for the large amount of material loss due to wear, equid teeth have long crowns (up to 9 cm; Hoppe, Stover, et al., 2004) with only a small fraction visible in the mouth at any given time. The part of the crown not visible is named the reserve crown and is located in the alveolar socket in the jaw bone (Staszyk et al., 2015). This means that equids have a lot of enamel along almost the complete length of their teeth. The reserve crown is covered in cementum in order to attach it to jaw bone.

The occlusal surface of equid cheek teeth is much more complex than in humans, as an adaptation to feeding on abrasive grasses (see figure 3.4). The tooth is surrounded by a continuous ring of enamel, but also possesses enamel folds (lophs) and protruding enamel ridges, visible on the occlusal surface (Staszyk et al., 2015). These enamel folds are covered by cementum and encircle dentin.

To further compensate for the wear experienced, equid teeth erupt continuously throughout life, but they do not grow indefinitely (Bendrey et al., 2015; Staszyk et al., 2015). Erupting is the process where a tooth enters the oral cavity and becomes visible, whereas growing is the process of the formation of new dental material. In equids, like in most mammals, the crown of the teeth forms first, and then the tooth grows downward, increasing its length. During the first year after eruption of cheek teeth (premolars and molars), tooth growth rate exceeds occlusal wear, increasing the length of the tooth (Staszyk et al., 2015). During the second year after eruption, the rate of tooth formation and occlusal wear are equal, maintaining the length of the tooth. After this time, tooth growth slows down and the teeth start reducing in length. It has been estimated that the amount of occlusal wear and compensatory tooth eruption is roughly 2-4 mm per year in equine cheek teeth, with rates up to 9 mm per year in young individuals (Staszyk et al., 2015). For incisors, the wear vs growth rate is quite different. However, that will not be discussed here since only third molars are analysed in this study.

The start of tooth growth, growth rate, eruption time, and enamel mineralization time differs per tooth. Here, I will shortly discuss these aspects for the third molar (M3) in modern equids. For a more complete overview regarding the other (pre)molars, see Hoppe, Stover, et al. (2004) and Bendrey et al. (2015). All molars reach approximately the same maximum length of 9 cm in modern horses. The M3 starts to form around 16 months of age (Bendrey et al., 2015), it starts to mineralize around 21 months of age, continues for about 34 months (Hoppe, Stover, et al., 2004), and it erupts around 3.5 years of age (Hoppe, Stover, et al., 2004). As Bendrey et al. (2015) and Nacarino-Meneses et al. (2017) show, both modern and archaeological equid molars show an exponentially decreasing tooth growth rate over time. This, however, does not mean that the teeth keep mineralizing until they reach their full length. After full mineralization (for M3s around 55 months of age), dentin continues to be deposited, extending the roots of the tooth. The average growth rate of a modern equid third molar is around 3 cm per year (Hoppe, Stover, et al., 2004). This means any bulk sample for stable isotope analysis would need to cover around 3 cm of enamel along the vertical axis of the tooth to not be influenced by seasonality. This is, however, also dependent on the location of sampling, since tooth growth rate decreases exponentially. There is thus more time averaging in the enamel closer to the root (Bendrey et al., 2015). It has to be noted that the timings mentioned here are based on data from modern horses and should thus not be directly applied to extinct equid species as absolute values.

In this study, third molars were collected, because, as explained above, the consumption of mother's milk influences the isotopic composition of tissues that form during this period. In equids, third molars only start to develop after the weaning period has ended, and are therefore perfect to avoid this confounding factor. Furthermore, due to the direction and duration of mineralization, the teeth were serially-sampled along the complete growth axis (crown to root) in order to establish a seasonality pattern based on the $\delta^{18}O$ values of the enamel.

3.4 Conclusion

Enamel is the hardest material in the mammalian body, as well as that it is highly resistant to diagenesis and chemical alteration. It preserves a small amount of nitrogen bound to the mineral matrix and therefore is an untapped resource for nitrogen isotope analysis. Equid teeth possesses high-crowned (hypsodont) teeth, which erupt continuously during life to compensate for the occlusal wear experienced due to their abrasive food diet. The third molar (the tooth type analysed for this study) start to form around 16 months of age (post-weaning), starts to mineralize around 21 months of age, and continuous to do so for another 34 months. Furthermore, it can reach a maximum length of 9 cm and has an exponentially decreasing tooth growth rate.

4 Isotope background

4.1 Introduction

In this chapter, I will focus on providing the necessary background information regarding stable isotopes and isotopic analysis, in particular stable carbon, oxygen, and nitrogen isotopes. First, I will explain what isotopes are, as well as the difference between stable and unstable isotopes. In addition, I will discuss two important mechanisms, fractionation and mixing, which influence the ratios of isotopes in nature, and I will explain the conventional delta notation used for isotopes. Then, I will describe the isotopes that are analysed here, their applications, and how their ratios can be influenced in nature. I will start with stable carbon and oxygen isotopes. The enamel samples were first analysed for these isotopes combined and based on those results, a selection was made for nitrogen analysis, as will be explained in more detail in chapter 5. I will end this chapter with a detailed description of nitrogen isotopes and what factors can influence them, as the main focus of this thesis is to see what affects nitrogen isotopes during the development of (equid) enamel.

4.2 Isotopes

4.2.1 What are isotopes?

Everything is made up of molecules and molecules in turn are made up of different atoms, or elements, in different ratios. At the present moment, 118 chemical elements are known of which 94 occur in nature. Each atom consists of a nucleus with protons and neutrons surrounded by a 'cloud' of electrons. The weight of protons and neutrons is roughly the same, while the weight of electrons is nearly negligibly small. The weight of protons and neutrons together forms the *atomic weight* of the atom. The *atomic number* of each element corresponds with the number of protons in the nucleus. The different elements are arranged by increasing atomic number in the period table (figure 4.1). The table starts with hydrogen, which has an atomic number of 1 and thus one proton. Helium has an atomic number 2 and thus two protons, and so on. Usually, atoms have a neutral charge, which is achieved by an equal number of protons and electrons.

However, it is also possible to have several variants of the same element. These versions are called isotopes. Isotopes of a single element differ from each other because of a slight variation in atomic mass, which is caused by a different number of neutrons in the nucleus. For example, carbon (C) has three different isotopes: carbon-12 (^{12}C), carbon-13 (^{13}C), and carbon-14 (^{14}C). The number in the name of the isotopes equals the number of protons and neutrons added together. Carbon has an atomic number of 6 in the periodic table, which means it has 6 protons in its nucleus. Carbon-12, which is by far the most common carbon isotope in nature, thus has 6 neutrons in the nucleus (12 – 6 = 6). Carbon-13 has 7 neutrons (13 – 6 = 7), and carbon-14 has 8 neutrons (14 – 6 = 8).

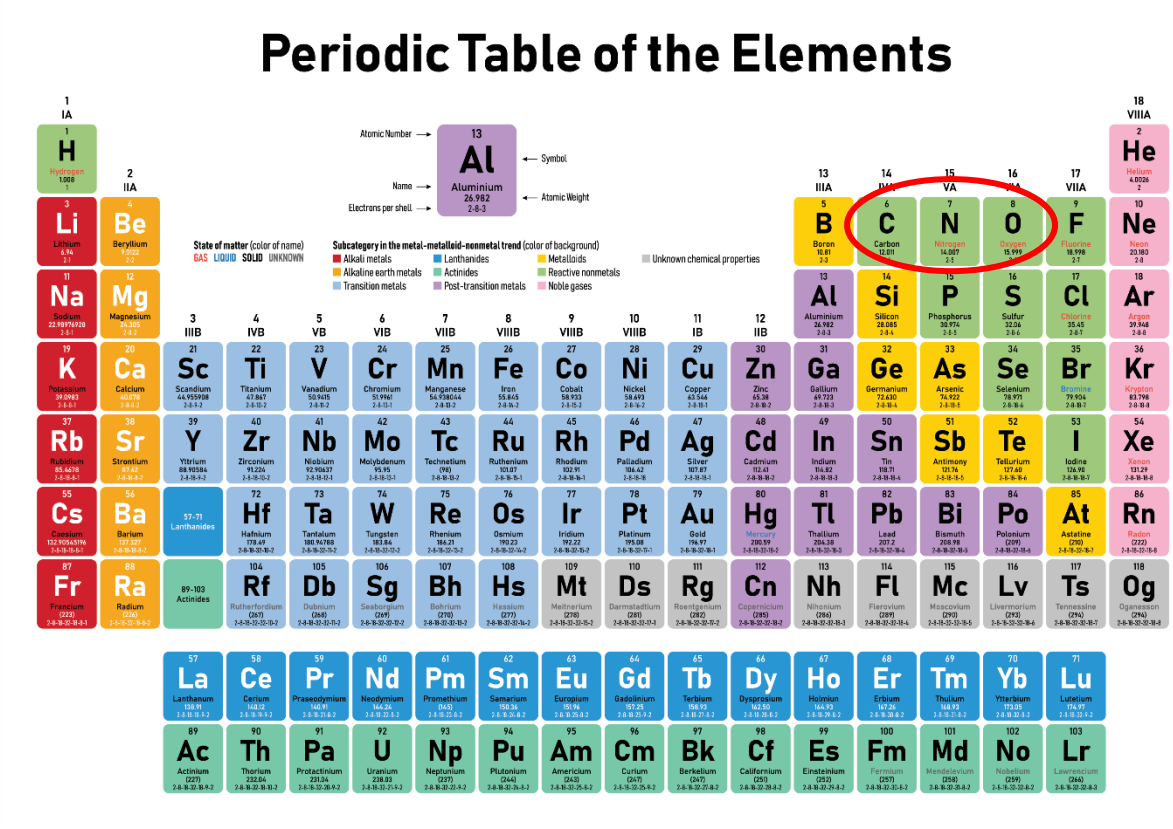

Figure 4.1: Periodic table with carbon (C), nitrogen (N), and oxygen (O) circled (https://www.snexplores.org/article/scientists-say-periodic-table (accessed on 03-02-2023)).

4.2.2 Stable and unstable isotopes

Two types of isotopes exist: stable and unstable (or radioactive) isotopes. Stable isotopes are isotopes that stay the same over time, whereas unstable isotopes fall apart into stable isotopes of other elements over time. Radioactive isotopes do not necessarily decay to stable isotopes immediately, but can go through a chain of other unstable isotopes until they reach a stable stage. Every unstable isotope has its own half-life. The half-life means the time it takes for a specific isotope to decay until there is only half of the initial amount of that isotope left.

Both stable and radioactive isotopes are used in archaeological research. In this study, only stable isotope analysis will be used. Stable isotope analysis is based on the measurement of the ratio between the most common naturally-occurring stable isotope of the element and (one of) the rarer naturally-occurring stable isotope(s) of the element in the sample being analysed. What such analyses can show will be explained in detail for carbon, oxygen, and nitrogen below.

4.2.3 Mixing and fractionation

There are two main mechanisms which influence the distribution of isotopes in nature: mixing and fractionation. Mixing is relatively straight-forward and occurs when two or more sources of isotopes are combined. Fractionation is a bit more complicated, but highly important, because it forms the

basis of most isotopic analyses and their interpretations, and thus also the analyses done in this study. This mechanism mostly influences concentrations of stable isotopes.

Fractionation is the result of the fact that the stable isotopes of one element are highly similar, but not *exactly* the same and thus behave slightly differently during certain chemical reactions and physical processes. According to Fry (2006, p. 12), the two most important rules are:

1. In kinetic reactions, the light isotopes tend to react faster than the heavy isotopes
2. In exchange reactions, the heavy isotopes concentrate where bonds are strongest

The first rule means that when a reaction needs a starting energy, the light isotopes (the isotopes with fewer neutrons in the nucleus) react faster and thus there will be a relatively higher ratio of light isotopes in the product compared to the source material. For example, during photosynthesis, carbon is taken up from the atmosphere in the form of CO_2 and converted into sugar. In this reaction the lighter isotope, ^{12}C, reacts faster than the heavier isotope, ^{13}C, and the light isotope is thus preferentially taken up. This leads to the conclusion that more ^{12}C relative to ^{13}C is present in plant sugar compared to atmospheric CO_2.

The second rule describes the heavy isotopes preferring the side of an equilibrium reaction where bonds are strongest. Equilibrium reactions are reactions that not only react forwards (from source to product), but both forwards and backwards (from product to source) until they reach a balance. Such a balance means that the forward and the backward reaction occur simultaneously with an equal speed. This means there are no net changes to the source and product concentrations in equilibrium. The heavier isotopes will be relatively more abundant on whichever side of this balance the bonds between atoms are stronger. This could be on the 'source' side, but also on the 'product' side depending on which reaction is happening.

4.2.4 Delta notation

Isotope values are reported using the δ (delta) notation, which denotes difference. In this case, it signifies the difference between the isotopic composition of a measured sample and the isotopic composition of a standard. Each isotope has its own standard, although some standards are used for more than one isotope. The δ values are calculated using the following formula (Fry, 2006, p. 31):

$$\delta^{H}X = (R_{sample}/R_{standard} - 1) * 1000 \quad (1)$$

which can also be written as:

$$\delta^{H}X = ((R_{sample} - R_{standard})/R_{standard}) * 1000$$

where the X is the specific element measured (carbon (C), nitrogen (N), or oxygen (O)), the superscript H denotes the heavy isotope mass of that element (^{13}C for carbon, ^{15}N for nitrogen, or ^{18}O for oxygen), and R stands for the ratio of the heavy isotope to the light isotope for that element ($^{13}C/^{12}C$, $^{15}N/^{14}N$, or $^{18}O/^{16}O$). As the differences between sample and standard are often incredibly small, the δ values are multiplied by 1000 and expressed in permille or parts per thousand (‰).

For most isotopes, the δ values range between -100 and +50 ‰ for natural samples (Fry, 2006, pp. 23-24). The δ values being negative means that there are relatively fewer heavy isotopes present in the sample than in the standard. Standards themselves have a δ value of 0 ‰, because if you measure them against themselves, the difference is 0. When the δ value is higher, the sample is enriched in heavy isotopes and thus heavier compared to the standard. When the δ value is lower, the sample is depleted in heavy isotopes and thus lighter. In other words, "higher heavier, lower lighter" (Fry, 2006, pp 22).

4.3 Carbon

As mentioned above, stable isotope analysis focusses on the ratio of the concentration of the most naturally occurring isotope vs the rarer naturally occurring isotope of the same element. In this section, the focus is on stable carbon isotopes, which are ^{12}C and ^{13}C. ^{12}C is the most naturally abundant isotope and accounts for roughly 98.9 % of atmospheric carbon, whereas ^{13}C is much rarer and accounts for roughly 1.1 % of atmospheric carbon (Nier, 1950).

Stable carbon isotope analyses are used to investigate the plant component of the diet of animals. This analysis is based on the fact that there are two main photosynthetic pathways used by terrestrial plants: the C_3 and C_4 pathway. C_3 plants get their name from the fact that the first photosynthetic product is a 3-carbon molecule, whereas with C_4 plants, the first photosynthetic product is a 4-carbon molecule. C_3 plants are by far the most abundant on earth, accounting for ~ 95 % of green plants. C_4 plants are a relatively recent adaptation (~ 20 million years ago) and only began to expand and be incorporated in the diet of mammals between 8 and 6 million years ago (Ehleringer & Cerling, 2002; Hobbie & Werner, 2004). The efficiency of C_4 photosynthesis is higher only in environments with higher temperatures and/or lower CO_2 concentrations than that of C_3 photosynthesis (Ehleringer & Cerling, 2002). C_4 plants are mostly tropical grasses and sedges and occur in Asia, Africa, North and South America.

One other photosynthetic pathway exists, called CAM (crassulacean acid metabolism). This occurs in succulent and epiphyte species from very arid regions. CAM plants usually fixate atmospheric CO_2 following the C_4 pathway, but separate certain activities of enzymes between day and night

(Marshall et al., 2007, p. 24). The carbon in such plants undergoes as much fractionation as in C_4 plants, and the $\delta^{13}C$ values are therefore similar. Some CAM plants (facultative-CAM plants) can switch between the C_3 pathway and the CAM pathway based on environmental conditions (Marshall et al., 2007; O'Leary, 1981). These plants will present with a $\delta^{13}C$ value intermediate to C_3 and C_4 plants. However, since their distribution is so restricted, they often do not play a (significant) role when analysing the diet of an animal.

As explained above (section 4.2), fractionation occurs during photosynthesis. There is a difference in the degree of fractionation between the two photosynthetic pathways (Ehleringer & Cerling, 2002; Kohn & Cerling, 2002). C_3 plants are very 'leaky', which means they have more free exchange between external and internal CO_2. Because of the first rule of fractionation, which says that light isotopes react faster than heavy isotopes, ^{12}C is preferably captured during photosynthesis, while ^{13}C is incorporated less before the internal CO_2 is exchanged with 'fresh' external atmospheric CO_2. This means that the internal CO_2 will be exchanged when it has a relatively increased concentration of ^{13}C compared to atmospheric carbon, while the plant material of the C_3 plant is relatively depleted of ^{13}C. This in turn results in a lower $\delta^{13}C$ value of C_3 plant material compared to the $\delta^{13}C$ value of the atmosphere. In contrast, C_4 plants are less 'leaky' compared to C_3 plants. They still adhere to the first rule of fractionation and thus have a $\delta^{13}C$ value that is lower than the atmospheric $\delta^{13}C$ value. However, their $\delta^{13}C$ value is higher than that of C_3 plants, because the internal CO_2 is exchanged with external CO_2 at a slower rate and the plant therefore has more time to incorporate ^{13}C isotopes in its products (see figure 4.2 for an illustration of this $\delta^{13}C$ separation). For a more detailed overview of how the two pathways work, see Ehleringer and Cerling (2002) and O'Leary (1981).

The two different photosynthetic pathways result in a relative ^{13}C depletion of ~18 ‰ for C_3 plants and ~4 ‰ for C_4 plants, compared to atmospheric carbon isotope ratios. Presently, the $\delta^{13}C$ value of the atmosphere is around -8 ‰ (compared to a standard, see below), the $\delta^{13}C$ values of C_3 plants range between -25 and -30 ‰, while

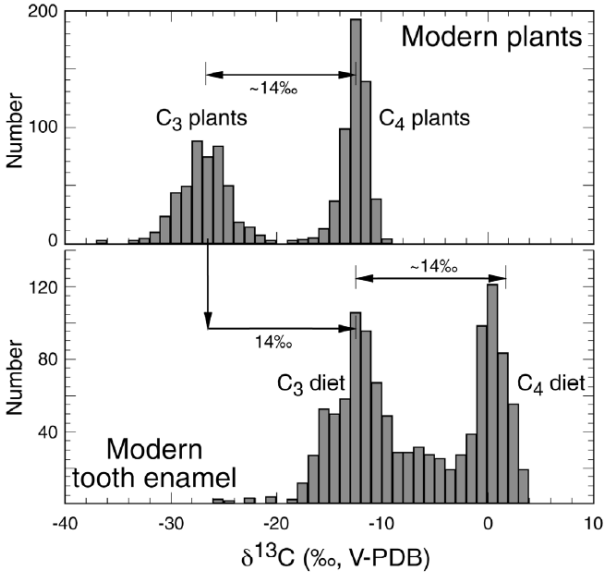

Figure 4.2: Separation of plant and tooth enamel $\delta^{13}C$ values. Histograms of the $\delta^{13}C$ values of modern plants (above) and of the structural carbonate component of African mammal tooth enamel (below). The differentiation between the two different photosynthetic pathways is clearly visible and corresponds with the separation visible in the diet. The enrichment factor of 14 ‰ between plants and enamel is based on Cerling and Harris (1999), but this study will use the enrichment factor of 13.5 ‰ calculated by Cerling at al (2021) for non-coprophagous hindgut fermenters as will be explained further down in this section (Kohn and Cerling, 2002, figure 3, p. 462).

the $\delta^{13}C$ values of most C_4 plants range between -9 and -19 ‰ (e.g., Bender, 1971; Cerling et al., 2003; Kohn, 2010; Kohn & Cerling, 2002). However, these values were different before the industrial revolution. Due to the enormous amount of CO_2 added to the atmosphere from fossil fuel combustion and deforestation, the $\delta^{13}C$ of the atmosphere has decreased by roughly 1.5 ‰ since 1850 (e.g., Dombrosky, 2019; Marino & McElroy, 1991). This is called the Suess effect. The CO_2 concentration of the atmosphere has also fluctuated before 1850, although generally less drastically than in the last 150 years (e.g., Hare et al., 2018). Hare et al. (2018) modelled the $\delta^{13}C$ of CO_2 in the atmosphere, as well as its concentration, over the last tens of thousands of years. They show that around 120,000 years ago, the $\delta^{13}C$ of the atmosphere was around -6.5 ‰, and the average $\delta^{13}C$ of C_3 plants around -26 ‰. This indicates that the range of $\delta^{13}C$ of C_3 plants during the Eemian was between -24 and -29 ‰, and the range for C_4 plants between -8 and -18 ‰.

Generally speaking, an animal's isotopic composition depends on the isotopic composition of its diet according to the "you are what you eat" principle (DeNiro & Epstein, 1981). In the case of carbon isotopes, the relative $\delta^{13}C$ of plants is transferred to the animal. So, animals with a C_3 diet have a lower $\delta^{13}C$ in their tissues than animals with a C_4 diet. Animals that feed on a mixed diet fall in between. However, it is important to remember that fractionation occurs during chemical reactions and physical processes. The incorporation of carbon into different body tissues is a chemical reaction and the carbon isotopes ratios present in the diet are thus affected by fractionation. The difference between the $\delta^{13}C$ value of the diet and the $\delta^{13}C$ value of the specific tissue is called the enrichment factor or ε^*. The enrichment factor is not only dependent on what specific tissue is measured, but also what type of digestive system an animal has and the specific isotope under analysis.

An enrichment factor of 14.1 ± 0.5 ‰ between tooth enamel and the diet of ungulate mammals was determined by Cerling and Harris (1999). Since then, multiple studies have explored what aspects of animal physiology influence the enrichment factor, and if this factor is different between species or groups of species. For example, Tejada-Lara et al. (2018) concluded that the enrichment factor between diet and bioapatite for herbivorous mammals is dependent on body mass. However, Cerling et al. (2021) show, based on modern mammal samples, that the enrichment factor between diet and breath (diet-breath enrichment factor) is mostly determined by methane production and that it is different for four different groups of mammals: non-coprophagous and coprophagous hindgut fermenters, and non-ruminant and ruminant foregut fermenters. Coprophagous animals are animals that incorporate their dung into their diet, rabbits for example. Hindgut fermenters have a single stomach and multiple enlarged fermentation compartments in their colon and/or cecum, whereas foregut fermenters have a pre-gastric fermentation chamber. Rhinos

and horses fall into the category of hindgut fermenters, while cattle fall in with foregut fermenters. Ruminants are animals that are able to regurgitate food from their rumen, such as cattle and giraffes. The diet-breath enrichment factor for each group can be used to estimate the diet-bioapatite enrichment factor for $\delta^{13}C$, because there is a near constant isotope enrichment between breath and enamel (Passey et al., 2005). Following Cerling et al. (2021), equids have a diet-enamel enrichment factor of 13.5 ± 1 ‰, since they belong to the non-coprophagous hindgut fermenter group (figure 4.2).

Because of the enrichment factor between the diet of herbivores and their enamel, modern browsers (>70 % C_3 diet) have a $\delta^{13}C_{enamel}$ values lower than -8 ‰, while grazers (>70 % C_4 diet) have $\delta^{13}C_{enamel}$ values higher than -2 ‰ (Cerling et al., 2003; Cerling & Harris, 1999; Uno et al., 2018). Any value in between is typical for a modern mixed feeder (>30 % C_3 and >30 % C_4 diet). On the other hand, the $\delta^{13}C_{enamel}$ values of carnivores are determined by the $\delta^{13}C_{enamel}$ values of their prey, with hardly any fractionation between the trophic levels (roughly 1 ‰; Bocherens & Drucker, 2003). This means that when analysing the enamel of a carnivore for stable carbon isotopes, it can indicate what type of prey (browser or grazer) it fed on. However, in complete C_3 environments, all modern herbivores will have a $\delta^{13}C_{enamel}$ value lower than -8 ‰. Due to the Suess effect, herbivores from the Eemian would have a $\delta^{13}C_{enamel}$ value of lower than -9 ‰.

Another effect that impacts the $\delta^{13}C$ of plants and animals is the so-called canopy effect. This effect states that below a closed canopy the plants are depleted in ^{13}C, so they have a more negative $\delta^{13}C$ value, because of two major factors. First, below a poorly ventilated canopy the CO_2 in the atmosphere is depleted in ^{13}C, due to CO_2 recycling from leaf litter (e.g, Medina & Minchin, 1980; Medina et al., 1986; Merwe & Medina, 1989). Second, below a canopy there is an overall depletion of CO_2 and a lack of light, which leads to a change in photosynthetic activity resulting in more negative $\delta^{13}C$ values (e.g., Broadmeadow et al., 1992; Gebauer & Schulze, 1991). The presence and degree of the canopy effect is the result of a combination of aspects influencing the two main factors, including air circulation and canopy complexity (Drucker et al., 2008). Not every forest will show a canopy effect in its $\delta^{13}C$ values, but when it is observed, it implies the presence of a mature, dense, complex forest (Drucker et al., 2008). This lower $\delta^{13}C$ value is also passed on up the food chain, but it may not affect the $\delta^{13}C$ values of all woodland-dwelling species to the same extent (Bonafini et al., 2013; Merwe & Medina, 1991).

Variation in $\delta^{13}C$ values within a single plant can be due to varying climate conditions over the year. For example, a higher temperature during the summer period is associated with a reduction of stomatal conductance in plants in order to decrease water loss (Farquhar et al., 1989; Hartman & Danin, 2010; Smedley et al., 1991). Stomata are the cell organs in the leaves or needles of plants that are responsible for the exchange of CO_2 and water between the plant tissues and the atmosphere.

The reaction of the stomata to temperature results in higher $\delta^{13}C$ values during the summer. In contrast, plants have more water loss in wet areas or during the growth/wet season, which results in lower $\delta^{13}C$ values (Kohn, 2010; Smedley et al., 1991). Related, water availability in the environment can also impact $\delta^{13}C$ values. In case water availability decreases, water-use efficiency of plants increases, which leads to an increase in $\delta^{13}C$ value of plants (Farquhar et al., 1989; Rao et al., 2017). In general, plants that are adapted to dry environments have higher $\delta^{13}C$ values than plants that are not.

Variation in $\delta^{13}C$ values can also occur between different plant species and between different organs of a single plant. Generally, woody plants (e.g., trees) have a higher $\delta^{13}C$ value (2 ‰ or higher) than herbaceous plants (e.g., grasses; Heaton, 1999). Different plant organs have different ratios of carbohydrates, proteins, and lipids, which have different $\delta^{13}C$ values (up to a couple permille), with carbohydrates typically the highest and lipids the lowest $\delta^{13}C$ (Heaton, 1999). Therefore, the $\delta^{13}C$ value of the plant depends on its composition and the measured organ. However, it should be noted that the variation caused by these climate and environmental conditions, as well as the species and organ differences, is very small compared (roughly 2 ‰; Heaton, 1999) to the difference in $\delta^{13}C$ values between C_3 and C_4 plants.

Stable carbon isotopes are measured in the structural CO_3 component of bioapatite (Kohn & Cerling, 2002). This component is present in the inorganic mineral phase of enamel, as explained in the previous chapter, but also collagen in bones and dentin. The values are measured against the standard VPDB (Vienna Pee Dee Belemnite). This standard is a virtual reference of the original carbon reference standard, called Peedee Belemnite (PDB; e.g., Brand et al., 2014). This standard was a calcium carbonate fossil from the Peedee formation in South Carolina, collected in the 1950s. However, the physical sample was exhausted by the end of the 1970s and replaced by VPDB in the early 1980s.

All in all, even though horses are considered grazers, with a diet of mainly grasses supplemented with a small percentage of shrubs, forbs, and herbs (e.g., Hoppe, Amundson, et al., 2004; Lazzerini et al., 2019), it is expected in this study to see $\delta^{13}C$ values corresponding with a complete C_3 diet. This is due to the fact that Germany, and thus the Neumark-Nord locality, experiences a climate that is too wet and does not sustain any C_4 or CAM plants.

4.4 Oxygen

Oxygen has three stable isotopes, ^{16}O, ^{17}O and ^{18}O. As with carbon, the lightest variant, ^{16}O, is the most common naturally-occurring stable isotope, representing around 99.76 % of all oxygen isotopes. ^{17}O is the least common naturally-occurring stable isotope with around 0.04 %, while ^{18}O accounts for

roughly 0.20 % (Nier, 1950). ^{17}O is can be used in oxygen isotope analysis, which is called triple isotope analysis (e.g., Gehler et al., 2016). However, this method is not employed in this study, and thus will not be discussed any further. Stable oxygen isotope analysis has a whole range of applications from reconstructing past environments to past culinary preparation techniques (Pederzani & Britton, 2019). In this study, the focus of the oxygen isotope analysis is on reconstructing seasonality at NMN2 during the Eemian.

Reconstructing seasonality based on $\delta^{18}O$ values works as follows: Local rainwater has a certain $\delta^{18}O$ value, which is dependent on a wide range of variables including the distance from its source area (Pederzani & Britton, 2019). However, seasonality is established on a local scale and the relative $\delta^{18}O$ values of winter compared to summer are more important than the absolute $\delta^{18}O$ values. In non-tropical regions, the temperature effect is the most important variable affecting local rain water $\delta^{18}O$ values. This effect says that the difference between winter and summer $\delta^{18}O$ values of precipitation is due to the fact that the isotopic fractionation during the condensation of rainwater is dependent on temperature (Pederzani & Britton, 2019, p. 79). This, in turn, results in higher $\delta^{18}O$ values of precipitation in summer compared to winter and thus a predictable seasonal $\delta^{18}O$ pattern for rainwater. In tropical regions, the amount effect is the most important variable affecting local rain water $\delta^{18}O$ values. However, I will not discuss this here as Neumark-Nord is located in a non-tropical region.

The $\delta^{18}O$ values of lakes, rivers, pools, or springs is partially dependent on the $\delta^{18}O$ values of precipitation but can deviate quite substantially due to, among other things, influxes of non-local water or evaporative enrichment (Pederzani & Britton, 2019). However, here, the small, shallow, calm pool Neumark-Nord 2 is studied, which will be mostly affected by evaporation. Based on the fact that ^{16}O is lighter than ^{18}O, this isotope will evaporate more quickly, meaning the pool water becomes depleted in ^{16}O and enriched in ^{18}O. In summer, when the temperature is higher, there is relatively more evaporation, and thus the $\delta^{18}O$ value of the water will be relatively high. In contrast, in winter the temperature is lower, there is less evaporation and thus the $\delta^{18}O$ value of the water will be lower than in summer. This results in a seasonal isotopic pattern of $\delta^{18}O$ values of the pool, with maximum $\delta^{18}O$ values in summer months, and minimum $\delta^{18}O$ values in winter months (figure 4.3; Pederzani & Britton, 2019). A study of the $\delta^{18}O$ values of mollusc shells from NMN2, as well as of modern precipitation and of a small lake located close to Neumark-Nord, shows that there would have been such a seasonal pattern visible in the $\delta^{18}O$ values of the pool water (Milano et al., 2020).

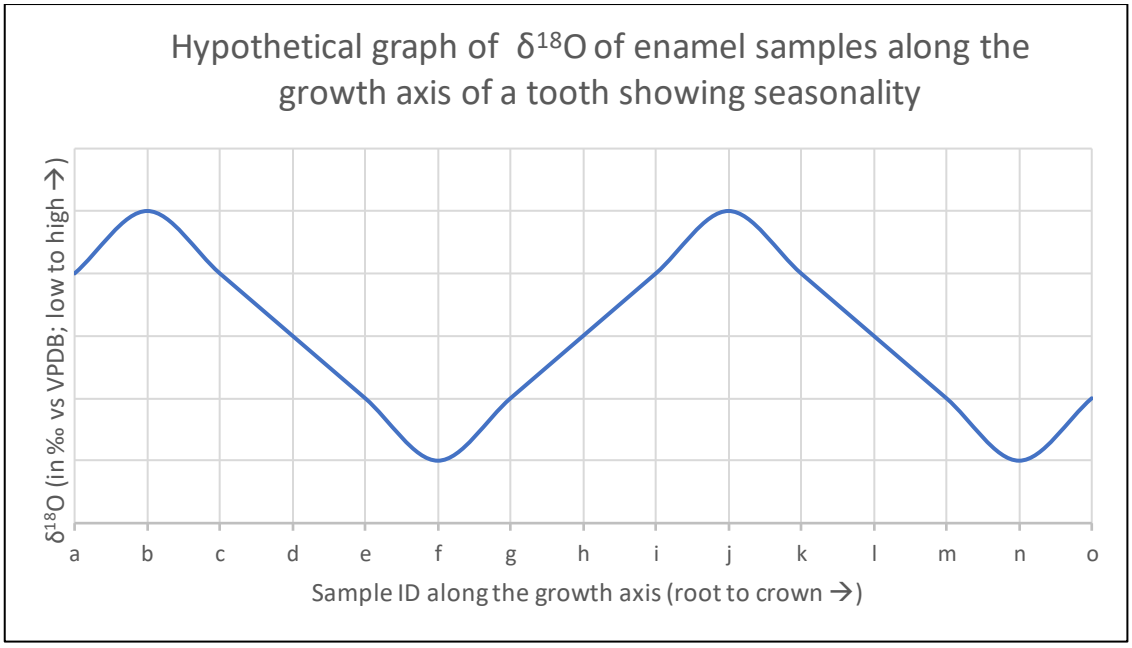

Figure 4.3: A hypothetical graph of $\delta^{18}O$ values showing seasonality. The peaks correspond to summer and the throughs to winter. In the hypothetical case that each summer has the same $\delta^{18}O$ value, each winter has the same value, and enamel mineralizes evenly, a $\delta^{18}O$ graph of equid enamel should look like this (figure by M. Vink).

To determine the $\delta^{18}O$ values of the NMN2 water, it is necessary to look at the $\delta^{18}O$ values of body water of animals who use this water as a drinking source. These values are dependent on the animal's habitat, climate (temperature, humidity), diet, drinking behaviour, and physiology (e.g., Bryant & Froelich, 1995; Kohn, 1996; Pederzani & Britton, 2019). However, it has been demonstrated that for large-bodied (>100 kg), obligate drinkers, which includes equids, the $\delta^{18}O$ values of their body water primarily reflect the $\delta^{18}O$ values of consumed water or drinking water, since this forms the largest proportion of their oxygen intake (Bryant & Froelich, 1995; Hoppe, 2006; Kohn, 1996). Obligate drinkers are animals that need to drink from a water source and are not able to get all of their water out of their diet. In order to determine the $\delta^{18}O$ values of body water, and thus of drinking water, it is necessary to look at the $\delta^{18}O$ values of bioapatite.

As explained above for carbon isotopes, there is an offset, due to fractionation, between the $\delta^{13}C$ values of the diet and the $\delta^{13}C$ values of the enamel. This is also the case between the $\delta^{18}O$ values of body water and the $\delta^{18}O$ values of bioapatite, including enamel. However, this is not as simple as with stable carbon isotopes and requires the following equation (Kohn & Cerling, 2002):

$$\delta^{18}O_{PO4} \approx 0.9 * \delta^{18}O_{bodywater} + 23 \quad (2)$$

This equation is an average used for the entire group of mammals. However, it can be different for any given species. There is an equation for horses specifically, which was also used in a recent paper on $\delta^{18}O$ values of horses at NMN2 (Britton et al., 2019). Because this study looks at equids from NMN2,

this horse specific equation will also be used in this study in order to be able to compare the results easily. This equation was first presented by Delgado Huertas et al. (1995, p. 4304) and improved upon by Pryor et al. (2014):

$$\delta^{18}O_{PO4} \approx 0.71 * \delta^{18}O_{bodywater} + 22.60 \quad (3)$$

As can be seen in this equation, the $\delta^{18}O$ values are measured in the PO_4 component, which is found in the inorganic mineral phase of bioapatite. When measured in this component, the values are determined by the reference standard called VSMOW (Vienna Standard Mean Ocean Water). This standard is a physical standard consisting of distilled ocean water from the equator and 180° longitude (e.g., Brand et al., 2014). It was first named SMOW (Standard Mean Ocean Water), but it was changed to VSMOW in 1976 to avoid confusion with the virtual SMOW scale.

It is also possible to measure $\delta^{13}C$ and $\delta^{18}O$ simultaneously in the structural CO_3 component, as will be done in this study. In this case, these values are determined against the standard VPDB and are thus different from the VSMOW values. It is possible to recalculate the $\delta^{18}O_{VPDB}$ values to $\delta^{18}O_{VSMOW}$ values using the International Union of Pure and Applied Chemistry (IUPAC) recommended formula (Brand et al., 2014; Kim et al., 2015), which is based on the equation listed in Coplen et al. (1983), in order to calculate $\delta^{18}O$ values of body water:

$$\delta^{18}O_{VSMOW} \approx 1.03092 * \delta^{18}O_{VPDB} + 30.92 ‰ \quad (4)$$

After this, it is also necessary to recalculate the carbonate (CO_3) $\delta^{18}O_{VSMOW}$ values to phosphate (PO4) $\delta^{18}O_{VSMOW}$, since the phosphate values are the ones necessary to calculate the $\delta^{18}O$ values of body water (equation 3). This recalculation has been recently re-established by Iacumin et al. (2022):

$$\delta^{18}O_{PO4} + 1 \approx 0.9787 * (\delta^{18}O_{CO3} + 1) + 0.0142 \quad (5)$$

All in all, a seasonal signal is expected to be visible in the $\delta^{18}O$ values of the enamel of the equids measured in this study, because of the position of the Neumark-Nord locality on the globe, which experiences a winter-summer seasonality. In addition, even though there can be considerable time lag present in the $\delta^{18}O$ values of enamel due to the mineralisation time (as explained in chapter 3), there have been plenty of studies using equid teeth to establish a seasonal cycle, to show that this is possible (e.g., de Winter et al., 2016; Nelson, 2005).

4.5 Nitrogen

Nitrogen has two stable isotopes, ^{14}N and ^{15}N. Comparable to both carbon and oxygen, the lightest isotope, ^{14}N, is the most naturally abundant accounting for 99.63 %, whereas ^{15}N accounts only for 0.37 % of all naturally occurring nitrogen (Robinson, 2001). The most important application of nitrogen stable isotope analysis is the investigation of the trophic level of animals. Trophic level indicates the position of a group of organisms who have a similar feeding strategy in the food web. So, in short, plants, which get their energy from the sun, have the lowest trophic level, while herbivores are a level above plants and carnivores in turn, occupy a level above herbivores. Nitrogen is a major nutrient and animals obtain it from their diet. Due to fractionation during metabolism (digestion) and the excretion of waste, an animal's $\delta^{15}N$ values are higher compared to the $\delta^{15}N$ values of the food they consume. On average, this difference is +2-5 ‰ based on large ecological studies and laboratory experiments (e.g., Bocherens & Drucker, 2003; Fox-Dobbs et al., 2007; Krajcarz et al., 2018; Leichliter and Lüdecke et al., 2023; Leichliter et al., 2021; Lüdecke and Leichliter et al., 2022; Schoeninger & DeNiro, 1984).

In a terrestrial food web, plants form the lowest trophic level, as mentioned above. Unlike carbon, which plants get from the air, they get their nitrogen typically from the soil (Robinson, 2001). Nitrogen in soils is derived from three main sources of which ammonium from biological fixation of atmospheric nitrogen gas is the most important (Ostrom & Ostrom, 1998). The $\delta^{15}N$ values of plants are affected by the $\delta^{15}N$ values of the soil they grown on (Codron et al., 2005). These $\delta^{15}N$ values are correlated with two aspects of the local climate, mean annual precipitation (MAP) and mean annual temperature (MAT; Amundson et al., 2003; Evans, 2001; Robinson, 2001). The $\delta^{15}N$ values of soil decrease with increasing MAP and decreasing MAT and thus, wetter and colder areas have lower $\delta^{15}N$ values (Amundson et al., 2003; Craine, Elmore, et al., 2009).

The $\delta^{15}N$ values of plants are generally lower than the $\delta^{15}N$ values of the soil (e.g., Amundson et al., 2003; Craine, Elmore, et al., 2009; Evans, 2001; Handley et al., 1999). This is due to fractionation occurring during the uptake and assimilation of inorganic soil nitrogen into organic nitrogen in the plant tissues (Kalcsits et al., 2014). The first rule of fractionation is applicable, since the uptake involves a process in which ^{14}N reacts faster, as this is the lighter isotope, and the plant tissue thus becomes enriched in ^{14}N and depleted in ^{15}N compared to the soil (Evans, 2001). Furthermore, the difference between $\delta^{15}N$ values of the soil and $\delta^{15}N$ values of the plant is also (mostly) correlated with MAT. The difference in $\delta^{15}N$ values increases with decreasing MAT (Amundson et al., 2003). So, in colder ecosystems, the difference between soil and plant $\delta^{15}N$ values is larger than in warmer ecosystems. In addition, on a global scale, leaf (or foliar) $\delta^{15}N$ values are correlated with MAP in the same way as the soil (Handley et al., 1999), so foliar $\delta^{15}N$ decreases with increasing MAP. However, at a smaller

regional or landscape scale, this pattern does not hold true; wet spots, topographical depressions in a landscape, have a higher $\delta^{15}N$ value in their soil and plants than surrounding dry areas (Handley et al., 1999). Lastly, even though foliar $\delta^{15}N$ is usually lower than soil $\delta^{15}N$, they do show a positive correlation (Craine, Ballantyne, et al., 2009; Craine, Elmore, et al., 2009).

Bulk soil contains many different forms of nitrogen, but only three of them are available to plants: ammonium (NH_4^+), nitrate (NO_3^-), and dissolved organic nitrogen (DON). This means that the $\delta^{15}N$ value of bulk soil is different from the $\delta^{15}N$ value of the nitrogen source of plants, because these three forms represent only a fraction of the nitrogen in bulk soil, and thus also influence the $\delta^{15}N$ of bulk soil relatively little (Marshall et al., 2007). Discrimination between N source/supply and plant N is often only observed when the nitrogen demand of the plant is low compared to the nitrogen supply (e.g., Evans, 2001; Kalcsits et al., 2014). In other words, when nitrogen supply increases or nitrogen demand decreases, discrimination, which is the difference between $\delta^{15}N$ values of source nitrogen and those of plant nitrogen (also written as $\Delta^{15}N$), increases. When nitrogen supply decreases or nitrogen demand increases, discrimination decreases (Kalcsits et al., 2014). Since in natural ecosystems nitrogen demand of plants usually exceeds nitrogen supply, $\delta^{15}N$ values of plants are generally good approximations of the $\delta^{15}N$ values of the available nitrogen sources, but not of bulk soil, as explained above (Marshall et al., 2007, p. 36).

Many plants show a distinct preference for one of the three sources. The preference of plants for the rates of ammonium (NH_4^+) vs. nitrate (NO_3^-) they take up can change depending on environmental conditions (Marshall et al., 2007). The $\delta^{15}N$ values of ammonium vs. nitrate can also differ based on certain processes, and thus the $\delta^{15}N$ values of plants grown on the same soil can differ if they have different nitrogen source preferences. For example, in soils with high nitrification rates, ammonium will be enriched in ^{15}N, and thus have a higher $\delta^{15}N$ value, than nitrate (e.g., Marshall et al., 2007; Schmidt & Stewart, 2003). Nitrification is the process of converting ammonia into nitrate. This process has a significant isotope effect, which follows the first rule of fractionation, where the light isotopes react first and form a product (nitrate) that is depleted in ^{15}N compared to the source (ammonium). Thus, in a soil with high nitrification rates, the $\delta^{15}N$ of plants, which preferentially take up ammonium, will be higher than plants that take up relatively more nitrate.

Denitrification, the process of converting nitrate into gaseous nitrogen, mainly N_2 or N_2O, is also associated with the same kind of isotopic discrimination, where the product (gaseous nitrogen (N_2 or N_2O)) is depleted in ^{15}N and the source (soil ammonium (NH_4^+)) is enriched in ^{15}N (e.g., Szpak, 2014). So, in soils where denitrification occurs, the plants that prefer ammonium have a higher $\delta^{15}N$ value. This process is likely to take place in swampy shallow water due to the high input of organic

matter (Muzuka, 1999). It is thus possible that NMN2 and its surrounding soil and vegetation was affected by denitrification. In circumstances of ammonium toxicity, greater discrimination has been observed between the $\delta^{15}N$ values of ammonium and plants than between nitrate and plants (Kalcsits et al., 2014). In these cases, plants will have lower $\delta^{15}N$ values when they take up more ammonium than nitrate.

The amount of salt in the soil can also impact plant $\delta^{15}N$ values. This can take the form of sea-spray, which contains nitrate enriched in ^{15}N and thus results in a higher $\delta^{15}N$ of plants (Heaton, 1987). High salinity in the soil, potentially caused by a nearby alkaline lake, is also correlated with enriched $\delta^{15}N$ values of plants (Muzuka, 1999), as are salt marches (Guiry et al., 2021). Seeing as the NMN2 pool contained brackish water at times (Bakels, 2012; chapter 2), the higher salinity could potentially have enriched the $\delta^{15}N$ values of the plants in the surrounding area.

Microhabitat, wet/dry seasonality, and species can have an effect on $\delta^{15}N$ values of plants, and thus also grasses. This was shown by Codron et al. (2005), who measured $\delta^{13}C$ and $\delta^{15}N$ values of different plant types (grasses, trees, and forbs) within the savanna biome of Kruger National Park (KNP) in South Africa. There was a relatively wide range of $\delta^{15}N$ values within each plant type. However, the plant types (grasses vs shrubs vs trees) did not differ significantly from each other in their $\delta^{15}N$ values. In addition, the $\delta^{15}N$ values of all groups followed similar geographical trends corresponding to their different microhabitats. The mean $\delta^{15}N$ value of the different microhabitats differed up to 4 ‰ between them and is most likely primarily influenced by local environmental factors, like water availability/precipitation, and soil type (Codron et al, 2005). This shows that the microhabitat can influence the $\delta^{15}N$ value of plants to a relatively large degree and that it is therefore important to establish a $\delta^{15}N$ baseline for each site/habitat.

All plant $\delta^{15}N$ values combined for KNP showed seasonal shifts, where the wet season showed higher $\delta^{15}N$ values than the dry season (Codron et al., 2005). This is mostly likely linked to the increase in water availability in the soil and thus soil denitrification and nitrogen loss, which drives the local $\delta^{15}N$ values upwards during the wet season (e.g., Lazzerini et al., 2019; Szpak, 2014). However, it needs to be noted that the KNP, which experiences a wet/dry seasonality based on changes in rainfall amounts, is different from the area of the present study, which experienced a winter/summer seasonality based on changes in temperature. In addition, the grasses studied at KNP consisted of only C_4 grasses, so their $\delta^{15}N$ range (up to 6 ‰ difference between species) reported by Codron et al. (2005) may differ from the range of C_3 grasses, which are the only type of grasses present at NMN2, as mentioned above.

The next part will discuss plant physiology in great detail. It will show that there is quite some variation in plant $\delta^{15}N$ values and thus that the $\delta^{15}N$ values of the diet of herbivores is not only dependent on the environment, but also on what type, species, and parts of plants these herbivores eat. This could lead to variation in the values observed in the equid tooth enamel and will be discussed in relation to the results of this study in chapter 7.

The $\delta^{15}N$ values of different plant types and/or species can not only differ from each other due to environment and soil features, but also due to certain aspects of plant physiology. One of these aspects is the symbiotic relationship with mycorrhizal fungi. Mycorrhizal fungi colonise the root system of a plant and supplies it with soil nutrients, including nitrogen. There are three main types of mycorrhizal fungi: arbuscular or endomycorrhizal, ectomycorrhizal, and ericoid mycorrhizal, which can all form relationships with a different group of plant species. The group of plant species, which cannot form a relationship with a mycorrhizal fungus, are called nonmycorrhizal plants. Arbuscular mycorrhizal fungi are by far the most common and can form relationships with up to 90 % of terrestrial plant species, including grasses. All these different fungi groups have a different impact on the foliar $\delta^{15}N$ values of plants. Generally, mycorrhizal plants are more depleted in ^{15}N, and thus have a lower $\delta^{15}N$ values, than nonmycorrhizal plants, with ericoid plants having the lowest $\delta^{15}N$ values, roughly 6 ‰ lower than nonmycorrhizal plants, then ectomycorrhizal plants, and then arbuscular plants being depleted by around 2 ‰ compared to nonmycorrhizal plants (Craine, Elmore, et al., 2009; Schmidt & Stewart, 2003).

Another aspect of plant physiology that can lead to differences in $\delta^{15}N$ values is the ability to fix N_2 from the atmosphere into a more useful form of nitrogen for the plant. These nitrogen-fixing plants have a symbiotic relationship with specific bacteria which are capable of converting N_2 into NH_3 (e.g., Stewart, 1977). There is hardly any discrimination during this process of fixation and therefore, the $\delta^{15}N$ of nitrogen-fixing plants should be highly similar to the $\delta^{15}N$ of atmospheric N_2, which is by definition 0 ‰ (Handley & Raven, 1992; Robinson, 2001). Generally, this means that the $\delta^{15}N$ values of N-fixing plants are lower than of non-N-fixing plants in a specific ecosystem (Codron et al., 2005; Dijkstra et al., 2003). A lot of leguminous plants and quite some tropical grass species are N-fixing plants (e.g., Boddey & Dobereiner, 1995; Döbereiner, 1977; Stewart, 1977). It is not likely that N-fixing played a large role for the grasses at NMN2.

Plant type can also potentially influence $\delta^{15}N$ value. For example, a paleoclimatic reconstruction of Beringian Megafauna used Alaskan vegetation values to distinguish grasses/sedges and herbs, with a slightly higher $\delta^{15}N$ value, from shrubs/trees, with a lower $\delta^{15}N$ value (Fox-Dobbs et al., 2008). Bonafini et al. (2013) even showed relatively large variation in $\delta^{15}N$ between four grass species as well as between individual plants from the same species.

Variations in $\delta^{15}N$ values can be present between different parts/organs of a plant. For example, in controlled experiments, the $\delta^{15}N$ value of leaves can be 3-7 ‰ higher than roots (e.g., Evans et al., 1996). This variation between different plant parts can be due to the loss of nitrogen in specific organs, reallocation of nitrogen, or a difference in nitrogen assimilation patterns between organs (Evans, 2001). Field studies point towards the $\Delta^{15}N$ of leaves vs root being ecosystem dependent. For example, Dijkstra et al. (2003) looked at $\Delta^{15}N$ of leaves vs roots in a forest compared to a meadow. They found that there were significant differences in foliar $\delta^{15}N$ compared to root $\delta^{15}N$ in almost all plant groups studied, but the range of $\Delta^{15}N$ was relatively small (-0.97 to +0.86 ‰). Some species were depleted in foliar $\delta^{15}N$ compared to the roots, while others were enriched in foliar $\delta^{15}N$. In addition, they show that the $\Delta^{15}N$ of forbs in the forest differed significantly from the ones in the meadow.

When focussing on grasses specifically, Craine et al. (2005) showed that there is no uniform global relationship between root and leaf traits that is consistent across four different environments. The only global relationship noted is the strong positive correlation between leaf and root nitrogen concentrations. C_4 grasses in South Africa showed significantly lower $\delta^{15}N$ values in their roots compared to the seeds (Codron et al., 2005). Leaves and stems had intermediate $\delta^{15}N$ values with considerable overlap with both roots and seeds. All this is to say that the differences in leaf vs root $\delta^{15}N$ in grasses, and other plants, at NMN2 are difficult to determine. A generalised overview of the different processes affecting nitrogen cycling in plants, as explained here, is visible in figure 4.4.

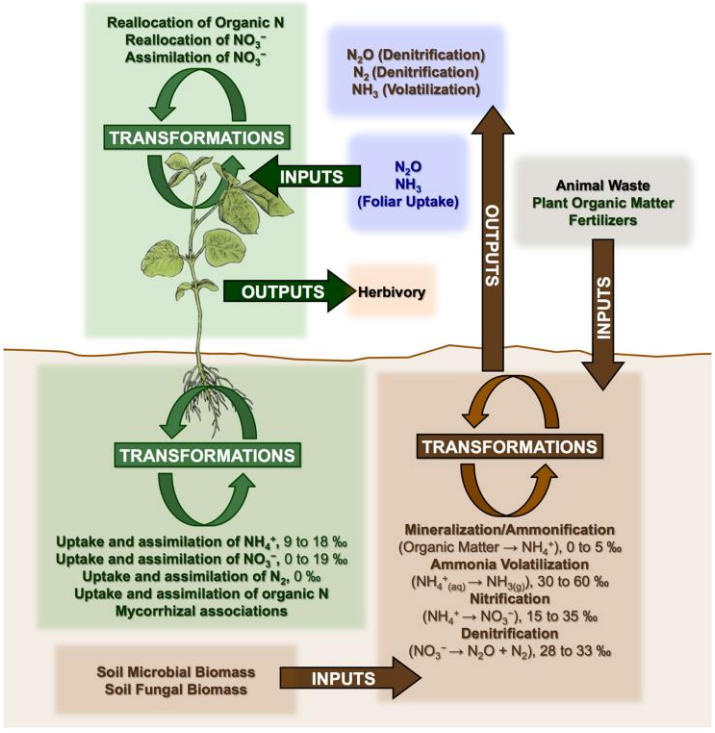

Figure 4.4: Generalized overview of all processes that affect nitrogen cycling in plants and soils. For some processes, fractionations are given according to Robinson, 2001 (Szpak, 2014, figure 3, p. 4)

The $\delta^{15}N$ values of an animal are higher than their diet, as explained above. The fractionation during metabolic processing thus preferentially includes ^{15}N in the consumers tissues and excretes ^{14}N as waste (Robinson, 2001). This results in a depletion of ^{15}N, and thus a lower $\delta^{15}N$, in waste material, and an enrichment, and thus a higher $\delta^{15}N$, in the consumers tissues. This fractionation occurs during amino acid synthesis and is dominated by the second rule of fractionation, which states that the heavy isotopes concentrate on the side of the reaction where bonds are strongest (e.g., Adams & Sterner, 2000; Gaebler et al., 1966; Gannes et al., 1998).

Seeing as animal $\delta^{15}N$ values are dependent on their diet, herbivore $\delta^{15}N$ values will vary with the plant, and thus also soil, $\delta^{15}N$ values between different climates and (micro)habitats. It is therefore important to keep in mind that the 2-5 ‰ stepwise trophic level separation does not correspond to the same absolute $\delta^{15}N$ values across the world, but to the $\delta^{15}N$ values within each specific ecosystem (Amundson et al., 2003). For example, African herbivores will have different $\delta^{15}N$ values compared to European herbivores, even though both of them are part of the same, low trophic level, just in different ecosystems. Despite the wide potential variations in $\delta^{15}N$ values of plants, as detailed above, the 3-5 ‰ trophic level separation seems to hold in well-constrained ecosystems (e.g., Lüdecke and Leichliter et al., 2022).

As explained, there are variations in $\delta^{15}N$ values in different ecosystems. So, when studying a trophic food web, it is vital to understand the baseline $\delta^{15}N$ values and its variations of that specific habitat (e.g., Codron et al., 2005). However, since this is nearly impossible for past ecosystems, analysing the $\delta^{15}N$ values of enamel of different species of herbivores can provide a baseline for the lowest trophic level in that habitat. It preferable to include herbivores of different diet types, both browsers and grazers, to encapsulate the complete $\delta^{15}N$ variation within the lowest trophic level of that ecosystem. This is because browsers mainly feed on trees and grazers mainly on grasses. Since these different plant types potentially have different $\delta^{15}N$ ranges, browsers may differ slightly in their $\delta^{15}N$ values from grazers. For example, even though the browsers and grazers in Gorongosa National Park, Mozambique, do not differ significantly in their $\delta^{15}N$ values, as expected, the mean $\delta^{15}N$ for each group is slightly different, which also influences the mean and the range for all herbivores together (Lüdecke and Leichliter et al., 2022). The complete range observed in the $\delta^{15}N$ values of the herbivores at Gorongosa National Park is 4.3 ‰ (Lüdecke and Leichliter et al., 2022), which corresponds to the 4 ‰ baseline variation in plant $\delta^{15}N$ values in the savannah biome of Kruger National Park reported by (Codron et al., 2005).

It has been suggested that not only climate and habitat baseline variation affect $\delta^{15}N$ values of animals, but that digestive physiology and water dependence do as well (Ambrose, 1991; Cantalapiedra-Hijar

et al., 2015; Hartman, 2010; Sealy et al., 1987). However, in a recent study on a well-constrained modern African ecosystem, no correlation between herbivore diet groups (browsing, grazing, mixed-feeding), digestive physiology (ruminant vs. non-ruminant) or water dependence and $\delta^{15}N$ values was found (Lüdecke and Leichliter et al., 2022). Furthermore, it has been shown that starvation has an effect on $\delta^{15}N$ values (e.g., Beaumont & Montgomery, 2016; Doi et al., 2017). The longer the starvation period lasts, the more $\delta^{15}N$ values increase due to an internal recycling of nitrogen isotopes. However, this should not affect the present study, since starvation periods usually have a relatively short duration, and enamel mineralization has a relatively long duration. Another potential factor influencing $\delta^{15}N$ values of animal tissue is seasonality. Lazzerini et al. (2019) showed that the $\delta^{15}N$ values of tail hair of modern domestic horses from Mongolia were influenced by seasonality (most likely associated with an increase in melt water) and seasonal diet preferences. Lastly, the canopy effect does not seem to influence $\delta^{15}N$ values of animal tissues (Bonafini et al., 2013).

Caut et al. (2009) reviewed a multitude of studies concerning the trophic enrichment factor or discrimination factor for both $\delta^{13}C$ and $\delta^{15}N$ in animals. This factor is the difference in $\delta^{13}C$ or $\delta^{15}N$ values between the diet and the animal and is usually shown as $\Delta^{13}C$ or $\Delta^{15}N$. So, the average of $\Delta^{15}N$, as mentioned above, is 2-5 ‰. Caut et al. (2009) showed that $\Delta^{15}N$ is significantly affected by the studied tissue and some of the tissues in turn by the isotopic ratios of the diet. They provide a decision model, in which each consumer group (mammals, bird, fish, invertebrates) and each tissue (liver, muscle, blood, hair, etc.) has its own regression equation for both $\Delta^{13}C$ and $\Delta^{15}N$, which includes the diet isotopic ratios if this affects that specific tissue. However, the decision diagram does not include either collagen, dentin, or enamel as a tissue in the mammal group. Therefore, in this study, the trophic enrichment factor ($\Delta^{15}N$) of 3-5 ‰ will be maintained, based on studies of $\delta^{15}N$ values in enamel in both modern and fossil material (Leichliter and Lüdecke et al., 2023; Lüdecke and Leichliter et al., 2022).

In addition, a laboratory study of $\Delta^{15}N$ in rats in different tissues showed that the $\Delta^{15}N$ between tissues and a diet based on animal proteins was lower than the $\Delta^{15}N$ between tissues and a plant protein-based diet (Poupin et al., 2011). This is likely due to plant proteins containing a lower amount of essential amino acids. Essential amino acids are amino acids that animals cannot produce themselves and thus they need to acquire them from their diet. Non-essential amino acids can be broken down and built into new non-essential amino acids by the body. So, foodstuffs with less essential amino acids (like plant proteins) are thus subjected to more digestion (break down of the amino acids) and thus more fractionation compared to foodstuffs with more essential amino acids (like animal proteins; Gaebler et al., 1966; Silfer et al., 1992). This results in a higher $\delta^{15}N$ compared to

the diet and thus a higher $\Delta^{15}N$ between plant-based diets and their consumers than in animal-based diets and their consumers. This is relevant for trophic level studies, since this might influence the 3-5 ‰ trophic spacing. However, since the present study only focusses on herbivores, this metabolic mechanism is not of high importance and will not be explored any further.

As explained in chapter 3, nitrogen isotopes in the fossil record are usually measured from the organic nitrogen in bone- and dentine-derived collagen, when it is well-preserved, which typically means less than 100,000 years old (Bocherens & Drucker, 2003; Britton et al., 2012; Jaouen et al., 2019). Older samples are much harder to get an original nitrogen signal from, since the organic material (mostly collagen) in bone and dentin is not very resistant to diagenetic alterations over time. This is due to the fact that bone is a porous material, has a large surface-to-volume ratio, and the bioapatite nanocrystals in its mineral phase have low crystallinity, which means they are not arranged in a highly regular manner (e.g., Clementz, 2012; Keenan, 2016), and therefore the organic matter in bone and dentin is more susceptible to diagenesis. In contrast, as explained previously, enamel is much more highly mineralized and more resistant to degradation. In this study, a new method (*oxidation-denitrification*) will be employed to measure the $\delta^{15}N$ of the organic nitrogen trapped in the mineral lattice of the enamel. The $\delta^{15}N$ values will be determined against the standard of atmospheric air (Air).

In this study, several individuals of a single herbivore species, equids from Neumark-Nord 2, were analysed. The goal of the nitrogen isotope analysis here is thus not to reconstruct the food web at NMN2, which is the usual application of such an analysis. This research focused on serially-sampled teeth and how the $\delta^{15}N$ values of an herbivore, and thus the species that is used as part of baseline for $\delta^{15}N$ values in past ecosystems when present, change during the development of the enamel. The combination of the nitrogen isotope analysis with stable carbon and oxygen isotope analysis will show if the $\delta^{15}N$ values observed in enamel over time are correlated to $\delta^{13}C$ and/or $\delta^{18}O$ values and then may likely be affected by the same factors. For example, if $\delta^{15}N$ values show a strong correlation with $\delta^{18}O$ values, it is likely that seasonality has an influence on the $\delta^{15}N$ values in enamel, as it does on $\delta^{15}N$ values in hair (Lazzerini et al., 2019). If the $\delta^{15}N$ values correlate with the $\delta^{13}C$ values, they are likely affected by the same factors associated with plants in the diet, since horses acquire both types of isotopes from their diet. This will influence future studies on fossil enamel $\delta^{15}N$ analysis, whether it be on sampling strategy or on interpretation of herbivore $\delta^{15}N$ values.

4.6 Conclusion

Stable isotope analysis has a plethora of applications, ranging e.g., from distinguishing C_3 from C_4 plants in the diet using stable carbon isotopes, to reconstructing the temperature based on stable oxygen isotopes, to reconstructing a trophic food web based on nitrogen isotopes. Stable isotope ratios are denoted using the δ-notation and expressed in ‰ compared to a standard. This standard is VPDB for stable carbon isotopes and in some cases also for stable oxygen isotopes. VSMOW is the most used standard for stable oxygen isotopes and Air is the standard used in nitrogen isotope analysis. The values of $\delta^{13}C$, $\delta^{18}O$, and $\delta^{15}N$ are dependent on a number of factors, and are often specific for each ecosystem. It is therefore important to be aware of the factors that could cause variation within the studied ecosystem. $\delta^{15}N$ variations in animal tissues are affected by the broadest range of factors, including soil type, plant species, nitrogen source, mean annual temperature, mean annual precipitation, starvation, and more. However, it is yet unknown if, and how, winter-summer seasonality impacts $\delta^{15}N$ in enamel.

5 Research Methods

5.1 Introduction

In this chapter, I will present the processes of sample selection and preparation. Then, I will provide a short overview of the cold trap method for $\delta^{13}C$ and $\delta^{18}O$ analysis. Next, I will discuss, in more detail, an overview of the *oxidation-denitrification* method used for $\delta^{15}N$ analysis. Lastly, I will shortly go into trace element analysis, which was performed on the samples of a single tooth by T. Tacail. All of the sample preparation and isotope analyses were done at the Max Planck Institute of Chemistry in Mainz, Germany; the trace element analysis was done at Johannes Gutenberg-Universität in Mainz, Germany; specimens are housed at the MONREPOS, Neuwied, Germany.

5.2 Sample selection

For this research, 14 fossilized *Equus sp.* teeth from NMN2 were selected. Equids were chosen mainly because of their great availability at NMN2 (Kindler et al., 2014). In addition, horses were present at NMN2 all year round, which indicates that they reflect the isotopic conditions of the immediate environment surrounding the pool (Britton et al., 2019). All horses at NMN2 are caballoid horses (true horses) and their larger, less gracile molars indicate that they belong to the Caballine clade (Britton et al., 2012, p. 170). The longest, fully erupted teeth available were selected (7 - 10 cm in length) in order to capture data over the longest possible span of time. As explained in chapter 3, equid teeth wear down during life, so the selection of long teeth with little wear indicates that they belonged to young individuals.

All of the teeth are third molars, which means there is no weaning signal, as explained in the chapter 3. Eight of the molars are left maxillary molars, two are right maxillary molars, one an undetermined maxillary molar, and three right mandibular molars. Left maxillary molars were mostly selected to ensure analysis of different individuals. However, due to the limited number of teeth in the primary selection, third molars from other positions were added. All of these added molars were found in areas of the excavation clearly separated from the left maxillary molars selected before (see figure 5.1). As discussed in chapter 2, there were very little post-depositional processes occurring at NMN2 and thus, it is assumed that the separated teeth do not belong to the same individual (MNI = 14).

The teeth all have an official collection identification number, but were renamed for this research with an MPIC ID for simplicity (table 5.1). In the rest of this paper, the teeth will be referred to by their MPIC ID.

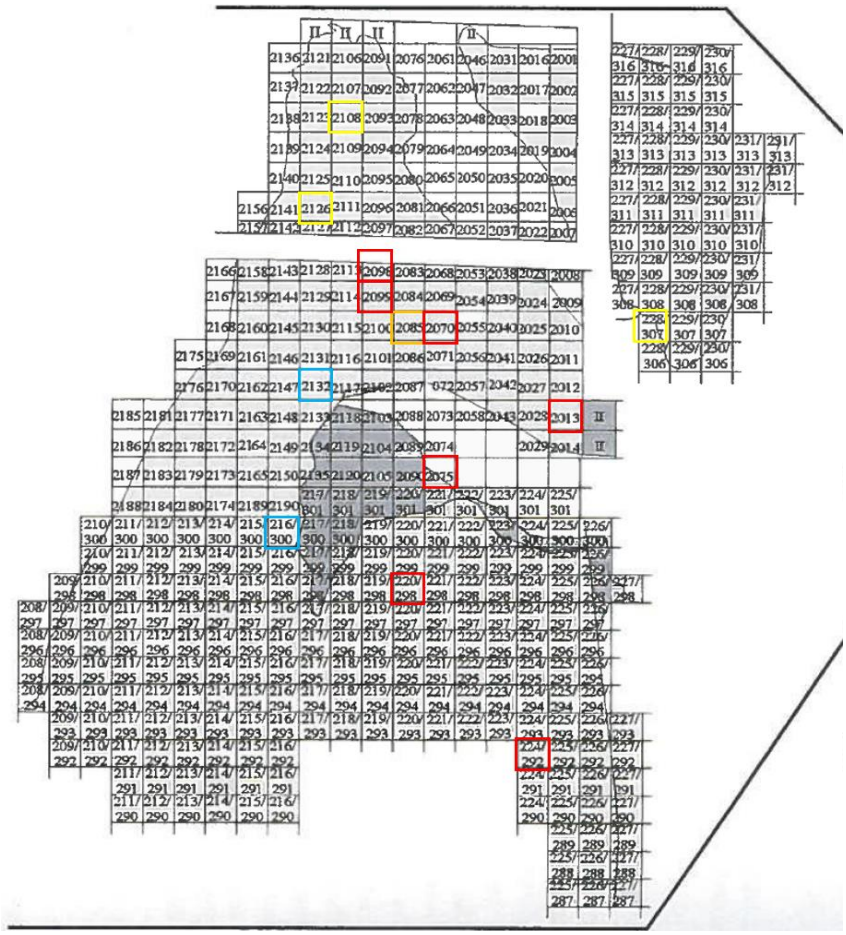

Figure 5.1: Excavation map of Neumark-Nord 2. The grid covers over 30 m from top to bottom. The squares where the teeth were found are highlighted (Red = superior left; Blue = superior right; Yellow = inferior right; Orange = superior of unknown side; after Kindler et al, 2014, p. 198).

Table 5.1: Basic information of each selected equid tooth. The square corresponds to the square of the excavation the tooth was found (see figure 5.1 for an excavation map). Tooth NMN-125 was found in HP10, which is a profile and not a square, and is thus also not a square, and is thus also not on the excavation map. Sup and Inf corresponds to superior (maxillary) and inferior (mandibular) molars respectively and side indicates the side of the jaw the molar is from. The teeth are colour coded to correspond with the colours of the excavation grid above in figure 5.1

Collection ID	MPIC ID	Find layer	Square	Sup or Inf	Side
NN2/2/14712	NMN-120	NN2/2b	2132	Sup	Right
NN2/2/22451	NMN-121	NN2/2b	220/298	Sup	Left
NN2/2/19018	NMN-122	NN2/2b	2075	Sup	Left
NN2/2/10135	NMN-123	NN2/2b	2085	Sup	Unknown
NN2/2/13833	NMN-124	NN2/2b	2126	Inf	Right
NN2/2/33160	NMN-125	NN2/2b	HP10	Sup	Left
NN2/2/32108	NMN-126	NN2/2b	224/292	Sup	Left
NN2/2/2720	NMN-127	NN2/2b	2013	Sup	Left
NN2/2/20372	NMN-128	NN2/2b	216/300	Sup	Right
NN2/2/10941	NMN-129	NN2/2	2098	Sup	Left
NN2/2/11096	NMN-130	NN2/2b	2099	Sup	Left
NN2/2/11938	NMN-131	NN2/2b	2108	Inf	Right
NN2/2/8818	NMN-132	NN2/2b	2070	Sup	Left
NN2/2/28869	NMN-133	NN2/2b	228/307	Inf	Right

5.3 Sample preparation

As explained in chapter 3, enamel maturation can result in significant time averaging of the isotopic signal. This fact can be partly mitigated by sampling the tooth in lines perpendicular to the growth direction to collect a sample over the smallest time period possible (Hoppe, Stover, et al., 2004; Passey & Cerling, 2002). However, there is still time averaging present since it can take up to a couple months for a small area of enamel to be fully mineralized from the EDJ (enamel-dentine junction) through to the outer layer.

The sampling area on each tooth was selected based on the thickness of the enamel. The enamel is thickest on the buccal and lingual side of the molar. Of these sides, the one with the least breakage and/or longest enamel cover was chosen for each tooth. Next, that area was cleaned of all cementum by using a Dremel with an abrasive stone head (silicon carbide grinding stone or aluminium oxide grinding stone). This material is not hard enough to flake off any enamel, which means the tooth could be cleaned thoroughly. The samples were collected in lines perpendicular to the growth direction, starting close to the root (figure 5.2), using a Dremel with a diamond-studded drill bit (2 mm diameter). Each sample was assigned an alphabetical sample ID based on the MPIC ID assigned to the tooth (e.g., NMN-120a, NMN-120b, NMN-120c, etc.). Between 13 and 26 samples were taken per tooth and collected in 4 ml combusted glass vials. To run carbon, nitrogen, and oxygen analyses in duplicate as well as to have enough material for other isotope analyses, e.g., calcium, strontium, and zinc isotopes, a minimum of 32 mg enamel powder per sample was collected. In total, 259 samples were collected from the fourteen teeth.

Table 5.2 shows the maximum length of each tooth and the maximum length of each tooth that was sampled, which is at least 10 mm shorter than the maximum length of each tooth. This is due to the enamel not extending completely along the maximum length of the tooth, the enamel being broken or damaged at either end of the tooth, and/or the side of the tooth that was sampled, not extending over the maximum length of the tooth.

5.4 Carbon and Oxygen analysis

All the collected samples were run for carbon and oxygen isotopes using a relatively new method of continuous-flow mass spectrometry called the cold trap method (Vonhof, de Graaf, et al., 2020). The carbonate in the bioapatite of the enamel is measured in the form of CO_2. For this method only between 70 and 100 µg of enamel powder is needed. The powder was directly weighted into a 12 ml glass exetainer vial with a septum. This method is fully automated and uses a Thermo Delta-V mass spectrometer in continuous flow configuration. It is directly interfaced with a GasBench II gas preparation unit, which has an integrated pneumatically operated cold trap system. First, the vials

Figure 5.2: Tooth NMN-130 before (a) and after (b) sampling. Scale in cm. Letters of samples on the right side. Lines from sample NMN-130a, NMN-130n, and NMN-130z to their respective samples (photographs by M. Vink).

Table 5.2: The maximum length of each tooth and the maximum length that was sampled.

MPIC ID	Max length (mm)	Max length sampled (mm)
NMN-120	80	70
NMN-121	91	68
NMN-122	79	63
NMN-123	83	70
NMN-124	76	60
NMN-125	89	76
NMN-126	80	64
NMN-127	75	51
NMN-128	85	67
NMN-129	87	72
NMN-130	92	84
NMN-131	84	71
NMN-132	95	83
NMN-133	82	68

containing the samples and standards are flushed with ultrapure helium, to make sure there is no more atmospheric CO_2 in the vial. Next, the enamel powder is dripped with acid (> 99 % H_3PO_4) to digest the solid bioapatite structural carbonate into measurable CO_2 gas, which takes 90 min. at 70 °C. Lastly, the sample gas is fed through the cold trap, where the CO_2 is cryogenically focused by cooling the trap with liquid N_2 for 6 to 7 min. This is done to separate the CO_2 from the other gasses present in the sample vial. After the cooling, the cold trap is lifted out of the liquid N_2 and the sample gas is sent through a standard Poraplot-Q Gas Chromatography (GC) column and carried to the mass

spectrometer. The carbon and oxygen isotope values are measured in a single peak, preceded by five reference gas peaks (Vonhof, de Graaf, et al., 2020).

With each batch, five different standards and five in-line blanks were included. All standards used are listed in table 5.3. Three of these are NBS18, NBS120c, and IAEA-603, of which two (NBS18 and IAEA-603) are internationally certified carbonate ($CaCO_3$) standards and one (NBS120c) is an internationally certified rock phosphate standard. The other two are VICS and AG-Lox, which are in-house standards. VICS is a carbonate standard (Carrara marble) used in several labs. AG-Lox is an enamel standard collected from the molar of an adult modern African elephant (*Loxodonta africana*; Leichliter et al., 2021). The AG-Lox standard was used to correct the isotope measurement of the equid samples, because both it and the sample are bioapatite, while all the other standards are pure carbonate or rock phosphate powders (Vonhof, de Graaf, et al., 2020).

In some of the later runs a new, not yet established, enamel in-house standard was included for the first time. This standard is called Mammy and the first values are reported in table 5.3. It was collected from the fossilized molar of a juvenile mammoth (*Mammuthus sp.*) from Siberia. This standard was not used to correct the samples analysed in this research. However, in the future it will be used together with AG-Lox to establish a two-point correction for carbon and oxygen isotopes analysis of bioapatite structural carbonate.

The measured stable carbon and oxygen values were normalized to Vienna Pee Dee Belemnite (VPDB). All samples were measured in duplicate. As a quality control, if the standard deviation of either the $\delta^{13}C$ value or the $\delta^{18}O$ value of a sample was above 0.5 ‰, the sample was measured in triplicate or more if necessary (appendix B). A total of 19 different batches were run with the cold trap, between the 7th of May 2022 and the 7th of July 2022. Each batch included between 20 and 35 enamel samples, 36 standards for batches excluding Mammy (11 AG-Lox, 11 VICS, 6 IAEA-603, 5 NBS-120c, and 3 NBS-18), 38 standards for batches including Mammy (11 AG-Lox, 11 Mammy, 5 VICS, 6 IAEA-603, and 5 NBS-120c), and 5 in-line blanks. The overall analytical uncertainties are better than 0.14 ‰ for $\delta^{13}C_{enamel}$ and 0.18 ‰ for $\delta^{18}O_{enamel}$ (1σ standard deviation of AG-Lox within batches). Carbonate contents of samples were calculated based on the standard vs sample total peak area ratios, where AG-Lox has a 7.5 % structural carbonate content (after Vonhof, Tutken, et al., 2020).

5.5 Nitrogen analysis

The cleaning and preparation of the samples needed before nitrogen analysis of enamel powder using the *oxidation-denitrification* method, makes it a much longer (5 to 7 working days) and more complicated process than carbon and oxygen analysis using the cold trap method (24 hours). A short overview of all the steps will be presented here, but for a detailed explanation of the cleaning process,

*Table 5.3: Values of all standards used in this study. References can be found in the "standard reference list" subsection of the bibliography. *Unpublished established in-house standards. **Unpublished values obtained from this study only.*

International standards	**Material**	**$\delta^{13}C$ (‰ vs. VPDB)**	**$\delta^{18}O$ (‰ vs. VPDB)**	**$\delta^{15}N$ (‰ vs. Air)**
NBS18	Carbonatite	-5.01 ± 0.035	-23.2 ± 0.1	-
NBS120c	Phosphate rock	-6.2	-2 ± 0.5	-
IAEA-603	Calcite	2.46 ± 0.01	-2.37 ± 0.04	-
USGS40	L-glutamic acid	-	-	-4.52 ± 0.06
USGS65	L-glutamic acid	-	-	20.68 ± 0.06
IAEA-NO-3	Potassium nitrate	-	-	4.7 ± 0.2
USGS34	Potassium nitrate	-	-	-1.8 ± 0.2
In-house standards				
VICS	Carrara marble	1.45 ± < 0.1	-5.44 ± < 0.1	-
MPIC-Cf1*	Coral fragments	-	-	5.7 ± 0.2
MPIC-Cf2*	Branching coral	-	-	3.5 ± < 0.2
AG-Lox	Modern enamel	-11.46 ± 0.05	-1.5 ± 0.08	4.2 ± 0.5
Mammy**	Fossil enamel	-13.5 ± <0.1	-14.8 ± 0.1	6.2 ± 0.5

see Leichliter et al. (2021), and for details on the bacteria process and mass spectrometer set-up see Sigman et al. (2001) and Weigand et al. (2016). The denitrification part of the method was first developed to measured $\delta^{15}N$ in water (Sigman et al., 2001), while the oxidation part was added later to measure diatom microfossil-bound $\delta^{15}N$ (Robinson et al., 2004). Currently, the entire method (*oxidation-denitrification*) is routinely used for research into both modern and fossil marine invertebrates, including foraminifera, corals, and diatoms, by measuring the $\delta^{15}N$ values of their mineral bound organic matter (e.g., Martinez-Garcia et al., 2014; Robinson et al., 2004; Studer et al., 2018).

Since $\delta^{15}N$ measurements require a large sample amount (ca. 6 mg), and pre-treatment and oxidation are time-consuming and labour-intensive compared to C and O, not all 259 samples were analysed. Instead a selection was made (table 5.4) in order to establish if and how $\delta^{15}N$ is correlated with $\delta^{13}C$ and/or $\delta^{18}O$ in equid tooth enamel. First, of four teeth (NMN-120, NMN-122, NMN-127, and NMN-129), two to three samples were selected based on extremes in oxygen. One of the samples corresponds with a high oxygen value, the other with a low oxygen value, which correlate with extremes in seasonality, as explained in chapter 4 (for a more in-depth discussion of the results, see chapter 7). Next, three teeth were selected for complete $\delta^{15}N$ serial sample analysis. NMN-126 was

selected based on its $\delta^{18}O$ results. It shows a relatively extended time span (multiple high and low extremes) compared to the $\delta^{18}O$ results of other teeth, with a relatively large intra-tooth variation. The other two teeth were selected based on their $\delta^{13}C$ results. NMN-130 shows relatively high intra-tooth variability in the $\delta^{13}C$ values, whereas NMN-133 shows relatively low intra-tooth variability in these values. In total, 72 samples were analysed with the *oxidation-denitrification* method, of which 63 were part of the three completely analysed teeth.

Table 5.4: Sample selection for nitrogen isotope analysis.

Tooth	Nitrogen isotopes analysis sample selection	n
NMN-120	NMN-120e and NMN-120h	2
NMN-122	NMN-122c and NMN-122n	2
NMN-126	All (NMN-126a – s)	19
NMN-127	NMN-127b and NMN-127d	2
NMn-129	NMN-129a, NMN-129n, and NMN-129s	3
NMN-130	All (NMN-130a – z)	26
NMN-133	All (NMN-133a – r)	18

For this method ca. 5 to 7 milligram of enamel powder is usually needed (Leichliter et al., 2021), with the aim of having 10 nmol N in the sample vial, of which half (5 nmol) is injected (see below) for measurement. However, after the first run of the Neumark-Nord 2 equid samples, it became clear that these teeth have a lower nitrogen content than most other fossil (or modern) tooth enamel samples that have been analysed with this method. This means that from the second run onwards, at least 8 milligram per sample was weighed in. In addition to the samples, three aliquots of three different in-house standards were weighted in. These standards include two coral standards (cf1 and cf2) and one enamel standard (AG-Lox, the same as used for the cold trap method; see table 5.3). In addition, the new Mammy standard was also included in all runs as a start in establishing it as the second in-house enamel standard. This will be used in the future as a two-point correction with AG-Lox.

The first step of the process is the removal of exogenous organic matter in the tooth enamel by means of a reductive cleaning followed by an oxidative cleaning. In the first part of the cleaning, 7 ml of sodium bicarbonate-buffered dithionite citrate (recipe in table 5.5) was added to the powders in 15 ml polypropylene centrifuge tubes to reduce the metal oxide coatings (Mehra & Jackson, 1958; Ren et al., 2012). These metals have the protentional to trap exogenous nitrogen, which is nitrogen from any outside source, during the fossilisation process and thus contaminate the nitrogen trapped in the mineralized enamel when they are not removed. After 10 min in a water bath of 80 °C, the samples were centrifuged (5 min. at 4000 rpm) and decanted. The samples were then rinsed three times with

10 ml Milli-Q water and centrifuged between each rinse. The rinsed powder was transferred to a pre-combusted 4 ml glass vial and after a final round of centrifuging, the remaining water was removed by suction (Leichliter et al., 2021).

Immediately following this reductive cleaning, 3 ml of a basic potassium persulfate solution (recipe in table 5.6) was added to the samples. The samples were then put into the autoclave for 65 min. at 120 °C. During this step, exogenous nitrogen in organic matter is oxidized to nitrate, which is removed with the solution by suction after a round of centrifuging. Again, the samples were rinsed using 4 ml Milli-Q water four times and centrifuged between every rinse. The samples were loosely covered by pre-combusted aluminium foil and then placed in an oven in the clean lab at 60 °C and dried overnight. Once the powder was completely dry, the clean samples were weighed, which is necessary to calculate the nitrogen content, and transferred to new pre-combusted 4 ml glass vials (Leichliter et al., 2021). During these two steps an average of 55-65 % of the material was lost.

The next step is the demineralization of the enamel and the conversion of organic nitrogen that was first trapped in the mineral structure of the enamel, to nitrate. To demineralize the enamel and free the organic matter in the mineral structure, 40 µl of 4N hydrochloric acid was added to the cleaned powder. Immediately after, 1 ml basic potassium persulfate solution (recipe in table 5.7) was added to oxidize the freed organic nitrogen to nitrate. To guarantee complete oxidation of the organic nitrogen, the samples were autoclaved again for 65 min. at 120 °C (Leichliter et al., 2021).

During this step, two new standards were oxidized along the samples. USGS-40 and USGS-65 are internationally certified amino acid isotope reference standards (see table 1), which serve as a control on the complete oxidation of the samples. They were treated exactly the same as the pre-treated samples. In addition to the two extra standards, fifteen blanks (empty pre-combusted glass vials) were added, which were prepared with the HCl and oxidizing solution. This is necessary in order to monitor the blank and correct for the N content and $\delta^{15}N$ of the solution used for oxidation. The blanks were spaced throughout the batch, with five at the beginning, five in the middle, and five at the end.

In order to minimize uncertainties related with nonlinearity in the mass spectrometer, it is important to guarantee a consistent final quantity of N_2O for samples and standards (Sigman et al., 2001; Weigand et al., 2016). Using 5 µl of each oxidized sample, the nitrate concentration was determined by the reduction of the nitrate to nitrous oxide with Vanadium (III) and by chemiluminescent detection of this nitrous oxide on a Teledyne NOx analyser (or NOxBox; Braman & Hendrix, 1989). This analysis resulted in an estimated nitrate content of the samples. This estimation

was used to calculate the volume of the sample which needed to be injected into the bacteria to ensure the desired 5 nmol nitrogen for measurement.

Table 5.5: Recipe for 100 ml of sodium bicarbonate-buffered dithionite citrate solution used in the reductive cleaning step.

Material	Amount
Milli-Q water	100 ml
Sodium Citrate	6.2 g
Sodium Bicarbonate	2 g
Sodium Dithionite	5 g
4N NaOH	400 µl

Table 5.6: Recipe for 100 ml of basic potassium persulfate solution used in the oxidative cleaning step.

Material	Amount
Milli-Q water	100 ml
NaOH (pellet)	2 g
Potassium persulfate ($K_2S_2O_8$)	2 g

Table 5.7: Recipe for 100 ml of basic potassium persulfate solution used in the oxidation step. Four-times recrystallized potassium persulfate is used to ensure a low nitrogen content that does not interfere with the sample signal.

Material	Amount
Milli-Q water	95 ml
6.25 N NaOH	4 ml
Four-times recrystallized potassium persulfate	0.67 – 0.70 g

The last step before measurement was the conversion of the nitrate to N_2O using denitrifying bacteria (*Pseudomonas chlororaphis*). The bacteria were grown, cultured, and harvested prior to injection of the samples (Sigman et al., 2001; Weigand et al., 2016). The samples were injected into 3 ml of media containing bacteria. The injection volume of the sample corresponded with the nitrate content of the sample as explained above. To avoid bacterial death due to a too high (too basic) pH of the injected solution, blanks and samples that required more than 750 µl of injection volume, were adjusted to a near-neutral pH (5-7) by stepwise addition of 4 N hydrochloric acid. Next to the samples and the standards mentioned above, another two internationally certified nitrate standards (IAEA-NO-3 and USGS34, see table 5.3) were also injected. These were injected at concentrations of 1, 3, 5, and 10 nmol nitrogen in order to calculate the nitrogen concentration and calibrate the isotopic composition of the samples relative to atmospheric nitrogen (Weigand et al., 2016).

Five 1 ml blanks were combined and injected into a single bacteria vial. So, the fifteen blanks that were added into the batch during the oxidation step result in three blanks for measurement. This is necessary because the blanks have extremely low nitrogen contents (between 0.4 – 0.5 nmol/ml in

this study) and it is important to accurately measure the nitrogen isotopic composition and nitrogen content of the blanks in order to calculate their impact on the nitrogen content and nitrogen isotope composition of the samples (Leichliter et al., 2021).

The $\delta^{15}N$ values of the converted N_2O were measured via gas chromatography-isotope ratio mass spectrometry (GC-IRMS) on a Thermo Scientific 253 Plus isotope ratio mass spectrometer. A purpose-built system was used for extraction and purification of the N_2O, which fed into the mass spectrometer (Casciotti et al., 2002; McIlvin & Casciotti, 2011; Weigand et al., 2016). In addition, standard N_2O gas aliquots at 5 nmol N were included in each run to monitor for potential instrumental drift. In none of the runs, significant drift was detected.

All samples of the chosen teeth were measured in duplicate, or triplicate where necessary ($1\sigma > 0.5$ ‰), in different batches, resulting in 149 individual measurements (appendix B). Duplicates and triplicates were run in five different batches. The nitrogen values were normalized to atmospheric nitrogen (Air) using the standards IAEA-NO-3 and USGS34 following Weigand et al. (2016). The $\delta^{15}N$ values of the samples were corrected for blank contribution using the nitrogen content and $\delta^{15}N$ values of the blanks added during the oxidation step. Taking the fraction of the blank (f_{blank}) and the fraction of the sample (f_{sample}) in the sample vial into account, the blank contribution is calculated as follows (Leichliter et al., 2021):

$$\delta^{15}N_{sample} = (\delta^{15}N_{measured} - (f_{blank} * \delta^{15}N_{blank})) / f_{sample} \quad (6)$$

where $\delta^{15}N_{measured}$ and $\delta^{15}N_{blank}$ were measured directly using GC-IRMS. $\delta^{15}N_{measured}$ corresponds to the $\delta^{15}N$ value of the sample vial in question and $\delta^{15}N_{blank}$ corresponds to the average $\delta^{15}N$ value of the three blanks included in each batch. f_{blank} and f_{sample} can be calculated using the following equations (Leichliter et al., 2021):

$$f_{blank} = N\ content_{blank} / N\ content_{measured} \quad (7)$$

$$f_{sample} = 1 - f_{blank} \quad (8)$$

where $N\ content_{blank}$ corresponds to the average nitrogen content (in nmol/ml) measured of the three blanks included in each batch, and $N\ content_{measured}$ to the nitrogen content measured of the sample vial in question.

The average nitrogen content of the blank was 0.43 ± 0.06 nmol/ml (n = 14). The average blank fraction was 0.05 ± 0.01, which means that the blank typically contributed around 5 % of nitrogen content in a given sample vial. Inter-batch precision (± 1σ) in measured $\delta^{15}N$ values for international standards is < 0.5 ‰ for USGS65 (n = 14) and < 0.9 ‰ for USGS40 (n = 15). This precision for in-house

standards is < 0.2 ‰ for coral standard cf1 (n = 15) and cf2 (n = 15) and < 0.3 ‰ for tooth enamel standard AG-Lox (n = 15) across all analytical batches.

5.6 Trace element analysis

Trace elements are minerals and metals that occur in small amounts (µg/g) in (fossilized) bones and teeth. The analysis of such trace elements has multiple applications (e.g., Reynard & Balter, 2014; Sponheimer & Lee-Thorp, 2006; Tacail et al., 2017), but here it is used look at the degree of diagenetic alteration of the enamel and if this changes over the length of the tooth. During fossilization, trace elements can be incorporated in bioapatite in two ways: they can substitute other elements in the crystal structure of the bioapatite, or they can fill miniscule voids in the crystal lattice (Parker & Toots, 1970). A high abundance of trace elements would thus indicate that the bioapatite is diagenetically altered and therefore that the isotopic composition of the fossilized bioapatite is likely different from the composition during life, while a low number of trace elements would indicate no to very little diagenetic change of the isotopic composition.

A single tooth was selected (NMN-126), which was analysed for all three isotopic systems, and send to T. Tacail at the Institut für Geowissenschaften at the Johannes Gutenberg-Universität, Mainz, Germany. The following elements were measured: aluminium (Al), boron (B), barium (Ba), iron (Fe), magnesium (Mg), manganese (Mn), sodium (Na), phosphorus (P), strontium (Sr), and zinc (Zn). Results of trace element analysis are routinely given normalized to calcium (Ca; e.g., Tacail et al., 2017), since this material is very abundant in bioapatites. This means that the results of for example aluminium will be given in Al/Ca, which is the ratio of aluminium abundance in µg/g compared to the abundance of calcium in µg/g. The values for this study fall in the range of 0.0001 – 0.1, depending on the element. The results of this analysis are given in appendix C and briefly discussed in chapter 7.

5.7 Statistical analyses

The isotopic data of each tooth were evaluated to determine if the data was normally distributed using a Shapiro-Wilks test. In all cases at least some of the teeth did not have normally distributed isotopic data. This means that the requirements of Analysis of variance (ANOVA) were not satisfied (data needs to be normally distributed), so a non-parametric Kruskal-Wallace test was used to determine if the isotopic values between teeth were statistically significantly different, followed by a Dunn's post-hoc test with a Bonferroni correction. To determine statistically significant correlations between paired isotopic values from the same tooth, a Pearson correlation (two-tailed) was used. The significance level was set to $p = 0.05$ and for correlation the Pearson correlation coefficient (r) is given. Statistical analyses were performed using R-studio version 4.2.3.

5.8 Conclusion

In this chapter, I discussed the materials and methods employed in this research. First, I selected long, third molars of equids, of which I collected enamel samples by drilling the enamel of either the buccal or lingual side of the tooth. For stable carbon and oxygen isotope analysis, all 259 samples were run using the cold trap method. Next, a sub-selection for nitrogen analysis was made based on the $\delta^{13}C$ and $\delta^{18}O$ results and a total of 72 samples were run with the *oxidation-denitrification* method. Trace element analysis was performed on a single tooth to estimate the degree of diagenetic alteration and to see if certain parts of the tooth enamel are more diagenetically affected than others. Statistical analyses were performed on isotopic data of the teeth to determine if the isotopic values between teeth were statistically significant and if there are statistically significant correlations between paired isotopic values from the same tooth.

6 Results

6.1 Introduction

In this chapter, I will present the results of the isotope analyses of tooth enamel from fourteen equid teeth from NMN2. Every tooth has between 15 and 26 C and O measurements (approximately every 2 mm). Four teeth have between two and three N measurements, while three teeth were selected for detailed nitrogen analysis, which have between 18 and 26 measurements. Firstly, I will discuss the results from analyses of the standards used in all three isotopic analyses. Next, I will show the cold trap results; carbon and oxygen isotope values were measured simultaneously. Then, the *oxidation-denitrification* nitrogen isotope ratios are shown. Both methods use the same aliquot of tooth enamel, but different machines (and pre-treatments). The results per tooth are given in figure 6.2 and 6.5, and in table 6.1, 6.3, and 6.4, while the results of each individual sample are given in appendix B. All standard deviations are given in 1σ.

The carbon and oxygen isotope ratios of the 259 equid tooth enamel samples were analysed in at least duplicates (total number of measurements = 543) in nineteen analytical batches. If the standard deviation of the duplicates of a sample was > 0.5 ‰, the sample were analysed again, resulting in a typical standard deviation between 0.0 and 0.4 ‰ (on average 0.1 ‰) for stable carbon and oxygen isotopes. Nitrogen isotope measurements were also conducted in duplicates in five analytical batches, and, whenever necessary, a triplicate analysis was performed when 1σ was > 0.5 ‰, resulting in 149 individual measurements with a standard deviation generally < 0.5‰ (on average 0.3 ‰).

6.2 Standards

The in-house enamel standard AG-Lox was used to correct the values for $\delta^{13}C$ and $\delta^{18}O$ of the NMN2 samples. The average standard deviation observed over all nineteen runs was 0.08 ‰ for $\delta^{13}C$ and 0.12 ‰ for $\delta^{18}O$ (n = 175), which falls in the normal range of variation (e.g., Leichliter and Lüdecke et al., 2023; Lüdecke and Leichliter et al., 2022). The other four standards that were included in each run were corrected against their official carbon and oxygen values. VICS has a standard deviation of 0.09 ‰ for carbon and 0.08 ‰ for oxygen (n = 168); IAEA-603 has a standard deviation of 0.10 ‰ for $\delta^{13}C$ and 0.06 for $\delta^{18}O$ (n = 95); NBS120c has a standard deviation of 0.11 ‰ for carbon and 0.12 ‰ for oxygen (n = 86); NBS18 has a standard deviation of 0.06 ‰ for carbon and 0.10 ‰ for oxygen (n = 43), which all fall in the normal range of variation for this method (Vonhof, de Graaf, et al., 2020). The new in-house enamel standard Mammy was corrected using AG-Lox and yielded a $\delta^{13}C$ value of -13.5 ± < 0.1 ‰ and a $\delta^{18}O$ value of -14.8 ± 0.1 ‰ (n = 67).

The $\delta^{15}N$ values of the NMN2 samples were calculated using the IAEA-NO-3 and the USGS34 internal standards and then corrected for the blank contribution, as explained in the previous chapter. The average standard deviation observed over all five runs for the $\delta^{15}N$ values of both IAEA-NO-3 and USGS34 is 0.06 ‰ (n = 51). The average blank content in each vial observed over all runs is 0.42 ± 0.07 nmol with a range between 0.37 and 0.50 nmol per vial. This content corresponds to a fraction of the blank between 0.02 and 0.08 (2 to 8 %; average = 0.05 ± 0.01) in each sample vial, which falls in the normal range for blank contribution (Leichliter et al., 2021). The other standards that were included in each run were corrected against their known nitrogen values. USGS 40 and USGS 65 both have an average standard deviation of 0.4 ‰ (n = 15 and n = 14 respectively); the average standard deviation of cf1 and cf2 is 0.1 ‰ (n = 15). AG-Lox has an average standard deviation of 0.2 ‰ (n = 15). The new in-house enamel standard Mammy was corrected using the same method as for the samples and yielded a $\delta^{15}N$ value of 6.2 ± 0.4 (n = 15). Given that all values reported above fall in the range of normal variation, I am confident that the results of the samples presented below are accurate.

6.3 Carbon

The carbon isotope ratios of the 259 equid tooth enamel samples show values between -10.6 and -13.1 ‰ (average = -12.3 ± 0.4 ‰; table 6.1 and figure 6.1, grouped according to table 6.2). The standard deviation ranges between 0.0 and 0.4 ‰, with an average of < 0.1 ‰. The $\delta^{13}C$ range is smaller within a single tooth, with an average amplitude of 1.1 ‰. The average $\delta^{13}C$ value of each tooth ranges between -11.6 and -12.7 ‰.

There is no cyclical pattern visible in the carbon isotope ratio variation within each tooth (figure 6.2), as might be expected if the diet varied seasonally. However, in some teeth, the carbon values increase significantly in the sample(s) closest to the root (e.g., samples NMN-123a and NMN-129a; figure 6.2).

A Kruskal-Wallis test (KW test) was performed to see if there is a significant difference between the $\delta^{13}C$ values of the 14 equid teeth. A Kruskal-Wallis test was preferred above a one-way ANOVA test, since four of the fourteen teeth (NMN-122, NMN-123, NMN-129, NMN-131) did not have normally-distributed $\delta^{13}C$ values based on the results of a Shapiro-Wilk Test ($\alpha = 0.05$). The KW test showed a statistically significant difference in the mean $\delta^{13}C$ value between at least two teeth ($\chi^2(13) = 122.27$, $p < 0.001$). Pairwise comparisons of average $\delta^{13}C$ values of teeth, using a Post-Hoc Dunn's test using a Bonferroni corrected alpha ($\alpha = 0.00055$), showed that certain pairs are statistically significantly different ($p < 0.001$), while others are not significantly different ($p > 0.05$; table 6.2). Two main clusters can be distinguished, which are highlighted in figure 6.1 and table 6.2.

Table 6.1: The results of the $\delta^{13}C$ analysis per tooth.

MPIC ID	n	Average $\delta^{13}C_{VPDB}$ (‰)	Range $\delta^{13}C_{VPDB}$ (‰)	Amplitude $\delta^{13}C_{VPDB}$ (‰)
NMN-120	13	-11.6 ± 0.3	(-12.0) – (-11.0)	0.9
NMN-121	17	-11.9 ± 0.4	(-12.5) – (-10.6)	1.9
NMN-122	17	-12.0 ± 0.5	(12.7) – (-11.5)	1.2
NMN-123	16	-12.2 ± 0.4	(12.6) – (-11.0)	1.6
NMN-124	17	-12.0 ± 0.3	(12.5) – (-11.4)	1.1
NMN-125	19	-12.7 ± 0.3	(13.1) – (-12.2)	0.9
NMN-126	19	-12.4 ± 0.2	(-12.9) – (-11.8)	1.1
NMN-127	14	-11.8 ± 0.2	(-12.1) – (-11.4)	0.7
NMN-128	20	-12.5 ± 0.2	(-12.8) – (-12.1)	0.6
NMN-129	23	-12.4 ± 0.4	(-12.9) – (-10.8)	2.1
NMN-130	26	-12.4 ± 0.1	(12.7) – (-12.1)	0.6
NMN-131	19	-12.4 ± 0.2	(-12.8) – (-11.8)	0.9
NMN-132	21	-12.5 ± 0.3	(-12.9) – (-12.1)	0.8
NMN-133	18	-12.1 ± 0.3	(-12.5) – (-11.5)	1.1
Total	259	-12.3 ± 0.4	(-13.1) – (-10.6)	1.1

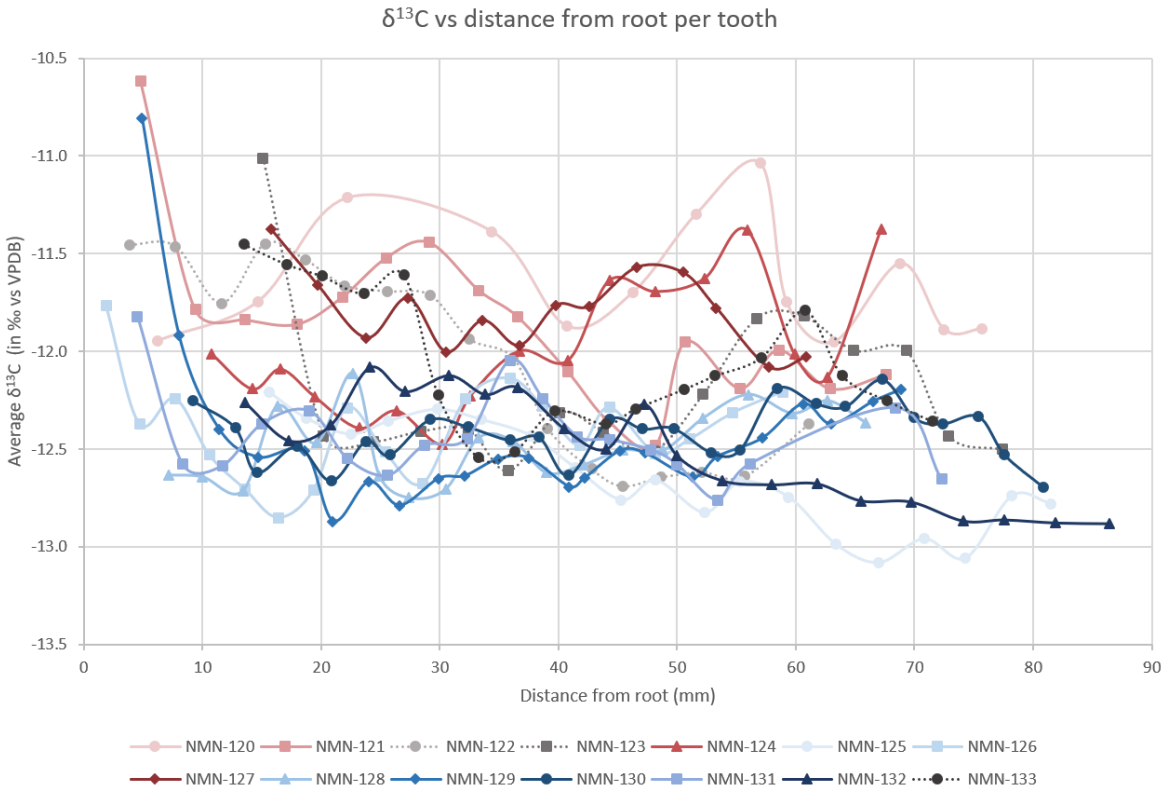

Figure 6.1: The $\delta^{13}C$ values of each sample compared to the distance from the root grouped per tooth. The colours correspond to the groups of teeth, whose average $\delta^{13}C$ value is statistically different from the other group (see table 6.2 on the next page). The teeth in the blue and red groups are statistically different from one another, while the grey, dashed group is different from neither the blue nor the red group.

Table 6.2: Results of the Post-Hoc Dunn's test with a Bonferroni corrected alpha (α = 0.00055) used on the carbon values per tooth in a pairwise table. In case the average $\delta^{13}C$ value of two teeth are statistically significantly different, the p-value is given. An empty cell means that the average $\delta^{13}C$ value of those two teeth are not different. The teeth are colour-coded according to the three groups visible in figure 6.1.

	NMN-120	NMN-121	NMN-122	NMN-123	NMN-124	NMN-125	NMN-126	NMN-127	NMN-128	NMN-129	NMN-130	NMN-131	NMN-132	NMN-133
NMN-120						< 0.001	< 0.001		< 0.001	< 0.001	< 0.001	< 0.001	< 0.001	
NMN-121						< 0.001	< 0.001		< 0.001	< 0.001	< 0.001	< 0.001	< 0.001	
NMN-122						< 0.001								
NMN-123														
NMN-124						< 0.001			< 0.001	< 0.001	< 0.001	< 0.001	< 0.001	
NMN-125	< 0.001	< 0.001	< 0.001		< 0.001			< 0.001						< 0.001
NMN-126	< 0.001	< 0.001						< 0.001						
NMN-127						< 0.001	< 0.001		< 0.001	< 0.001	< 0.001	< 0.001	< 0.001	
NMN-128	< 0.001	< 0.001			< 0.001			< 0.001						< 0.001
NMN-129	< 0.001	< 0.001			< 0.001			< 0.001						< 0.001
NMN-130	< 0.001	< 0.001			< 0.001			< 0.001						
NMN-131	< 0.001	< 0.001			< 0.001			< 0.001						
NMN-132	< 0.001	< 0.001			< 0.001			< 0.001						< 0.001
NMN-133						< 0.001			< 0.001	< 0.001			< 0.001	

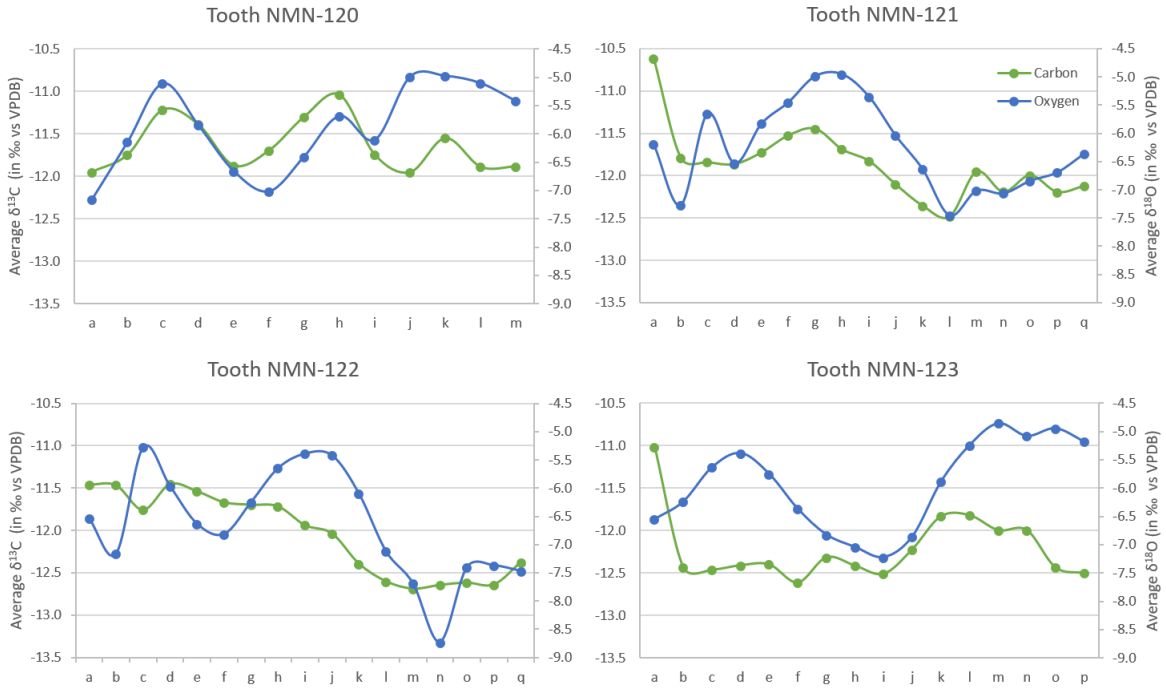

Figure 6.2: Continued on the next page

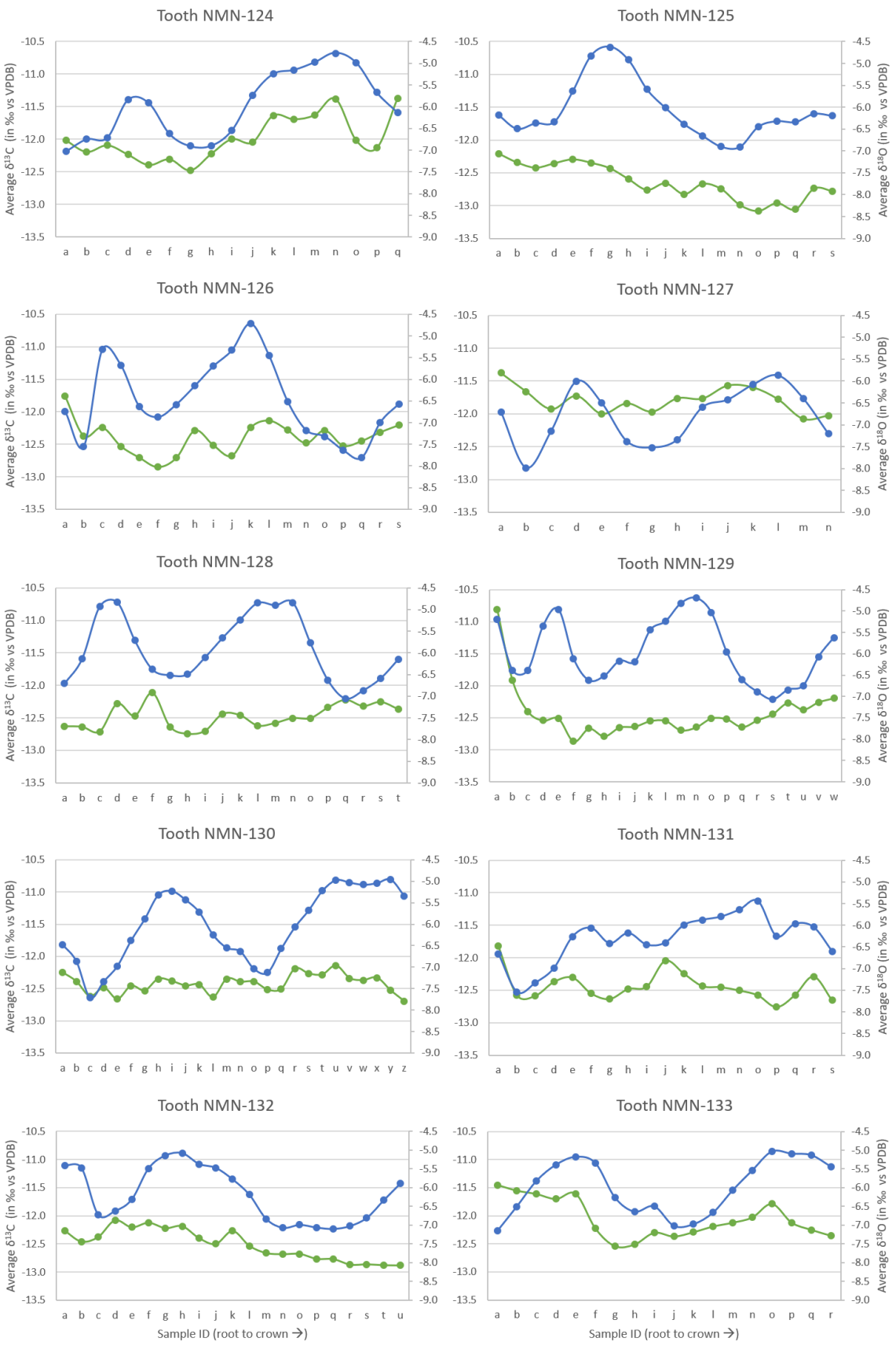

Figure 6.2: The results of the carbon and oxygen analysis visualized per tooth. Green lines correspond to $\delta^{13}C$ values on the left y-axis, blue lines correspond to $\delta^{18}O$ values on the right y-axis. The samples IDs that were taken along the growth axis from root to crown per tooth are shown on the x-axis.

6.4 Oxygen

The oxygen isotope ratios of the 259 equid tooth enamel samples show values between -4.6 and -8.7 ‰ (average = -6.2 ± 0.8 ‰; figure 6.3 and table 6.3). The standard deviation ranges between 0.0 and 0.4 ‰ (average = 0.1 ‰). Again, within a single tooth, the average $\delta^{18}O$ range is smaller than the range for all 259 samples combined, with an average range of 2.4 ‰ for each tooth. The average $\delta^{18}O$ value of a single tooth ranges between -5.9, and -6.8 ‰.

In contrast to the carbon isotope values, there is a clear cyclical pattern visible in the oxygen isotope ratios of each tooth (figure 6.2), which indicates seasonality, as explained in chapter 4. As mentioned, the average amplitude of the oxygen isotope values is 2.4 ‰ per tooth. Tooth NMN-122 has the largest amplitude (3.5 ‰), while tooth NMN-132 has the smallest amplitude (2.0 ‰).

A Kruskal-Wallis test was performed to see if there is a significant difference between the average $\delta^{18}O$ values of the fourteen equid teeth. Three of the fourteen teeth (NMN-125, NMN-128, and NMN-132) did not distribute normally in their $\delta^{18}O$ values based on the results of a Shapiro-Wilk Test ($\alpha = 0.05$), and so ANOVA could not be performed. The KW test showed a statistically significant difference in the mean $\delta^{18}O$ value between the different teeth ($\chi^2(13) = 24.21$, $p = 0.029$). However, when performing a pairwise comparison of the teeth using a Post-Hoc Dunn's test, none showed a significant difference in $\delta^{18}O$ mean value.

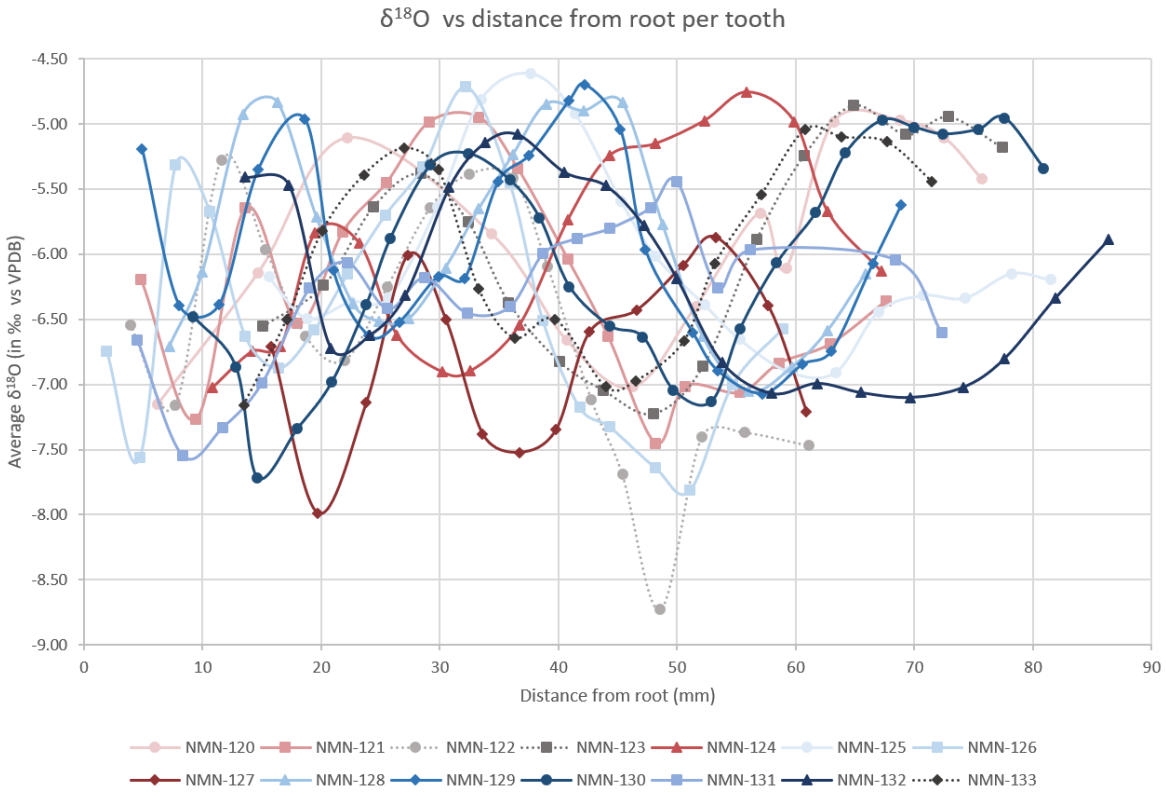

Figure 6.3: The $\delta^{18}O$ values of each sample compared to the distance from the root grouped per tooth. The colour of each tooth corresponds to the colour of that tooth in figure 6.1. However, for the $\delta^{18}O$ values there are no teeth that have an average $\delta^{18}O$ value statistically different from another tooth based on pairwise analysis.

Table 6.3: The results of the $\delta^{18}O$ analysis per tooth.

MPIC ID	n	Average $\delta^{18}O_{VPDB}$ (‰)	Range $\delta^{18}O_{VPDB}$ (‰)	Amplitude $\delta^{18}O_{VPDB}$ (‰)
NMN-120	13	-5.9 ± 0.7	(-7.2) – (-5.0)	2.2
NMN-121	17	-6.3 ± 0.8	(-7.5) – (-5.0)	2.5
NMN-122	17	-6.7 ± 0.9	(-8.7) – (-5.3)	3.5
NMN-123	16	-5.9 ± 0.8	(-7.2) – (-4.9)	2.4
NMN-124	17	-6.0 ± 0.8	(-7.0) – (-4.8)	2.3
NMN-125	19	-6.1 ± 0.7	(-6.9) – (-4.6)	2.3
NMN-126	19	-6.5 ± 0.9	(-7.8) – (-4.7)	3.1
NMN-127	14	-6.8 ± 0.6	(-8.0) – (-5.9)	2.1
NMN-128	20	-5.9 ± 0.7	(-7.1) – (-4.8)	2.2
NMN-129	23	-6.0 ± 0.7	(-7.1) – (-4.7)	2.4
NMN-130	26	-6.0 ± 0.8	(-7.7) – (-5.0)	2.8
NMN-131	19	-6.3 ± 0.5	(-7.6) – (-5.4)	2.1
NMN-132	21	-6.2 ± 0.7	(-7.1) – (-5.1)	2.0
NMN-133	18	-6.0 ± 0.7	(-7.2) – (-5.0)	2.1
Total	259	-6.2 ± 0.8	(-8.7) – (-4.6)	2.4

6.5 Nitrogen

A selection of 72 of the 259 enamel samples were analysed for nitrogen isotope composition using the *oxidation-denitrification* method, as explained in the previous chapter. The nitrogen isotope values range between 2.4 and 4.8 ‰ (average = 3.5 ± 0.6 ‰; figure 6.4 and table 6.4). The standard deviation ranges between 0.0 and 0.9 ‰ (average = 0.3 ‰). Within a single tooth, the average range of $\delta^{15}N$ values is 1.0 ‰. When focussing only on the three teeth that were analysed for nitrogen in detail, the range and average $\delta^{15}N$ values do not change much (2.5 – 4.8 ‰ and 3.6 ± 0.6 ‰ respectively, n = 63). However, the average range within a single tooth does increase to 1.5 ‰.

As with carbon values, there is no clear cyclical pattern visible for the nitrogen isotopes in the three teeth, as might be expected if the $\delta^{15}N$ varied seasonally (figure 6.4). Sample NMN-126a (enamel sample closest to the root/cervical margin) does show a marked increase in $\delta^{15}N$ value, following the pattern observed in carbon values for this same tooth.

A Kruskal-Wallis test was performed to see if there is a significant difference between the average $\delta^{15}N$ values of the 3 teeth. The $\delta^{15}N$ values of two of the three teeth (NMN-126 and NMN-133) do not distribute normally based on the results of a Shapiro-Wilk Test ($\alpha = 0.05$). The KW test showed a statistically significant difference in the mean $\delta^{15}N$ value between the different teeth ($\chi^2(2) = 34.99$, $p < 0.001$). In addition, a pairwise comparisons using a Post-Hoc Dunn's test with a Bonferroni corrected alpha of 0.017, indicated that all pairs of the teeth are different in their $\delta^{15}N$ values (NMN-126 vs NMN-130, $p < 0.001$; NMN-126 vs NMN-133, $p < 0.001$; NMN-130 vs NMN-133, $p = 0.005$).

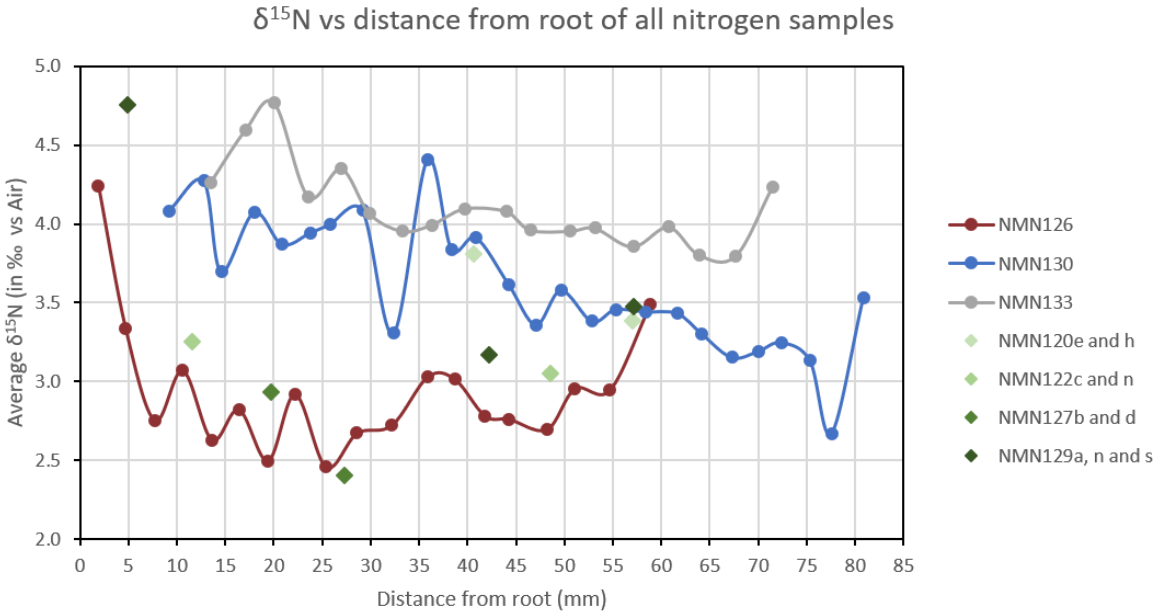

Figure 6.4: The $\delta^{15}N$ values of each sample (n = 72) compared to the distance from the root grouped per tooth. The green diamonds represent the samples of the four teeth that were not completely analysed.

Table 6.4: The results of the $\delta^{15}N$ analysis per tooth.

MPIC ID	n	Average $\delta^{15}N_{Air}$ (‰)	Range $\delta^{15}N_{Air}$ (‰)	Amplitude $\delta^{15}N_{Air}$ (‰)
NMN-120	2	3.6	3.4 – 3.8	0.4
NMN-122	2	3.1	3.0 – 3.2	0.2
NMN-126	19	2.9 ± 0.4	2.4 – 4.2	1.8
NMN-127	2	2.6	2.4 – 2.9	0.5
NMN-129	3	3.8	3.1 – 4.7	1.6
NMN-130	26	3.6 ± 0.4	2.6 – 4.4	1.8
NMN-133	18	4.1 ± 0.3	3.8 – 4.8	1.0
Total	72	3.5 ± 0.6	2.4 – 4.8	1.0

6.6 Pairing of Carbon, Oxygen, and Nitrogen

Results of the Pearson correlation of all 259 samples indicated that there is a significant small positive relationship between $\delta^{13}C$ and $\delta^{18}O$ ($r(257) = 0.137$, $p = 0.028$). However, when looking at the correlation between $\delta^{13}C$ and $\delta^{18}O$ within each tooth, only four show a significant relationship between $\delta^{13}C$ and $\delta^{18}O$: NMN-121 shows a significant medium positive relationship ($r(15) = 0.487$, $p = 0.048$), NMN-122 shows a significant large positive relationship ($r(15) = 0.574$, $p = 0.16$), NMN-124 shows a significant large positive correlation ($r(15) = 0.605$, $p = 0.010$), and NMN-132 also shows a significant large positive correlation ($r(19) = 0.599$, $p = 0.004$; figure 6.2 and table 6.5).

Table 6.5: The correlation between the $\delta^{13}C$ and $\delta^{18}O$ values of each tooth. The p-value, significance, and R^2 are based on a Pearson correlation test.

MPIC ID	n	p-value	Significance	R^2
NMN-120	13	0.581	Non	0.03
NMN-121	17	0.049	Significant	0.24
NMN-122	17	0.016	Significant	0.33
NMN-123	16	0.843	Non	0.00
NMN-124	17	0.010	Significant	0.37
NMN-125	19	0.081	Non	0.17
NMN-126	19	0.677	Non	0.01
NMN-127	14	0.576	Non	0.03
NMN-128	20	0.244	Non	0.08
NMN-129	23	0.621	Non	0.01
NMN-130	26	0.068	Non	0.13
NMN-131	19	0.927	Non	0.00
NMN-132	21	0.004	Significant	0.36
NMN-133	18	0.553	Non	0.22

Results of the Pearson correlation of all samples (n = 72) analysed for nitrogen isotope ratios indicates a significant medium positive relationship between $\delta^{13}C$ and $\delta^{15}N$ values ($r(70) = 0.386$, $p < 0.001$). When looking at the correlation between $\delta^{13}C$ and $\delta^{15}N$ within the three teeth that were completely analysed for nitrogen isotopes, both NMN-126 and NMN-133 show a significant large positive relationship ($r(17) = 0.723$, $p < 0.001$ and $r(16) = 0.633$, $p = 0.005$, respectively), while NMN-130 shows a non-significant relationship ($p > 0.05$; figure 6.5 and table 6.6).

The results of the correlation between $\delta^{15}N$ and $\delta^{18}O$ values of all nitrogen analysed samples (n = 72), show a non-significant very small positive relationship ($r(70) = 0.0623$, $p = 0.603$). When looking at this relationship within each of the three fully analysed teeth, both NMN-126 and NMN-133 show a non-significant relationship ($p = 0.417$ and $p = 0.649$ respectively), while NMN-130 shows a significant very small negative relationship between $\delta^{15}N$ and $\delta^{18}O$ ($r(24) = 0.441$, $p = 0.024$; figure 6.5 and table 6.7)

Table 6.6: The correlation between the $\delta^{13}C$ and $\delta^{15}N$ values of each tooth. The p-value, significance, and R^2 are based on a Pearson correlation test.

MPIC ID	n	p-value	Significance	R^2
NMN-126	19	< 0.001	Significant	0.52
NMN-130	26	0.306	Non	0.04
NMN-133	18	0.005	Significant	0.40

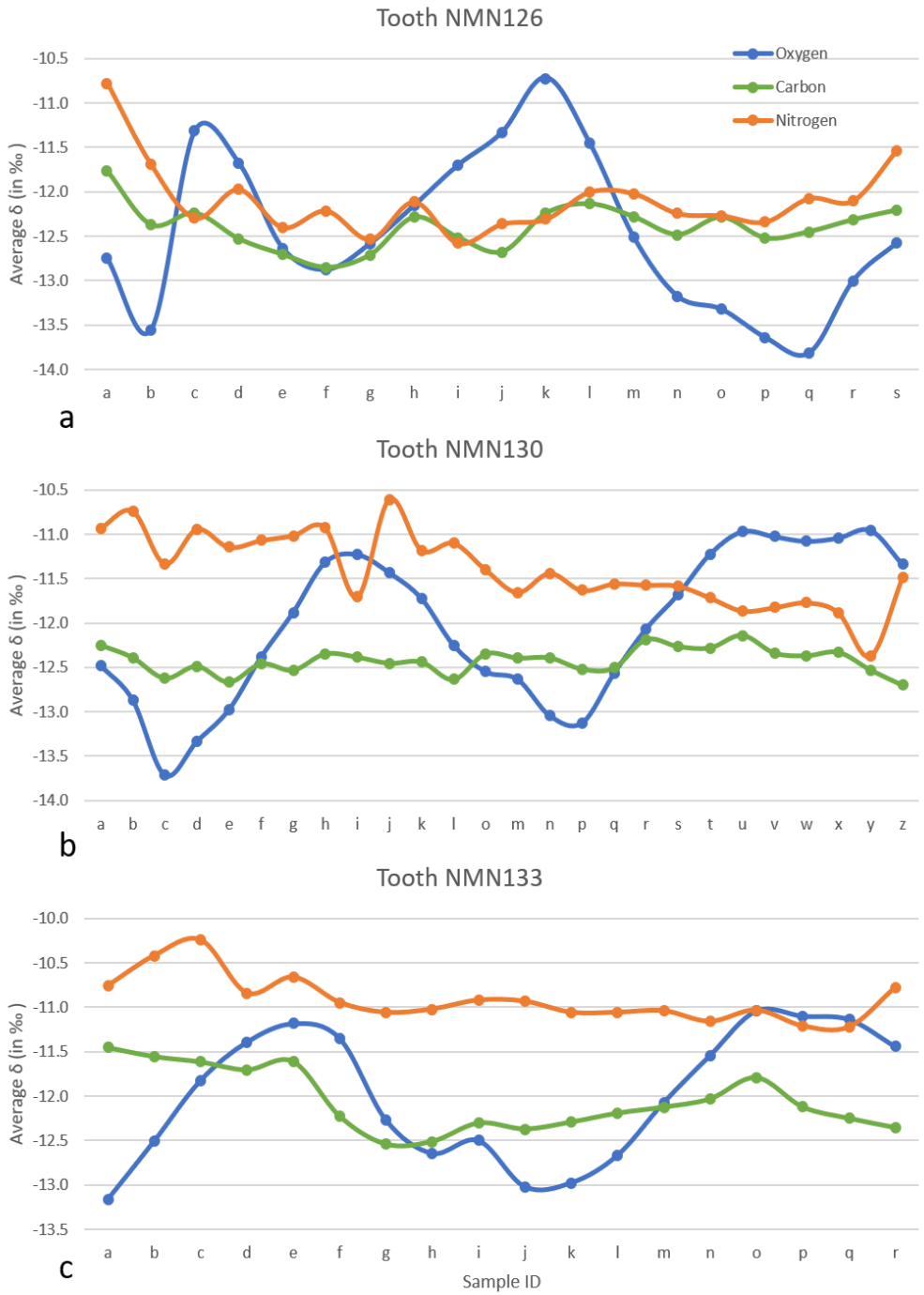

Figure 6.5: Pairing of $\delta^{13}C$, $\delta^{15}N$ and $\delta^{18}O$ for tooth NMN-126 (a), NMN-130 (b), and NMN-133 (c). Green lines represent $\delta^{13}C$ (in ‰ vs VPDB), orange lines represent $\delta^{15}N$ (in ‰ vs Air), and blue lines represent $\delta^{18}O$ (in ‰ vs VPDB). To get all values on the same scale, I subtracted 15 from the average $\delta^{15}N$ values of each sample and 6 from the average $\delta^{18}O$ values of each sample. The samples IDs per tooth are shown on the x-axis.

Table 6.7: The correlation between the $\delta^{18}O$ and $\delta^{15}N$ values of each tooth. The p-value, significance, and R^2 are based on a Pearson correlation test

MPIC ID	n	p-value	Significance	R^2
NMN-126	19	0.417	Non	0.04
NMN-130	26	0.024	Significant	0.19
NMN-133	18	0.649	Non	0.01

6.7 Carbonate and nitrogen content

The carbonate content in the equid enamel samples is on average 7 % (± 1 %), which is normal for enamel, as explained in chapter 3. AG-Lox has a carbonate content between 7 and 8 % (Wacker et al., 2016) and was used to calculate the carbonate content in the NMN2 samples. There is no significant correlation between carbonate content and $\delta^{13}C$ ($p = 0.382$; figure 6.6) or carbonate content and $\delta^{18}O$ ($p = 0.239$; figure 6.7).

The average nitrogen content in all 72 samples is 3.1 ± 0.5 nmol/mg. Tooth NMN-126 has an average content of 2.9 ± 0.5 nmol/mg, NMN-130 has an average of 3.1 ± 0.2 nmol/mg, and NMN-133 of 3.4 ± 0.4 nmol/mg, which is on the low side of the range observed in modern and fossilized enamel (Leichliter and Lüdecke et al., 2023; Lüdecke and Leichliter et al., 2022). Results of the Pearson correlation indicated that there is a significant large positive relationship between $\delta^{15}N$ and nitrogen content, ($r(70) = 0.698$, $p < 0.001$; figure 6.8), which is also visible when focussing only on the three complete analysed teeth ($r(61) = 0.731$, $p < 0.001$). In addition, the cervical margin sample of tooth NMN-126 (NMN-126a), which shows both a high $\delta^{13}C$ and $\delta^{15}N$ value compared to the rest of the tooth, also has a high nitrogen content. This pattern is also visible in one other cervical margin sample of tooth NMN-129 (NMN-129a). It has the highest nitrogen content of all enamel samples measured, as well as a high $\delta^{13}C$ and $\delta^{15}N$ value compared to other samples of this tooth.

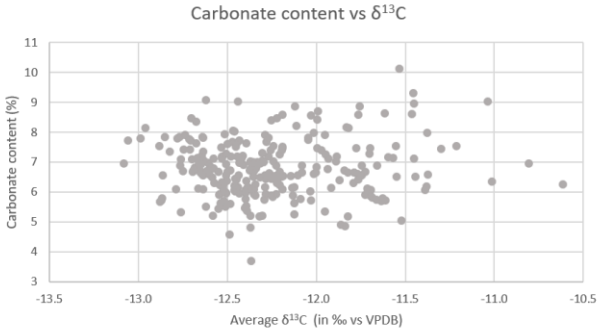

Figure 6.6: The $\delta^{13}C$ value of each tooth enamel sample compared to its carbonate content. Each dot represents a single sample.

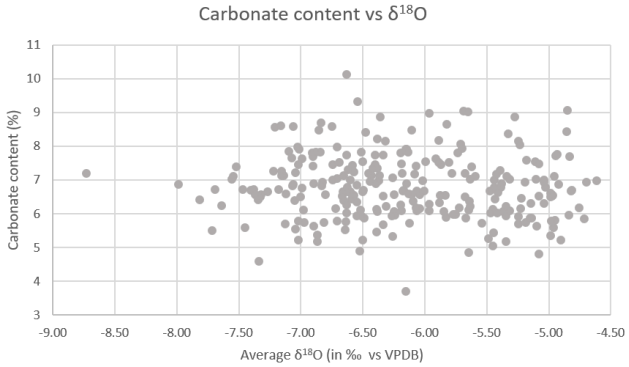

Figure 6.7: The δ18O value of each tooth enamel sample compared to its carbonate content. Each dot represents a single sample.

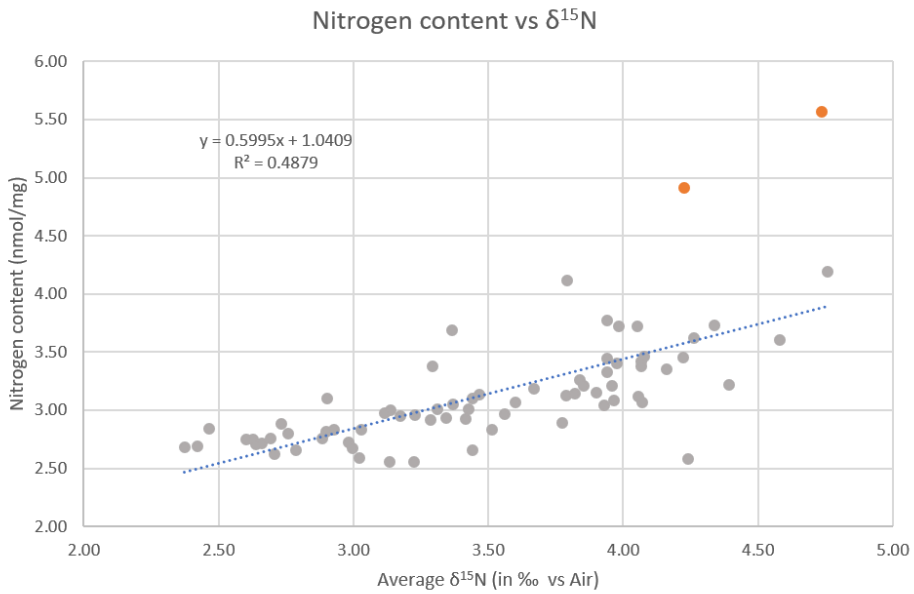

Figure 6.8: The δ15N value of each tooth enamel sample compared to its nitrogen content. A significant large positive correlation is visible. The trend line, its equation and its R2 value are displayed. Each dot represents a single sample. The two orange dots represent cervical margin samples NMN-126a and NMN-129a.

6.8 Conclusion

In this chapter, I presented the results from the stable carbon, oxygen, and nitrogen isotope analyses. All standards fall within the normal range expected for the two methods (cold-trap for stable carbon and oxygen analysis and *oxidation-denitrification* for nitrogen analysis). The overall average of the $\delta^{13}C$ values is -12.3 ± 0.4 ‰ (n = 259), the average is -6.2 ± 0.8 ‰ for $\delta^{18}O$ (n = 259), and 3.5 ± 0.6 ‰ for $\delta^{15}N$ (n =72). Four or the fourteen teeth (NMN-121, NMN-122, NMN-124, and NMN-132) show a positive relationship between $\delta^{13}C$ and $\delta^{18}O$. Two of the three teeth (NMN-126 and NMN-133) completely analysed for nitrogen isotope ratios, show a significant large positive relationship between $\delta^{13}C$ and $\delta^{15}N$, while the other tooth (NMN-130) shows a significant very small negative relationship between $\delta^{15}N$ and $\delta^{18}O$. The carbonate content of the enamel samples falls into the normal range and is not correlated with either $\delta^{13}C$ or $\delta^{18}O$. The nitrogen content of the enamel is on the low side of the range and does show a significant large positive correlation with $\delta^{15}N$.

7 Discussion

7.1 Introduction

In this chapter, I will start with a discussion on the possibility of diagenetic alteration of the tooth enamel analysed in this study. It is important to examine this, since diagenesis can impact the isotopic ratios in the enamel. Next, I will discuss the implications and interpretations of the results presented in the previous chapter. In addition, I will compare the equid data to previously published and unpublished isotopic data. These data cover stable carbon, oxygen, and nitrogen isotopes from bone collagen as well as tooth enamel from equids, and some other species from Neumark-Nord 2. At the end of the chapter, I will make some suggestions for future research.

7.2 Diagenesis

As explained in chapter 3, enamel as a biological material is highly resistant to diagenetic alteration. In addition, isotope analysis of bone collagen from Neumark-Nord 2 reflected the isotopic signal of the animal (chapter 2, Britton et al., 2012), which indicates that the preservation at the site is extremely good, because it preserved collagen for approximately 120,000 years and presents one of the oldest $\delta^{15}N$ collagen datasets published so far. Since enamel is more diagenetically resistant than collagen, it can be inferred that the enamel at this site is also well persevered.

The enamel samples that are nearest to the lowest point of the root (the cervical margin) show a relatively sharp increase in $\delta^{13}C$ value, as well as $\delta^{15}N$ where measured, in 5 different teeth (n = 6; e.g., figure 6.5a). This increase in isotopic values could be explained by the fact that equid teeth grow from the crown to the root and thus also mineralize in this direction (as explained in chapter 3). In case the individual died before the root part of the tooth was fully mineralized, this portion is much more porous and thus more susceptible to diagenetic alteration, which in turn can affect the stable isotope values (e.g., Kohn et al., 1999).

Tooth NMN-126 has undergone trace element analysis (appendix C). It indicates that the tooth is not diagenetically altered, because the concentrations of the trace elements that are present are low. When excluding the two samples NMN-126a and NMN-126b, which are within 5mm of the tip of the root, there is even less correlation visible between calcium and trace elements indicative of diagenesis. This indicates that these two samples are potentially more diagenetically altered than the rest of the tooth. This corresponds with the fact that the $\delta^{13}C$ and $\delta^{15}N$ values of these two samples show a relatively sharp increase in their values compared to the rest of the samples of this tooth.

Tooth NMN-133 is the only tooth that has a part of the enamel near the root that has a black colour (figure 7.1a). Bendrey et al. (2015, p. 1108) show a figure of a third molar belonging to a modern

domesticated horse, of which the lower half of the enamel is a much darker, almost black colour. This is enamel that is still mineralizing. It could be the case that the black enamel of tooth NMN-133 is also not fully matured yet. However, discoloration can also be a result of fossilization and does not necessarily imply diagenetic alteration. For example, all the sampled teeth have a brown-yellow to grey colour (e.g., tooth NMN-130 in figure 7.1b), but the teeth of living horses are white. The dark coloured part of the enamel was sampled and encompasses samples NMN-133a to e. These samples will be included in all analyses because it is undetermined whether the discolouration is due to immature enamel or fossilization. In addition, the stable carbon, oxygen, and nitrogen isotope values do not show outliers in these five samples. To determine if these five samples were affected by diagenesis, a trace element analysis could be performed on this tooth in the future.

Summarizing, the tooth enamel analysed in this research show no indicators for diagenetic alteration and thus reflect the isotope signal of the animal. However, there is the possibility that the enamel nearest to cervical margin is slightly affected by diagenesis. These samples (n = 6) will be included in the majority of interpretations. It will be explicitly mentioned when, and why, they are excluded from certain analyses and interpretations.

Figure 7.1: Tooth NMN-133 (a) and NMN-130 (b) after sampling. Scale in cm. The black enamel of tooth NMN-133 near the root is indicated by the bracket in a. Tooth NMN-130 shows the usual colour of equid tooth enamel from NMN2, ranging from brown-yellow to grey (photographs by M. Vink)

7.3 Carbon

The enrichment factor between diet and bioapatite in carbon isotopes for herbivorous ungulate mammals was determined by Cerling and Harris (1999) to be approximately 14 ‰. However, as

explained in chapter 4, a new enrichment factor was determined for four groups of herbivorous mammals: non-coprophagous and coprophagous hindgut fermenters, and non-ruminant and ruminant foregut fermenters (Cerling et al., 2021). They show that the enrichment factor (ε*) is mostly dependent on methane production. Equids belong to the category of non-coprophagous hindgut fermenters, which has a $\varepsilon^*_{enamel\text{-}diet}$ of 13.5 ± 1 ‰.

The average $\delta^{13}C$ value of the enamel samples studied here is -12.3 ± 0.4 ‰, which corresponds with a $\delta^{13}C$ value of the diet of -25.8 ± 1.4 ‰ after subtracting the enrichment factor (ε* = 13.5 ± 1 ‰; see table 7.1 for the average $\delta^{13}C_{diet}$ per tooth). This value falls well within the range of Eemian C_3 plants (-29 and -24 ‰; chapter 4), and is even very close to the average (-26 ‰, chapter 4). This is as expected, since there are no wild C_4 plants (or CAM plants) at the latitude Neumark-Nord is located. The range of $\delta^{13}C_{enamel}$ (-13.1 – -10.6 ‰; n = 259) corresponds with a range of $\delta^{13}C_{diet}$ between -26.6 and -24.1 ± 1 ‰. When excluding the enamel samples near the cervical margin, as explained above, neither the average nor the standard deviation changes. The range does become a little smaller for the $\delta^{13}C_{enamel}$ values (-13.1 – -11.0 ‰). However, since the average and standard deviation do not change when the enamel samples near the cervical margin are excluded, they will be included in the rest of the analyses on stable carbon isotopes.

Table 7.1: The average $\delta^{13}C$ value of the diet per tooth (calculated by subtracting the enrichment factor (ε = 13.5) from the $\delta^{13}C_{enamel}$ values).*

MPIC ID	n	Average $\delta^{13}C_{enamel}$ (‰)	Average $\delta^{13}C_{diet}$ (‰)
NMN-120	13	-11.6	-25.1
NMN-121	17	-11.9	-25.4
NMN-122	17	-12.0	-25.6
NMN-123	16	-12.2	-25.7
NMN-124	17	-12.0	-25.5
NMN-125	19	-12.7	-26.2
NMN-126	19	-12.4	-25.9
NMN-127	14	-11.8	-25.3
NMN-128	20	-12.5	-26.0
NMN-129	23	-12.4	-25.9
NMN-130	26	-12.4	-25.9
NMN-131	19	-12.4	-25.9
NMN-132	21	-12.5	-26.0
NMN-133	18	-12.1	-25.6

The average $\delta^{13}C_{diet}$ value (-25.8 ± 1.4 ‰) is slightly on the less negative end of the $\delta^{13}C$ range of C_3 plants (-29 and -24 ‰). This indicates that the $\delta^{13}C$ values of the plants were likely not affected by the canopy effect. In chapter 4 I explained that the canopy effect can lead to depleted $\delta^{13}C$ values of C_3

plants, which would result in a $\delta^{13}C_{diet}$ value on the lower/more negative end of the C_3 plant range (e.g., Bonafini et al, 2013; Drucker et al, 2008). Horses have a diet of grasses, shrubs, and herbs (chapter 4), which are below the canopy height, a canopy effect would therefore be expected to be visible in the $\delta^{13}C_{diet}$ in case the area surrounding NMN2 where the equids fed was a dense forest. However, as explained in chapter 2, the area surrounding the small lake was likely an open habitat (Bakels, 2012; Pop & Bakels, 2015), which is reflected in the slightly more positive $\delta^{13}C_{diet}$ values calculated here. In addition, if the horses fed in a wider area around the Neumark-Nord complex, there was either no mature, complex, and dense forest close by, or the portion of their diet consisting of plants originating in such a forest was not big enough for the ^{13}C depletion to remain visible in their tissues.

The variation of $\delta^{13}C_{enamel}$ values between individual teeth (range = -12.7 – -11.6 ‰), as well as the intra-tooth variation (average variation = 1.1 ± 0.4 ‰, range = 0.6 – 2.1 ‰), can be explained by variations in the $\delta^{13}C$ values of the plants the equids ate, as explained in chapter 4. For example, when consuming varying proportions of different plant species, which have different $\delta^{13}C$ values, the $\delta^{13}C$ values of two individuals can differ from each other corresponding with these different plant proportions. In addition, the $\delta^{13}C_{enamel}$ values of an individual can change over its lifetime (e.g., during the time of tooth formation) due to changes in climate, different proportions of different plant species in the diet, etc., which all affect the $\delta^{13}C$ values of the plants.

The Kruskal-Wallis test showed that there is a statistically significant difference in the mean $\delta^{13}C$ value of the thirteen teeth ($\chi^2(13) = 122.27$, $p < 0.001$). The results of the Post-Hoc Dunn's test, using a Bonferroni corrected alpha ($\alpha = 0.00055$; chapter 6; table 6.2, p. 61) show between which pairs of teeth the $\delta^{13}C$ mean value is statistically significantly different. Table 6.2 shows that most of the teeth can be clustered in two different groups based on their $\delta^{13}C$ values; the teeth in the first group have statistically higher mean $\delta^{13}C$ values compared to the teeth in the other group (figure 6.1, p. 60). NMN-133 could potentially be clumped in with the first group, since it is different from NMN-125, NMN-128, NMN-129, and NMN-132, but none of the other teeth. NMN-122 and NMN-123 fall outside of either of the groups, because NMN-122 is only statistically different from NMN-125, while NMN-123 is not statistically different from any other tooth.

The relatively clear division of the teeth in these two groups can indicate that the individuals with higher $\delta^{13}C$ values had a relatively similar diet source during enamel development, which in turn was different from the diet source of the specimens with lower $\delta^{13}C$ values. This small difference in $\delta^{13}C$ could be caused by a geographical separation of the feeding area of the two groups and/or by a temporal separation of the two groups. It has been suggested that equids were present year-round in

the vicinity of NMN2 (Garcia-Moreno et al., 2015; Kindler et al., 2020; Kindler et al., 2015), but this does not necessarily mean that they all have the same feeding area around the lake. In addition, the find layer was accumulated over a span of 455 years (chapter 2; Kindler et al., 2014). In archaeological terms, this is a relatively short period, but it is long when compared to the lifespan of horses, especially young ones as studied here. Furthermore, within 455 years, it is definitely possible for the $\delta^{13}C$ values of the area surrounding NMN2 to change. It was also explored whether the location of the tooth in the site might have been correlated with the group it belongs to. When looking at the geographical distribution of these groups in the excavation grid, there is no obvious pattern visible (figure 7.2).

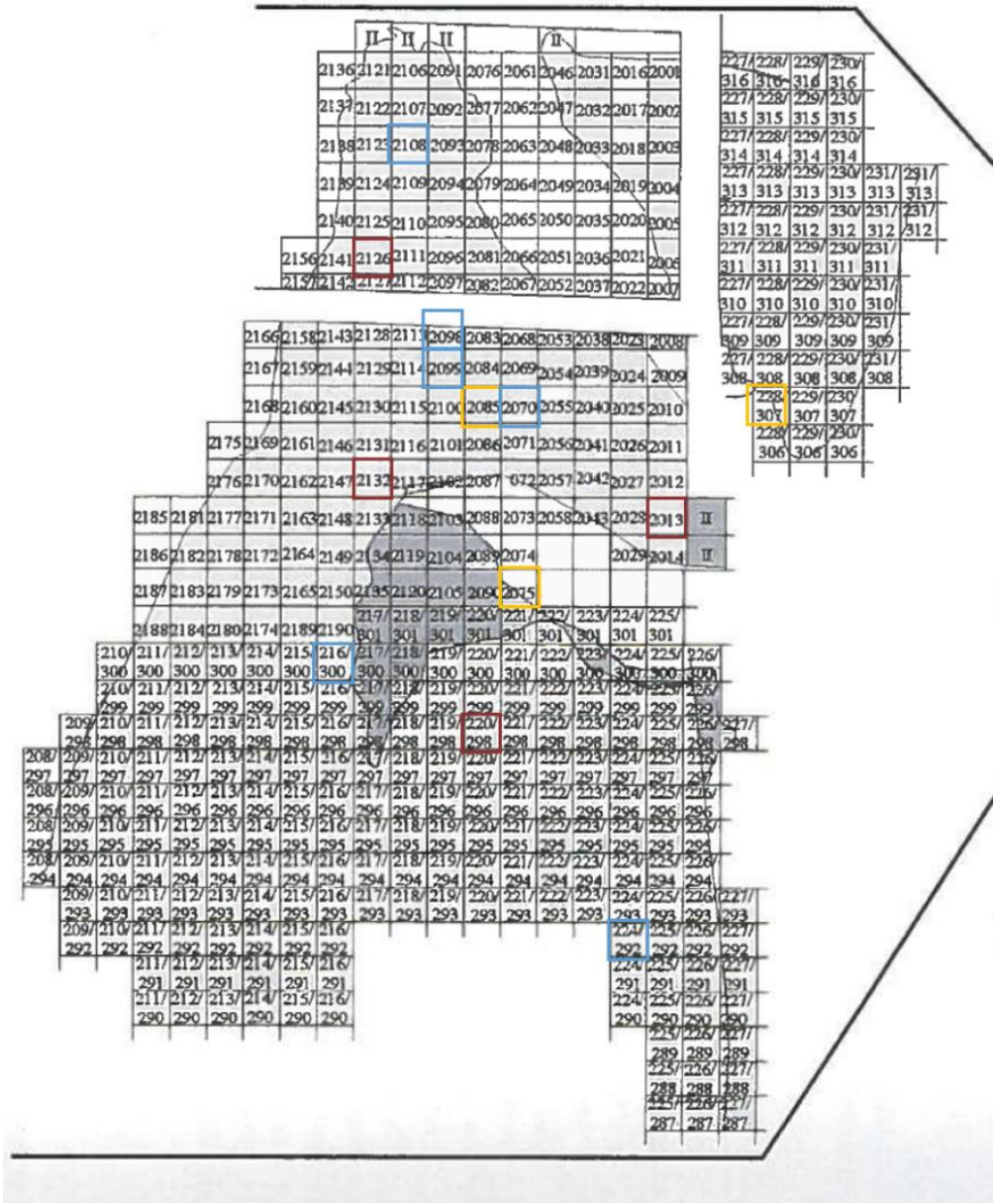

Figure 7.2: Excavation grid with the squares where the teeth were found highlighted. The colours correspond to the colours in figure 6.1 and table 6.2 and represent the statistically different groups. The yellow squares correspond to the three teeth that do show a significant difference with any other tooth and are represented with the grey colour in figure 6.1 and table 6.2. As can be seen, there is no obvious geographical pattern visible (after Kindler et al, 2014, p. 198).

Britton et al. (2012) analysed bone collagen from both *Bos* and *Equus* species from NMN2 for stable carbon and nitrogen isotopes. They analysed individuals from layer NN2/2 and all its three sublayers (a, b, and c). The results of the *Equus* (n = 6) from layer NMN2/2b will be discussed and compared to my tooth enamel results in this thesis. The nitrogen results will be discussed below (section 7.5). The average $\delta^{13}C_{collagen}$ value of the equids analysed by Britton et al. (2012) is -21.5 ± 0.5 ‰. This value cannot be directly compared to the $\delta^{13}C$ values produced in this research, because they were measured on collagen while the results here are determined based on enamel powder. These two different tissues have different enrichment factors between their $\delta^{13}C$ values and the $\delta^{13}C$ values of the diet. Here, the calculated $\delta^{13}C$ values of the diet will be compared. The enrichment factor between $\delta^{13}C_{diet}$ and $\delta^{13}C_{collagen}$ is between +3.7 and +6 ‰ (Bocherens & Drucker, 2003), but Britton et al. (2012) mentions an enrichment factor of around +5 ‰, which is the value used here. This would make the average $\delta^{13}C$ of the diet of the equids analysed by Britton et al. (2012) around -26.5 ± 0.5 ‰. Even though this value is 0.7 ‰ lower than the average $\delta^{13}C_{diet}$ of the equids analysed in this study (-25.8 ± 1.4 ‰), it still falls within the 1σ of the average, as well as within the range of the $\delta^{13}C_{diet}$ calculated in this study (-24.1 – -26.6 ± 1 ‰). This shows, in combination with the fact that the enrichment factor between $\delta^{13}C_{diet}$ and $\delta^{13}C_{collagen}$ covers several permille, that the equids analysed by Britton et al. (2012) and the equids analysed presently had a diet with the same $\delta^{13}C$ values, which is expected since they lived during the same short period at the same locality.

The isotopic values of collagen and enamel do not necessarily reflect the same period in the life of an individual. As explained in chapter 3, enamel mineralizes during a specific period of an animal's life and only captures the isotopic values during that time frame. In contrast, bone collagen remodels throughout life and is completely replaced after a number of years, depending on the species (e.g. Vander Zanden et al., 2015). This means that isotopic values of bone collagen reflect the last years of life. As the age of the horses analysed by Britton et al. (2012) is unknown, it is impossible to say if they represent the same period of life as the enamel does. However, the fact that the $\delta^{13}C$ values of both the collagen and enamel are the same could indicate that the equids fed on a diet source with the same $\delta^{13}C$ values during their life.

J. N. Leichliter (personal communication, March, 2023) analysed both enamel and bone material of different herbivore, omnivore, and carnivore species from Neumark-Nord 2, including five equids. The equid material is made up of a right maxillary second premolar and three left inferior third molars. All enamel samples were analyzed with the cold trap for stable carbon and oxygen isotope analysis and with the *oxidation-denitrification* method for nitrogen isotope analysis.

Only the $\delta^{13}C$ values of the third molars will be compared to my data, because those are the only type that was analysed in this research. The average of the $\delta^{13}C_{enamel}$ values of the three third molars analysed by Leichliter is -12.5 ± 0.1 ‰, which corresponds well with the presently measured $\delta^{13}C_{enamel}$ value of -12.3 ± 0.4 ‰.

7.4 Oxygen

As mentioned in section 7.2, some enamel samples (n = 6) nearest to the cervical margin show an increase in their $\delta^{13}C$ and/or $\delta^{15}N$ values compared to the value of the rest of the teeth. However, none of these samples show this pattern in their $\delta^{18}O$ values. Even when, as a control, excluding the cervical margin samples with higher $\delta^{13}C$ values from the $\delta^{18}O$ average, the average, standard deviation and range of $\delta^{18}O$ values do not change. So, these samples will be included in all analyses and comparisons of the $\delta^{18}O$ values.

To calculate the $\delta^{18}O$ of the body water of the equids, which equates to drinking water (e.g., Pederzani & Britton, 2019), the measured $\delta^{18}O$ values need to be transformed to the correct values in three steps. First, it is necessary to recalculate $\delta^{18}O_{enamel}$ from the values calibrated with the VPDB standard to VSMOW standard values. This standard is used to calibrate $\delta^{18}O$ measurements of oxygen isotopes in phosphate and water. Second, the $\delta^{18}O$ values were measured on the carbonate part (CO_3) of the enamel. This needs to be recalculated to $\delta^{18}O$ values of phosphate (or PO_4), because the phosphate oxygen values are necessary for the next calculation. The last step is to transform the enamel $\delta^{18}O_{PO4}$ values to $\delta^{18}O_{bodywater}$ by using the fractionation equation between body water and phosphate in enamel. Each step will be detailed below for this study. A list of equations can be found at the beginning of this thesis (p. 10).

The $\delta^{18}O_{VPDB}$ values were recalculated to carbonate $\delta^{18}O_{VSMOW}$ values using the IUPAC recommended equation (Brand et al., 2014; Kim et al., 2015), which is based on the equation listed in Coplen et al. (1983), as mentioned in chapter 4:

$$\delta^{18}O_{VSMOW} \approx 1.03092 * \delta^{18}O_{VPDB} + 30.92\ ‰ \quad (4)$$

The results of this first calculation per tooth are given in table 7.2. The average $\delta^{18}O_{VPDB}$ value of -6.2 ‰ is 24.6 ‰ $\delta^{18}O_{VSMOW}$.

As explained in chapter 4, to recalculate carbonate $\delta^{18}O_{VSMOW}$ (written as $\delta^{18}O_{CO3}$) to phosphate $\delta^{18}O_{VSMOW}$ (written as $\delta^{18}O_{PO4}$), the following formula is used (Iacumin et al., 2022):

$$\delta^{18}O_{PO4} + 1 \approx 0.9787 * (\delta^{18}O_{CO3} + 1) + 0.0142 \quad (5)$$

Table 7.2: $\delta^{18}O$ values recalculated from VPDB ($\delta^{18}O_{VPDB}$) to VSMOW ($\delta^{18}O_{VSMOW}$) per tooth, following equation 4.

MPIC ID	Average $\delta^{18}O_{VPDB}$ (‰)	Range $\delta^{18}O_{VPDB}$ (‰)	Average $\delta^{18}O_{VSMOW}$ (‰)	Range $\delta 18O_{VSMOW}$ (‰)
NMN-120	-5.9	(-7.2) – (-5.0)	24.9	23.5 – 25.8
NMN-121	-6.3	(-7.5) – (-5.0)	24.5	23.2 – 25.8
NMN-122	-6.7	(-8.7) – (-5.3)	24.1	21.9 – 25.5
NMN-123	-5.9	(-7.2) – (-4.9)	24.8	23.5 – 25.9
NMN-124	-6.0	(-7.0) – (-4.8)	24.7	23.7 – 26.0
NMN-125	-6.1	(-6.9) – (-4.6)	24.7	23.8 – 26.2
NMN-126	-6.5	(-7.8) – (-4.7)	24.3	22.9 – 26.1
NMN-127	-6.8	(-8.0) – (-5.9)	23.9	22.7 – 24.9
NMN-128	-5.9	(-7.1) – (-4.8)	24.8	23.7 – 25.9
NMN-129	-6.0	(-7.1) – (-4.7)	24.8	23.6 – 26.1
NMN-130	-6.0	(-7.7) – (-5.0)	24.7	23.0 – 25.8
NMN-131	-6.3	(-7.6) – (-5.4)	24.4	23.1 – 25.3
NMN-132	-6.2	(-7.1) – (-5.1)	24.5	23.6 – 25.7
NMN-133	-6.0	(-7.2) – (-5.0)	24.8	23.6 – 25.7
Total	**-6.2**	**(-8.7) – (-4.6)**	**24.6**	**21.9 – 26.2**

Multiple different sources have proposed equations to recalculate carbonate $\delta^{18}O$ to phosphate $\delta^{18}O$ over the past 25 years (Bryant et al., 1996; Iacumin et al., 1996; Miller et al., 2019; Pellegrini et al., 2011; Zazzo et al., 2004). However, the Iacumin et al. (2022) equation was chosen in this study, because it is the most recent one, as well as that it takes almost all previously mentioned sources in consideration.

In equation 4, the $\delta^{18}O$ values are not given in permille, but in the proportional delta values. (e.g., a $\delta^{18}O$ value of 24.7 ‰ would be given as 0.0247). The equation was rewritten in the same format as the Iacumin et al. (1996) equation, because this is the equation used in most $\delta^{18}O$ studies (e.g., Bershaw et al., 2010; Lüdecke and Leichliter et al., 2022) and gives values in permille. Iacumin et al. (1996) presented the following equation:

$$\delta^{18}O_{PO4} \approx 0.98 * \delta^{18}O_{CO3} - 8.5 \quad (9)$$

What stands out is that the slope of equations 5 and 6, as well as the others analysed by Iacumin et al. (2022), are equal (≈ 0.98). This means that only the y-intercept (the last number of equation 6: 8.5) has to be determined to rewrite equation 5 into the same format as equation 6. This was done by taking the average $\delta^{18}O_{CO3}$ value, recalculated to VSMOW using equation 4, of tooth NMN-120 (24.8 ‰) and converting it to the proportional delta value (0.0248). Then, equation 5 was used to calculate the phosphate $\delta^{18}O_{VSMOW}$ of tooth NMN-120:

$$\delta^{18}O_{PO4} + 1 = 0.9787 * (0.0248 + 1) + 0.0142$$

$$\delta^{18}O_{PO4} + 1 = 1.0172$$

$$\delta^{18}O_{PO4} = 0.0172$$

$$\delta^{18}O_{PO4} = 17.2 ‰$$

Next, the equation was rewritten in the proper format with an unknown y-intercept (x in the equation):

$$\delta^{18}O_{PO4} = 0.9787 * \delta^{18}O_{CO3} - x$$

To calculate x, the previously calculated $\delta^{18}O_{CO3}$, using equation 4, and $\delta^{18}O_{PO4}$, using equation 5, values in permille of tooth NMN-120 were filled in:

$$17.2 = 0.9787 * 24.8 - x$$

$$17.2 = 24.3 - x$$

$$x = 7.1$$

which leads to a rewritten formula of:

$$\delta^{18}O_{PO4} \approx 0.9787 * \delta^{18}O_{CO3} - 7.1 \quad (10)$$

The validity of this formula was checked by filling in the $\delta^{18}O_{CO3}$ values of three other, randomly chosen, teeth in both the original and rewritten Iacumin et al. (2022) equations (eq. 5 and 7), which gave the same $\delta^{18}O_{PO4}$ values for both equations in all cases. In addition, the difference between the $\delta^{18}O_{PO4}$ value calculated using the Iacumin et al. (1996) formula (equation 6) and the $\delta^{18}O_{PO4}$ value calculated using the rewritten Iacumin et al. (2022) formula (equation 7) is in all cases 1.4 ‰, which is also the difference between the y-intercept values for both equations (8.5 – 7.1 = 1.4). This shows that equation 7 is rewritten correctly and that the most recent presented calculation gives $\delta^{18}O$ values of 1.4 ‰ higher than the previously used calculation. Table 7.3 shows the results of the carbonate to phosphate $\delta^{18}O$ calculations per tooth. The average $\delta^{18}O_{CO3}$ value of 24.6 ‰ is 16.9 ‰ $\delta^{18}O_{PO4}$.

The last step is to recalculate the $\delta^{18}O_{PO4}$ values of the enamel to $\delta^{18}O$ values of body water. This is done by using the formula (equation 3) given by Delgado Huertas et al. (1995) and following Pryor et al. (2014), as mentioned in chapter 4:

$$\delta^{18}O_{PO4} \approx 0.71 * \delta^{18}O_{bodywater} + 22.60 \quad (3)$$

or rewritten as:

$$\delta^{18}O_{bodywater} \approx (\delta^{18}O_{PO4} - 22.60) / 0.71$$

The results of this calculation are given in table 7.4. The average $\delta^{18}O_{PO4}$ value of 16.9 ‰ becomes a $\delta^{18}O_{bodywater}$ value of -8.0 ± 1.1 ‰. The results of the complete recalculation per sample (n = 259) are given in appendix D.

Table 7.3: $\delta^{18}O$ values recalculated from the VSMOW $\delta^{18}O_{CO3}$ to VSMOW $\delta^{18}O_{PO4}$ values per tooth, following equation 10.

MPIC ID	Average $\delta^{18}O_{CO3}$ (‰)	Range $\delta^{18}O_{CO3}$ (‰)	Average $\delta^{18}O_{PO4}$ (‰)	Range $\delta^{18}O_{PO4}$ (‰)
NMN-120	24.9	23.5 – 25.8	17.2	16.0 – 18.2
NMN-121	24.5	23.2 – 25.8	16.9	15.7 – 18.2
NMN-122	24.1	21.9 – 25.5	16.5	14.4 – 17.9
NMN-123	24.8	23.5 – 25.9	17.2	15.9 – 18.3
NMN-124	24.7	23.7 – 26.0	17.1	16.1 – 18.4
NMN-125	24.7	23.8 – 26.2	17.0	16.2 – 18.5
NMN-126	24.3	22.9 – 26.1	16.6	15.3 – 18.4
NMN-127	23.9	22.7 – 24.9	16.3	15.1 – 17.3
NMN-128	24.8	23.7 – 25.9	17.2	16.1 – 18.3
NMN-129	24.8	23.6 – 26.1	17.2	16.1 – 18.5
NMN-130	24.7	23.0 – 25.8	17.1	15.4 – 18.2
NMN-131	24.4	23.1 – 25.3	16.8	15.6 – 17.7
NMN-132	24.5	23.6 – 25.7	16.9	16.0 – 18.1
NMN-133	24.8	23.6 – 25.7	17.1	16.0 – 18.1
Total	**24.6**	**21.9 – 26.2**	**16.9**	**14.4 – 18.5**

Table 7.4: $\delta^{18}O$ values recalculated from $\delta^{18}O_{PO4}$ to the $\delta^{18}O$ values of body water per tooth, following equation 3.

MPIC ID	Average $\delta^{18}O_{PO4}$ (‰)	Range $\delta^{18}O_{PO4}$ (‰)	Average $\delta^{18}O_{bodywater}$ (‰)	Range $\delta^{18}O_{bodywater}$ (‰)
NMN-120	17.2	16.0 – 18.2	-7.6	(-7.6) – (-6.3)
NMN-121	16.9	15.7 – 18.2	-8.1	(-9.8) – (-6.3)
NMN-122	16.5	14.4 – 17.9	-8.7	(-11.6) – (-6.7)
NMN-123	17.2	15.9 – 18.3	-7.6	(-9.5) – (-6.1)
NMN-124	17.1	16.1 – 18.4	-7.7	(-9.2) – (-6.0)
NMN-125	17.0	16.2 – 18.5	-7.8	(-9.0) – (-5.8)
NMN-126	16.6	15.3 – 18.4	-8.4	(-10.3) – (-5.9)
NMN-127	16.3	15.1 – 17.3	-8.9	(-10.6) – (-7.6)
NMN-128	17.2	16.1 – 18.3	-7.6	(-9.2) – (-6.1)
NMN-129	17.2	16.1 – 18.5	-7.7	(-9.3) – (-5.9)
NMN-130	17.1	15.4 – 18.2	-7.8	(-10.2) – (-6.3)
NMN-131	16.8	15.6 – 17.7	-8.2	(-9.9) – (-6.9)
NMN-132	16.9	16.0 – 18.1	-8.0	(-9.3) – (-6.4)
NMN-133	17.1	16.0 – 18.1	-7.7	(-9.4) – (-6.4)
Total	**16.9**	**14.4 – 18.5**	**-8.0**	(-11.6) – (-5.8)

Equids are obligate drinkers. Therefore, they are likely to record stable oxygen isotope inputs from their water source(s) with great fidelity (e.g., Britton et al., 2019; Pederzani & Britton, 2019). An animal that is an obligate drinker is water dependant and thus requires a water source in addition to their diet to obtain enough water to survive. Furthermore, the $\delta^{18}O$ of body water of ungulate mammals is largely determined by their drinking water (e.g., Bershaw et al., 2010; Pederzani & Britton, 2019). In addition, based on juvenile bone development and biomass estimates, it has been suggested that equids were present year-round in the vicinity of NMN2 (Garcia-Moreno et al., 2015; Kindler et al., 2015; Kindler et al., 2020). This indicates that the $\delta^{18}O_{bodywater}$ values of the equids were partly determined by the $\delta^{18}O$ values of the water from the NMN2 lake. However, it needs to be noted that it is unlikely that NMN2 was the only drinking source used by the equids, because not only do horses have relatively large home ranges (e.g., Hennig et al, 2018; King, 2002), one other, larger water source, Neumark-Nord 1, was located immediately next to NMN2. This means that the $\delta^{18}O_{water}$ values calculated here are a combination of all the drinking sources used by each individual and do likely not directly correspond to $\delta^{18}O_{water}$ values from the NMN2 pool.

Milano et al. (2020) measured oxygen isotopes in freshwater molluscs from Neumark-Nord 2, to reconstruct palaeoenvironmental conditions. They also analysed $\delta^{18}O$ in modern freshwater molluscs for oxygen isotopes, as well as the water they were living in, in order to establish a calibration for the molluscs from NMN2. The small modern river where these molluscs and the water was taken from is called Hundewasser and is located about 30 km east of Neumark-Nord. The results of the water $\delta^{18}O$ values show a clear seasonal signal, with lower values in the winter months and higher values in the summer months, a similar cyclical signal is visible in the $\delta^{18}O$ results of the equid teeth analysed here. As the modern $\delta^{18}O$ values were measured on water collected close to NMN2, and the Eemian is considered to have had a similar climate as the present (e.g., chapter 2.3; Britton et al., 2019), it can be concluded that the $\delta^{18}O$ signal of the equids show the same seasonality, with the lower values corresponding to winter/colder periods and the higher values to summer/warmer periods during the year.

Based on the $\delta^{18}O$ results of molluscs from NMN2 compared to modern molluscs from Hundewasser, Milano et al. (2020) concluded that the isotopic composition of paleolake NMN2 was different from the modern Hundewasser water composition. This is likely due to the small size of the NMN2 lake, which might have been affected by evaporative processes, and to the fact that Hundewasser is a small river and not a small lake (Milano et al, 2020). In addition, the fact that the $\delta^{18}O$ values of the NMN2 molluscs do not correspond with the $\delta^{18}O$ values of Hundewasser water (Milano et al., 2020), but the $\delta^{18}O$ values of the equid tooth enamel analysed here do, indicates that

the equids did not have NMN2 as their only water source. In the case that the equids did only get their water from the NMN2 pool, it would have been expected that their $\delta^{18}O$ values would corresponds with the $\delta^{18}O$ values of the molluscs, because these lived in the NMN2 paleolake, which was thus their only source of water. This again indicates that the $\delta^{18}O$ values of drinking water calculated in this study likely represent the average of different types of water sources in the area surrounding NMN2.

The water samples collected from Hundewasser have $\delta^{18}O$ values, calibrated against VSMOW, between approximately -6.5 and -8.1 ‰ (range = 1.6 ‰; Milano et al., 2020). The range of $\delta^{18}O$ values of the water at NMN2 calculated here, is between -11.6 and -5.8 ‰ (see table 7.4). It is not unexpected that the total range of $\delta^{18}O$ values of the equid teeth is much wider than the Hundewasser values. This is might be connected with the fact that water from Hundewasser was only collected and measured over a single year. In contrast, the $\delta^{18}O$ values of the equid teeth were collected from layer NMN2/2b, which spans roughly 455 years. In these four and a half centuries, it is possible, and highly likely, that some summers were hotter and some winters were colder than the ones in the single year measured at Hundewasser. This results in the summer extremes of the $\delta^{18}O$ values among the equids to be higher and the winter extremes to be lower, and thus the total range of $\delta^{18}O$ values to be larger, than the $\delta^{18}O_{water}$ range of Hundewasser.

The range of $\delta^{18}O_{water}$ values in each analysed molar is larger than the 1.6 ‰ range measured at Hundewasser. The average range of $\delta^{18}O_{water}$ values in each individual is 3.4 ± 0.6 ‰, and all ranges are above 2.8 ‰. This might indicate that the temperature differences between summer and winter, and their related $\delta^{18}O_{water}$ values, were bigger in the Eemian compared to the present day. A recent study on seasonal variations of modern lake water $\delta^{18}O$ values in north eastern Germany shows a maximum range of about 2.5 ‰ in one lake (Aichner et al, 2022). This range in $\delta^{18}O$ values was measured in the shallowest lake in the river-lake system over a period of eight months (Aichner et al, 2022). This modern lake water $\delta^{18}O$ range is still lower than the ones observed in the equid teeth, which could indicate that the temperature differences between summer and winter would indeed have been larger in the Eemian than in the present day. However, it would be necessary to measure more than one consecutive year of modern lake water, preferably in multiple, smaller lakes, some of which are part of a closed system, to confirm this hypothesis, because the equids analysed here likely drank from multiple water sources, one of which was NMM2, a small, shallow, closed lake.

Each tooth studied in this research should encompass around three years of growth based on the maximum length of the tooth (see table 5.2, p. 50) in combination with the mineralisation rates of modern horse teeth (3 cm/year for third molars; chapter 3; Hoppe, Stover, et al., 2004). When looking at the maximum length that was sampled, each tooth should represent a little less than two years to

almost three years of tooth growth (table 5.2). In contrast, in most $\delta^{18}O_{enamel}$ graphs, around two years of time is represented, based on the seasonal signal of high values in summer and low values in winter. This is likely in part related to the fact that, as shown by Bendrey et al. (2015) and explained in chapter 3, modern horse teeth show an exponentially decreasing tooth growth rate over time. This means that the earliest mineralized enamel has the least time-averaging visible in the stable isotope values, whereas the latest mineralized enamel has the most time-averaging. In case the teeth were already erupted and experienced wear, the enamel that is still present and sampled in this study, contains a more time averaged $\delta^{18}O$ signal than when the earliest formed enamel was still present, and this time-averaging increases the closer the samples get to the root of the tooth.

All of this is visible in the $\delta^{18}O$ graphs (figure 6.2 and 6.3), which show that the dips and peaks are much narrower on the left of the graphs, and correspond to the samples that are nearest to the root. Furthermore, when there is time averaging present, one would expect the high and low $\delta^{18}O$ values closest to the root to be less extreme than the high and low $\delta^{18}O$ values closest to the occlusal surface. This is visible in most of the graphs (e.g. tooth NMN-121, NMN-123, and NMN-126). In addition, slower mineralization rates can result in such big time averaging that one sample could have mineralized over months. This could result in the $\delta^{18}O$ value of that specific sample representing all of the warmer months of a year in a single point. This possibility makes it hard to interpret the $\delta^{18}O$ graphs of the teeth near the root. For example, in tooth NMN-121, it is difficult to determine if NMN-121b represents all of the colder months of a year and NMN-121c all of the warmer months in one point or if they represent an average of two colder and two warmer months respectively. With the interpretation here, a conservative estimation is given on how much time is represented in the $\delta^{18}O$ graphs of each tooth (about two years).

Of note is that in some other teeth (e.g., NMN-130) the values of either the winter or summer season closest to the root are more extreme than the one present closer to the occlusal surface. This could be due to the year in which the root enamel mineralized having a relatively large difference in temperatures (either higher or lower) than the year(s) previously, in which the enamel closer to the occlusal surface mineralized. This could result in $\delta^{18}O$ values that, even after time averaging, are still lower than the $\delta^{18}O$ values of the previous year which are affected by less time averaging.

The average length that covered a complete year based on $\delta^{18}O$ values in the tooth enamel of the equid teeth analysed in this study, is 34 mm. This length is calculated excluding both the samples near the root, because of slower mineralization rates and potential diagenetic alterations, and the samples near the occlusal surface, because this surface can be used for other analyses, like microwear analysis, and it should thus be avoided in order to not damage it. In two teeth (NMN-125 and NMN-132), a full year based on $\delta^{18}O$ values is covered by samples spanning 41 mm along the length of the

tooth. Based on these results, it is recommended to sample around 35 to 40 mm of enamel along the length of the tooth roughly in the middle of the buccal or lingual side, when bulk sampling caballoid horse teeth for $\delta^{18}O$ analysis.

The breeding season of modern domesticated horses in the Northern Hemisphere starts in April and ends at the beginning of October (e.g., Trundell, 2020). The average gestation period is 11 months, but can vary anywhere between 10.5 and 13 months (Abraham, 2014). This means that foals are generally born between early spring and mid-autumn. In addition, as explained in chapter 3, equid third molars start to mineralize around 21 months of age, with a variation of roughly three months based on the various growth rates of individuals (Hoppe, Stover et al, 2004). This shows that third molars can start mineralizing in any season of the year, but this is dependent on the season of birth and individual growth. Furthermore, as soon as these teeth erupt, they begin to wear down in the same direction as they mineralize (crown to root, chapter 3), which means that the season of initial mineralization is the first that is removed from the isotopic record of that tooth. All of this is to say that it is nearly impossible to make a prediction on what part of the enamel mineralizes in what season.

As mentioned above, Leichliter (personal communication, March, 2023) analysed horse teeth from NMN2, including three third molars. The cold trap results of these molars show an average $\delta^{18}O_{VPDB}$ value of -8.2 ± 2.0 ‰, which falls outside of the 1σ range of the average $\delta^{18}O_{VPDB}$ analysed here (average = -6.2 ± 0.8 ‰). However, the average does fall within the range of $\delta^{18}O_{VPDB}$ measured in this study (-8.7 – -4.6 ‰). Considering that these samples were bulk samples, it is possible that the $\delta^{18}O$ values are skewed due the sample only including tooth enamel that mineralized during the warm months or during the cold months. Seeing as the average $\delta^{18}O_{VPDB}$ value (-8.2 ± 2.0 ‰) measured by Leichliter is on the low side of the range measured here (-8.7 – -4.6 ‰), the enamel likely mineralized during winter, since it is a relatively low $\delta^{18}O$ value.

Britton et al. (2019) analysed 26 equid teeth from Neumark-Nord 2, including eight from layer NMN2/2b, for oxygen isotopes in order to reconstruct paleotemperatures during the early Eemian and early Weichselian. They took a bulk sample of enamel along the growth axis of each tooth (~3-3.5 cm in length), to ensure the coverage of a full year of growth and eliminate the seasonal signal according to the growth rate of equid (pre)molars established by Hoppe, Stover, et al. (2004). The NMN2/2b samples analysed by Britton et al. (2019) show a mean $\delta^{18}O_{PO4}$ value of 16.1 ± 0.4 ‰ (1 σ) with a range between 15.6 and 16.9 ‰. This value falls within the range of the calculated $\delta^{18}O_{PO4}$

values of the samples analysed in this study, which range between 14.4 and 18.5 ‰ (see table 7.3). This indicates that even though the $\delta^{18}O$ values were measured on different parts of the enamel (phosphate in case of Britton et al. (2019) and structural carbonate in the present study), the results are the same. The range of the $\delta^{18}O$ values of this study is larger than the one of Britton et al. (2019), which is the results of the different sampling strategies. This study employs serial sampling and thus includes summer and winter extremes, whereas bulk sampling, as done by Britton et al. (2019), resulted in the averaging of the $\delta^{18}O$ values over the year and thus a smaller range.

The $\delta^{18}O$ values of water calculated by Britton et al. (2019) show a mean value of -9.1 ± 1.1 ‰ in layer NMN2/2b. This looks different from the mean $\delta^{18}O$ value of water (-8.0 ± 1.1 ‰) calculated in this study, but both the averages fall within 1σ of the other average. The difference might have been caused by the fact that Britton et al. (2019) used bulk samples, which might not have covered the complete year, and the present study used serial samples.

7.5 Nitrogen

The average of the $\delta^{15}N$ values of all samples (n = 72) is 3.5 ± 0.6 ‰, with an amplitude of 2.4 ‰. This amplitude is lower than the differences between trophic levels (3 – 5 ‰, chapter 4). This is expected, since only a single species was analysed in this study, which thus falls within a single trophic level. When excluding the samples that might be affected by diagenesis due to incomplete mineralization (NMN-126a and NMN-129a), as mentioned in section 7.2, the average $\delta^{15}N$ value and standard deviation do not change. For the rest of the analyses and comparisons of the $\delta^{15}N$ values, only the completely analysed teeth (NMN-126, NMN-130, and NMN-133), including root samples, will be used.

The variation in $\delta^{15}N$ values, as well as the statistical separation between the three teeth ($\chi^2(2) = 34.99$, $p < 0.001$), can be explained by differences in $\delta^{15}N$ values of the plants in the diet of the equids. As explained in chapter 4, there are relatively few factors relating to the physiology of animals that impact the $\delta^{15}N$ values of their tissues. In addition, the individuals that are analysed here all belong to the same species, so even if the $\delta^{15}N$ values of animals were majorly affected by their physiology, this is not expected to be visible in members of the same species, since they have the same physiology. The range of $\delta^{15}N$ values visible in the three completely analysed teeth will, thus, be discussed based on differences in plant $\delta^{15}N$ and how likely certain aspects were present in the environment surrounding NMN2.

The range of factors affecting plant $\delta^{15}N$ is very extensive, however there are a couple that are more likely to have been at play at Neumark-Nord 2. This includes denitrification, which is likely to occur in swampy shallow water (Muzuka, 1999) and could have been present at NMN2. This results

in plants that prefer to take up ammonium (NH_4^+) having a higher $\delta^{15}N$ than plants that prefer to take up nitrate (NO_3^-; e.g., Szpak, 2014). The individuals analysed here lived spread over a period of around 455 years (chapter 2, Sier et al., 2011). So, in the case that equids eat ammonium plants preferentially, the individual to which tooth NMN-126 belongs could have lived in a period with less denitrification than the other two individuals, since the $\delta^{15}N$ values of NMN-126 are substantially lower than the values of the others. In the case that they lived in the same period, the difference between the $\delta^{15}N$ values of the individuals might partially be explained by NMN-126 incorporating a great proportion of nitrate plants in their diet compared to ammonium plants, whereas NMN-133 would have incorporated a great portion of ammonium plants and thus have a higher $\delta^{15}N$ value average.

Higher salinity in the soil can also cause enriched $\delta^{15}N$ values in plants (e.g., Guiry et al., 2021; Muzuka, 1999). This could partially explain the difference in $\delta^{15}N$ values between the teeth in the case the individuals did not live during the exact same time. Salinity results in an overall enrichment of the $\delta^{15}N$ values of plants, and thus also of animals, NMN-130 and NMN-133 may have lived in a period where NMN2 contained more brackish water and the environment was more saline than during the period NMN-126 lived.

As Codron et al. (2005) showed, there can be a difference of up to 4 ‰ in $\delta^{15}N$ values between plants from different microhabitats within the same ecosystem, as well as a nearly 6 ‰ difference between different grass species. However, this study uses a savannah habitat in South Africa and the grass species studied were all C_4 plants, as explained in chapter 4. This means that these variations cannot be directly applied to Neumark-Nord 2, because the site represents a single microhabitat with only C_3 grasses, forbs, and shrubs as potential food sources for the equids. Such variation in $\delta^{15}N$ values should be separately established for European habitats with C_3 plants. In addition, Codron et al. (2005) suggest that the major reason for the variability observed in $\delta^{15}N$ values is the difference in soil type and climate between the different microhabitats. To see if this might be a reason for $\delta^{15}N$ variety at Neumark-Nord, the surrounding areas need to be tested on past soil type and climate.

In an experimental setting, Bonafini et al. (2013) grew four grass species native to the UK, all C_3 grasses, and measured each individual plant for $\delta^{13}C$ and $\delta^{15}N$ in different environments. The first measurement was based on individuals that all endured the same exact circumstances and showed a maximum difference between species of 4.1 ‰ in $\delta^{15}N$ and a range of 0.5 to 1.2 ‰ between individuals of a single species. This already gives an indication that the differences in $\delta^{15}N$ values between the equids seen here could be explained by different proportions of different grass and shrub species in their diet. This is even more likely when taking into consideration the results of the pollen analysis, which shows that a wide variety of plants were present at NMN2 (Appendix A; Sier et al., 2011). However, this should further be investigated in a wild setting, since the plants might respond

differently when growing in varying and uncontrolled environmental conditions. This could result in either less variation in the $\delta^{15}N$ values between or within plants species or, what is more likely, even more variation between species.

There are a number of factors related to plant physiology that can impact the $\delta^{15}N$ values of plants. Plants that can form a relationship with arbuscular mycorrhizal fungi (roughly 90 % of plant species) are about 2 ‰ more depleted in $\delta^{15}N$ than non-mycorrhizal plants (Craine, Elmore, et al., 2009; Schmidt & Stewart, 2003). When equids incorporate different kind of proportions of such plants in their diet, the overall $\delta^{15}N$ values of their tissues will differ from one another.

Different plant parts/organs can also have different $\delta^{15}N$ values. As explained in chapter 4, there is nearly always a difference between leaf and root $\delta^{15}N$ of plants, as well as stems and seeds in some cases (e.g., Codron et al., 2005; Dijkstra et al., 2003; Evans et al., 1996). When horses are grazing, they usually only eat the leaves of the grass, shrubs, or herbs. An individual that ingests a lot more roots, seeds, or stems than another might have a different average $\delta^{15}N$ value in their tissues. The amount of variation in $\delta^{15}N$ values between plant parts, however, is also dependent on the species of plant.

Summarizing, the variation in $\delta^{15}N$ between and within the three teeth likely reflects variation in the $\delta^{15}N$ values of the plants that these individuals consumed. The near complete separation in values between NMN-126 and NMN-133 (figure 7.3) might indicate that these two equids had a different food source. However, this is not necessarily the case, because even individuals of the same species that were fed the exact same diet in an experimental setting show $\delta^{15}N_{enamel}$ variations (Leichliter et al., 2021, Suppl. table A2). In addition, wild individuals of the same species living in the same natural environment (Gorongosa National Park) also show variation in their $\delta^{15}N_{enamel}$ (Lüdecke and Leichliter et al., 2022).

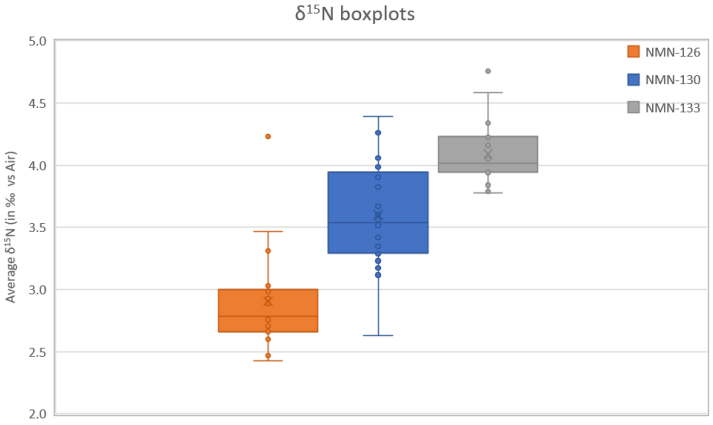

Figure 7.3: Boxplots of the $\delta^{15}N$ values of the three completely analysed teeth. Boxplots shows the interquartile range, with the median indicated by the solid line and the mean indicated by the x. Note the near complete separation of δ15N values of tooth NMN-126 and tooth NMN-133.

As mentioned above, Britton et al. (2012) performed stable carbon and nitrogen isotope analysis on collagen of equids and bovids from Neumark-Nord 2. In contrast to $\delta^{13}C$ values in collagen and enamel, $\delta^{15}N_{collagen}$ values can be directly compared to $\delta^{15}N_{enamel}$ values. The important thing to note with such

a comparison, is that collagen represents the last couple of years of life, while enamel represents the period of life during which it mineralized, as explained above. The average $\delta^{15}N_{collagen}$ value of equids measured by Britton et al. (2012), is 3.6 ± 0.6 ‰, excluding the individual from layer C. This corresponds perfectly with the average $\delta^{15}N_{enamel}$ value (3.5 ± 0.6 ‰) measured in the present study. Furthermore, the range in equid $\delta^{15}N_{collagen}$ (2 ‰) also corresponds well with the range in $\delta^{15}N_{enamel}$ (2.4 ‰).

After comparing the $\delta^{15}N_{collagen}$ values of equids to the ones of bovids, Britton et al. (2012) reports a niche separation between these two species, with bovids having around ca. 2 ‰ higher $\delta^{15}N$ values. The range of $\delta^{15}N_{collagen}$ values of both species combined is between 2.6 and 6.7 ‰ for layer NMN2/2b. This range and the separation of species show that the variation in $\delta^{15}N$ of plants at NMN2 is larger than just the variation observed in the equids analysed here. This confirms the importance to include different herbivore species to capture the entire $\delta^{15}N$ variation that is present at the base of a trophic food web.

The nitrogen values from Leichliter (personal communication, March, 2023) of equid third molars from NMN2/2b are 4.8 ± 1.1 ‰ (n = 3) on average, with a range between 3.3 and 5.8 ‰. The average is much higher than the one measured in the present study (3.5 ± 0.6 ‰) and falls outside of the 1σ. The average is just on the outer range of the $\delta^{15}N_{enamel}$ values measured in the serial samples (2.4 – 4.8 ‰), as well as outside the range of $\delta^{15}N_{collagen}$ values measured by Britton et al. (2012; 2.6 – 4.6 ‰). However, it has to be noted that Leichliter measured only three bulk enamel samples of equid third molars for $\delta^{15}N$, of which two in duplicate and one only a single time. If the single measured sample is excluded, the average drops to 4.3 ± 1.0 ‰, with a range between 3.3 and 5.3 ‰. In addition, the $\delta^{15}N_{enamel}$ values measured by Leichliter do fall in the range of the $\delta^{15}N_{collagen}$ values when combining both the $\delta^{15}N_{collagen}$ values from equids and bovids from NMN2/2b (Britton et al., 2012). Concluding, the Leichliter NMN sample set is very small and even though the $\delta^{15}N$ values do not fall within the values measured in this study, they do still fall within the range of $\delta^{15}N$ values of herbivores in layer NMN2/2b.

An interesting result of the nitrogen isotope analysis is the significant large positive correlation between $\delta^{15}N$ and nitrogen content. The pattern persists when including all samples (n = 72; Pearson correlation: $r(70) = 0.698$, $p < 0.001$), or when excluding the root samples (NMN-126a and NMN-129a; n = 70; Pearson correlation $r(68) = 0.728$, $p < 0.001$). This shows that this correlation is not driven by the root samples, which might not be fully mineralized yet and might be affected by diagenetic alteration, as explained in section 7.2.

A correlation between nitrogen content and $\delta^{15}N$ could be associated with diagenesis. Nitrogen can be removed from enamel that is affected by diagenesis. Leaching follows rule 1 of fractionation, which states that the lighter isotope (in this case ^{14}N) reacts faster than the heavier isotope (^{15}N), which results in the source being depleted in ^{14}N and enriched in ^{15}N and thus a having a higher $\delta^{15}N$. In addition, leaching means that the overall nitrogen content decreases, since nitrogen is taken out of the enamel. The correlation between $\delta^{15}N$ values and N-content would thus be a negative correlation: the lower the N-content, the higher the $\delta^{15}N$ value of the tissue, since it is depleted of ^{14}N. However, the fact that the correlation observed here is positive instead of negative, in combination with the other points on why the samples from NMN2 were likely not diagenetically altered, as explained in section 7.2, means that the positive correlation needs to be explained using a different hypothesis.

A potential theory could revolve around the amino acids, proteins, and proteases involved with enamel mineralization. During mineralization, the organic content of enamel decreases (e.g., Gil-Bona & Bidlack, 2020), and thus the amount of organic nitrogen in the enamel also decreases. In case the proteins and proteases that are involved in enamel maturation preferentially extract the heavy isotope ^{15}N from the mineralizing enamel, this would result in both the $\delta^{15}N$ value as well as the nitrogen content of the enamel to drop. However, to confirm such a mechanism, more research is necessary. For example, non-mineralized enamel could be analysed and compared to mineralized enamel, preferably of the same individual. This was already done on a small sample set (n = 4) in modern rodents teeth, which showed a higher nitrogen content in immature enamel, but a lower $\delta^{15}N$ value (Leichliter et al, 2021). However, mammals might have a completely different enamel mineralization mechanism compared to rodents. Such an experiment would thus preferably be done on modern horses, or other mammals, to avoid diagenetic alteration of immature enamel, as well as that the diet can be controlled and analysed for $\delta^{15}N$ and N-content. Serial sampling a still-mineralizing third molar would be best for such a study, because then there is no weaning signal and the mature and immature enamel of the same tooth can be compared. Another option would be to study the processes responsible for and proteins involved with enamel mineralization in more detail. This is already happening with the recent advances in proteomic analyses (e.g., Gil-Bona & Bidlack, 2020).

The nitrogen content of the equid teeth (average = 3.1 ± 0.4 nmol/mg, range = 2.6 – 4.9 nmol/mg) falls within the range of previously reported values for modern mammals (Leichliter and Lüdecke et al., 2023; Lüdecke and Leichliter et al., 2022). However, the here analysed nitrogen contents are low within this reported range. This is likely not an effect of diagenesis, as thoroughly discussed above. Leichliter (pesonal communication, March, 2023) analysed enamel of multiple different species at

NMN2, whose results also show a relatively low N-content (3.6 ± 1.1 nmol/mg). Since not only equids but also other species, including omnivores and carnivores, from NMN2 have a relatively low nitrogen content in their enamel, it is likely that an aspect of the locality is responsible for this and not a species-specific aspect. Such an aspect might be related to the climate or soil nitrogen content, but more research is necessary to establish this.

7.6 Pairing of Carbon, Oxygen, and Nitrogen

As explained in chapter 5, preferentially left superior/maxillary third molars were selected to ensure the analysis of different individuals. However, this was not possible for all teeth, and thus third molars from different positions were also selected. In order to avoid analysing the same individual, the teeth were selected from completely different squares of the excavation (see figure 5.1 and table 5.1). Third molars mineralize around the same age in equids, and a single individual has a specific diet at that time, it is expected that third molars from the same individual show the same $\delta^{13}C$, $\delta^{18}O$, and $\delta^{15}N$ values compared to the distance from the root. As can be seen in figure 6.1, 6.3, and 6.4, none of the teeth analysed show a complete overlap in all three values. This indicates that the fourteen molars did in fact belong to fourteen different individual horses that died near the NMN2 lake during the 455 years in which the layer NMN2/2b formed (MNI = 14).

As shown in the previous chapter, there are four teeth that demonstrate a significant correlation between $\delta^{13}C$ and $\delta^{18}O$, based on a Pearson correlation (table 6.5). The four teeth all show a similar relationship between $\delta^{13}C$ and $\delta^{18}O$, namely a medium to large positive one. This indicates that this correlation is likely caused by the same mechanism in each of these four individuals.

A positive variation between two variables means that if one increases in value, the other does as well. In this case, as the higher $\delta^{18}O$ values have been established to represent summer, while the lower values represent winter, the higher $\delta^{13}C$ values are also present in summer, and the lower ones in winter. This is likely due to the reduction of stomatal conductance in plants during summer in order to decrease water losses, as explained in chapter 4. This results in an increase in $\delta^{13}C$ values of plants and thus also an increase in $\delta^{13}C$ values in the enamel of herbivores. However, even though this mechanism was probably active at NMN2, it did not play a major role, because only four out of fourteen teeth show a correlation between $\delta^{13}C$ and $\delta^{18}O$. Furthermore, the R^2 value of the significant correlations are relatively small (R^2 = 0.24 for NMN-121, R^2 = 0.33 for NMN-122, R^2 = 0.37 for NMN-124, and R^2 = 0.36 for NMN-132). The R^2 value of a correlation correspond with the amount of variation in one variable that can be explained by the variation in the other variable. For example, the R^2 value for tooth NMN-132 is 0.36. This means that 36 % of the variation in $\delta^{13}C$ values of this tooth can be

explained by the variation in the $\delta^{18}O$ values. This also shows that 64 % of the variation in $\delta^{13}C$ values cannot be explained by seasonality (or $\delta^{18}O$ values) and thus needs to be explained in a different way, as done in section 7.3.

Focusing in on the three teeth that were analysed for all three isotopes (NMN-126, NMN-130, and NMN-133), there is no correlation between the $\delta^{13}C$ and $\delta^{18}O$ values as mentioned above. In contrast, there is a large positive relationship between the $\delta^{13}C$ and $\delta^{15}N$ of teeth NMN-126 ($r(17) = 0.723$, $p < 0.001$) and NMN-133 ($r(16) = 0.633$, $p = 0.005$; figure 6.5a and c and table 6.6). Furthermore, the R^2 value is relatively high for both teeth: 0.52 for NMN-126 and 0.40 for NMN-133. As explained above, this means that 52 % of the variation in $\delta^{13}C$ in tooth NMN-126 can be explained by the variation in $\delta^{15}N$. However, as explained in sections 7.3 and 7.5, there are a lot of factors possibly influencing the $\delta^{13}C$ and $\delta^{15}N$ values observed in these teeth. It is likely that, due to the statistical significance, the correlation is caused by a mechanism that influences both $\delta^{13}C$ and $\delta^{15}N$ in a similar manner, because the relationship is positive. The variation in both $\delta^{13}C$ and $\delta^{15}N$ in the equid enamel is expected to be based on variation in the $\delta^{13}C$ and $\delta^{15}N$ values of the plants, which the individuals ate, because there are no physiological factors that influence $\delta^{15}N$ values, as explained in chapter 4.

Tooth NMN-130 does not show a correlation between its $\delta^{13}C$ and $\delta^{15}N$ values ($p = 0.306$), but a very small negative relationship between its $\delta^{15}N$ and $\delta^{18}O$ values ($r(24) = 0.441$, $p = 0.024$). A negative relationship means that if, in this case, the $\delta^{15}N$ value increases, the related $\delta^{18}O$ value decreases (figure 6.5b and table 6.7). This indicates that during the winter/cold season, the $\delta^{15}N$ values where higher compared to the values during summer/warm season. However, it has to be noted that the R^2 value is relatively low (0.19) and that the relationship is small. Taken together this shows that 19 % of the variation in $\delta^{15}N$ values can be explained by variation in $\delta^{18}O$ values, but that the amount of $\delta^{15}N$ variation, relative to related $\delta^{18}O$ variation, is very small.

Lazzerini et al. (2019) observed seasonal variation in $\delta^{15}N$ in tail hairs of modern horses in Mongolia. Because hair grows much faster than enamel mineralizes, and the authors samples the hair over an extended period of time, their resolution on the time scale is much greater. The pattern in $\delta^{15}N$ values in equid tail hair observed by Lazzerini et al. (2019) does not correspond with the pattern visible in the $\delta^{15}N$ of the equid enamel from NMN2. First of all, the variation within a year is much greater in hair than in enamel. This can potentially be explained by the fact that hair grows faster and that there is time averaging present in enamel, as explained in chapter 3. In addition, based on the negative correlation of $\delta^{15}N_{enamel}$ with $\delta^{18}O_{enamel}$, we would expect higher $\delta^{15}N_{hair}$ values in winter and lower ones in summer if the same mechanism would have worked at NMN2 and in Mongolia. This

does not seem the case, as the only part of the patterns that overlap is when the $\delta^{15}N$ in Mongolia decreases for two months in the summer, due to a change in the diet of the horses.

Based on this comparison, it is clear that the correlation between $\delta^{15}N$ and $\delta^{18}O$ is not driven by an increase in melt water, since this would result in a positive correlation. It is possible that the individual at NMN2 shifted its diet source to a group of plants with a slightly lower $\delta^{15}N$ value during summer. However, since this correlation is only visible in a single individual and it is a very small relationship, the mechanism responsible for it did likely not play a major role at the Neumark-Nord locality. Future research should address if this is also the case at other localities in different environments.

7.7 Recommendations and future research

Based on the $\delta^{18}O$ results of the equid teeth discussed in section 7.4, it is recommended for future studies focussing on stable oxygen isotope analysis in bulk samples of enamel from the third molars of caballoid *Equus sp.* in a similar environment to Neumark-Nord, to sample at least 35 to 40 mm along the growth axis of the tooth. This is to make sure that the sample covers an entire year of mineralization in enamel and thus represent a correct average value of $\delta^{18}O$ during the year. Furthermore, it is advised to avoid the enamel near the root when dealing with younger individuals at least, because this enamel might not have fully mineralized yet and thus be more susceptible to diagenetic alteration, as well as to avoid the enamel near occlusal (bite) surface of the tooth, which can be used for microwear analysis. Sample location-wise, the same goes for bulk samples for stable carbon and/or nitrogen analysis. It is important to avoid both the enamel near the root in younger individuals, and to avoid damaging the occlusal surface. However, since both $\delta^{13}C$ and $\delta^{15}N$ show very little to no correlation with $\delta^{18}O$, and thus seasonality, in the fourteen teeth, bulk samples do not need to extent over the same length as they do for $\delta^{18}O$ samples.

One option for future research would be strontium isotope analysis on the equid teeth analysed here. Strontium isotopes are used to look into migration patterns (e.g., Kohn & Cerling, 2002), which could be an explanation for the differentiation between the two groups of individuals visible in the $\delta^{13}C$ values. Migration might also be a reason for the variation in $\delta^{15}N$ between individuals.

Isotopic analysis of other serially-sampled species, both herbivore and carnivore, from Neumark-Nord, or similar environments, could show if the patterns observed in equid teeth are also present in other species or if other patterns are visible. This would show if it is necessary to have different sampling strategies for $\delta^{13}C$, $\delta^{15}N$ and/or $\delta^{18}O$ isotope analysis when sampling teeth from different species. $\delta^{15}N$ analysis of all herbivore species present at NMN2 would also demonstrate the

$\delta^{15}N$ variation within this trophic level, and thus the indicate the minimum variation in $\delta^{15}N$ at the site. Furthermore, serial sampling equid teeth from completely different environments, like an African environment with a different seasonality, would show if the patterns observed here, especially the correlation between $\delta^{13}C$ and $\delta^{15}N$ and the non-correlation between $\delta^{18}O$ and $\delta^{15}N$, is something that is visible in all environments. This would in turn also lead to better recommendations when it comes to bulk sampling teeth.

To better understand the variation observed in $\delta^{13}C$ and $\delta^{15}N$ values within and between individuals, a study like Codron et al. (2005) did at Kruger National Park could be done on a temperate C_3 environment in Europe. Seeing as the variation in plant $\delta^{15}N$ observed in Kruger National Park corresponds well with the observed variation in herbivore enamel $\delta^{15}N$ in Gorongosa National Park, which have a similar environment (Lüdecke and Leichliter et al., 2022), it would be interesting to see if this is also the case for the variation in herbivore enamel $\delta^{15}N$ from Neumark-Nord compared to the variation in plant $\delta^{15}N$ of a modern comparable environment. Moreover, such a study could confirm if the correlation between $\delta^{13}C$ and $\delta^{15}N$, visible in the equid teeth analysed here, is also present in the plants in a temperate C_3 environment. In addition, observation of modern horse's feeding behaviour and subsequent isotope analysis, might indicate where the variation in both $\delta^{13}C$ and $\delta^{15}N$ between individuals living in the same habitat originates from.

As mentioned in section 7.5, the correlation between nitrogen content and the $\delta^{15}N$ value of the enamel might be related to the amino acids and proteins involved in enamel mineralization/maturation. If this is the case, this pattern should also be visible in modern horse teeth. A comparative study on modern horse teeth could also give more insight in the rate and timing of enamel mineralization, especially around the root of the tooth. Such a study could also be done on teeth from other herbivore species to better understand their enamel development, which is important when researching an archaeological site without any horses.

Trace element analysis could be done on more of the teeth here, especially the one that show outliers in the sample closest to the root, as explained in section 7.2. This could indicate if and to what extent these samples might be affected by diagenetic processes. A study on the effects of diagenesis on immature, not fully mineralized enamel, could be done on archaeological specimens from a site which has a wide range of ages and development stages represented in the herbivore teeth.

Lastly, a study on the (dis)colouration of equid teeth could be done. This would include an analysis on the colouration of modern horse teeth to figure out if mineralizing/maturing enamel always presents with a darker/black colour compared to mature enamel. Furthermore, archaeological specimens in different stages of development should be analysed to see if darker enamel represents not fully mineralized enamel or if it is potentially a result of diagenetic alterations.

7.8 Conclusion

This chapter discussed the patterns and variations visible in the isotopic data of fourteen equid teeth from NMN2/2b and tried to explain what these could mean. The $\delta^{13}C$ values correspond, as expected, to a C_3 diet. The $\delta^{18}O$ results show a clear seasonal pattern, and the $\delta^{15}N$ values are consistent with herbivore values from NMN2. In addition, comparisons with already published isotopic data from NMN2 were made, which show very similar results. There is no consistent correlation observed between the $\delta^{15}N$ values and $\delta^{18}O$ values, which shows that $\delta^{15}N$ in equid tooth enamel is not influenced by seasonality. There is a strong positive correlation noted between $\delta^{15}N$ and $\delta^{13}C$ values, which indicates that the mechanism behind the isotopic fractionation of these two isotopes are related in some way. Lastly, some recommendations and suggestions for future research were made.

8 Conclusion

In this chapter, I will summarise the most important findings of this study and answer the research questions posed in the introduction. Trace element analysis shows hardly any evidence for diagenetic alteration of the equid tooth enamel analysed in this study. Based on the results of both trace element and stable carbon and nitrogen isotope analysis, the enamel samples closest to the roots of the teeth may not be fully mineralized yet and thus more susceptible to diagenetic alteration. This may especially be the case in teeth with black enamel near the root, although this requires more research in the colour of mineralizing enamel in horses, as well as discoloration of enamel in different environments during the fossilization process.

The results of the stable carbon isotope analysis of the tooth enamel correspond to the $\delta^{13}C$ values associated with a diet consisting of C_3 plants, as expected for this locality. The closed canopy effect did likely not affect the plants the horses ate, which corresponds to the previously established open habitat surrounding NMN2. The relatively small variation in $\delta^{13}C$ values between individual specimens can be explained by variations in the $\delta^{13}C$ values of the plants they ate. Most of the individuals can be separated into two groups. The individuals in each group have an average $\delta^{13}C$ value which does not significantly differ within the group, but does differ from the $\delta^{13}C$ value of the individuals in the other group. The feeding area of these groups could have been separated in time and/or in space. There is also a third group consisting of three individuals, whose average $\delta^{13}C$ value does not differ from any other individual. Based on these groups, there is no observable spatial pattern in the excavation grid of NMN2. The $\delta^{13}C$ values measured here correspond to previously published and unpublished data from the same site and taxa.

As expected, the $\delta^{18}O$ data show a clear seasonal summer-winter pattern in each tooth. The average range of the calculated $\delta^{18}O_{water}$ values per tooth is more than double the range of the $\delta^{18}O$ values of a modern water source, which was measured over the span of a year. This could indicate that the difference in summer and winter temperature at this locality in the Eemian was larger than the difference in modern temperature, but this requires more research. Approximately 2 years is represented in the $\delta^{18}O$ values of each third molar. The $\delta^{18}O$ values from this study are in agreement with previously published and unpublished data.

The results of the nitrogen isotope analysis show less variation within all equid enamel samples than between trophic levels, which is as expected. The variation in $\delta^{15}N$ values between individuals can be explained by variation in $\delta^{15}N$ values of the plants they ate. More research is necessary to establish which factors played a role in this variation at NMN2. Both the $\delta^{15}N$ values and nitrogen content of the enamel correspond to previously published and unpublished data. The relatively low nitrogen content could be explained by a specific aspect of the locality, which would

need to be confirmed in future research. The large positive relationship observed here between $\delta^{15}N$ values and nitrogen content in the tooth enamel might be the results of processes involved in the enamel mineralization of equids. This would also require more research to confirm.

Four specimens show a significant positive relationship between their $\delta^{13}C$ and $\delta^{18}O$ values. This is likely the result of the plants the equids consumed having a reaction to temperature changes, which influenced their $\delta^{13}C$ values. The large positive relationship between $\delta^{13}C$ and $\delta^{15}N$ values seems to indicate that, in temperate environments, the mechanisms controlling carbon and nitrogen isotope fractionation are related. There is no strong, consistent relationship observed between $\delta^{15}N$ and $\delta^{18}O$ values of the equid teeth, which means that the $\delta^{15}N$ values of the enamel are not influenced by seasonality. This indicates that in temperate environments, bulk samples of tooth enamel from equids – and likely other large herbivores – do not need to cover an entire year of growth in order to measure an accurate average $\delta^{15}N$ value.

Lastly, when bulk sampling equid enamel, it is recommended to avoid the enamel close to the root in young individuals, since this enamel might not be fully mineralized and thus more susceptible to diagenetic alteration. In addition, it is also recommended to avoid the enamel near the crown, to ensure the occlusal surface stays intact for potential future microwear analysis. When performing $\delta^{18}O$ analysis on the equid enamel, it is recommended to bulk sample between 35 and 40 mm of enamel along the growth axis on the buccal or lingual side of the tooth, to ensure a full year is covered and an accurate average $\delta^{18}O$ value will be measured. For both $\delta^{13}C$ and $\delta^{15}N$ analysis it is not necessary to cover an entire year when bulk sampling, and thus the sample can be much shorter.

To answer the research questions posed in the introduction chapter of this thesis:

1. Seasonality does not seem to impact the $\delta^{15}N$ pattern observed in serially-sampled tooth enamel of equid third molars from the Eemian site Neumark-Nord 2, Germany.
    a. The $\delta^{13}C$ and $\delta^{18}O$ values of the serially-sampled equid teeth do not show a strong correlation.
    b. The $\delta^{13}C$ and $\delta^{15}N$ values of the serially-sampled equid teeth show a large positive correlation.
    c. The $\delta^{15}N$ and $\delta^{18}O$ values of the serially-sampled equid teeth do not show a strong correlation.
    d. The lack of a relationship between seasonality and the $\delta^{15}N$ values of the tooth enamel shows that it is not necessary to cover an entire year of growth when bulk sampling equid – and likely other large herbivores – teeth from temperate environments in order to measure an accurate average $\delta^{15}N$ value.

2. The previously published $\delta^{15}N$ values of equid collagen do not differ from the $\delta^{15}N$ values of equid tooth enamel measured in this study, which is as expected and shows once again that the *oxidation-denitrification* method can be applied to fossilized tooth enamel, which is highly resistant to diagenesis. This means that $\delta^{15}N$ research can be extended into deep time and help answer questions about the trophic position of our early ancestors.

Summarizing, this study showed that, by analysing the correlation between $\delta^{18}O$ and $\delta^{15}N$ values of the same aliquots of serially-sampled equid third molars, $\delta^{15}N$ values in tooth enamel of equids, in temperate environments, are not influenced by seasonality. This means that a bulk sample for the measurement of $\delta^{15}N$ taken from equid – and likely other large herbivores - tooth enamel from temperate environments does not need to cover an entire year of growth. Furthermore, the positive correlation between the $\delta^{13}C$ and $\delta^{15}N$ values of the same samples indicates that the carbon and nitrogen isotope fractionation are controlled by related mechanisms. Lastly, this thesis expanded the isotopic data set of the Middle Palaeolithic Neanderthal site of Neumark-Nord 2, Germany, by providing serially-sampled data which enables seasonality reconstruction of the Middle Palaeolithic environment.

Abstract

Stable carbon ($\delta^{13}C$), nitrogen ($\delta^{15}N$), and oxygen ($\delta^{18}O$) isotopes are well-established proxies for the reconstruction of past diet and environment. $\delta^{13}C$ and $\delta^{18}O$ can be used to reconstruct the plant-based diets of animals and seasonal environmental patterns. These isotopes are regularly measured in the non-organic component of tooth enamel, which is highly resistant to diagenetic alteration. Likewise, $\delta^{15}N$ can be used to reconstruct trophic level and food webs. Up until recently, $\delta^{15}N$ could only be measured on relatively young samples (<100,000 years old), because it requires organic material, usually bone collagen or dentin, which rarely preserves in the fossil record. However, in 2021, an *oxidation-denitrification* method was developed. This method allows for the measurement of the nitrogen isotopic composition of the organic material trapped in the crystalline structure of (fossil) tooth enamel. Thus, we can now measure $\delta^{13}C$, $\delta^{15}N$, and $\delta^{18}O$ on the same aliquot of tooth enamel.

Here, combined $\delta^{13}C$, $\delta^{15}N$, and $\delta^{18}O$ isotope data from tooth enamel of 14 serially-sampled fossil equid (*Equus* sp.) third molars from the ~120,000-year-old Middle Paleolithic Neanderthal site of Neumark-Nord 2, Germany, is presented. Each tooth was sampled along the growth axis and yielded up to 26 sub-samples (total n = 259). Neumark-Nord is a well-preserved archaeological site with a rich vertebrate fauna. It has yielded a large isotopic dataset, which includes some of the oldest stable carbon and nitrogen isotope measurements on bone collagen. This study allows us to expand the isotopic dataset of Neumark-Nord 2 by serially-sampled data, which enables us to reconstruct seasonality for the Last Interglacial (Eemian; MIS 5e/5d transition).

$\delta^{13}C$ and $\delta^{18}O$ of all enamel samples (n = 259) was measured using the cold trap method. Based on these isotope patterns, 72 samples (including all serial measurements of three of the equid teeth) were selected for $\delta^{15}N$ measurement, to assess potential seasonal variation in the $\delta^{15}N$ values of the enamel. The enamel $\delta^{13}C$, $\delta^{15}N$, and $\delta^{18}O$ results are consistent with previously published equid collagen $\delta^{13}C$, $\delta^{15}N$, and bulk enamel $\delta^{18}O$ values. A clear seasonal signal is present in the $\delta^{18}O$ values of each tooth, with higher values in summer than in winter. This seasonal signal is absent in both the $\delta^{13}C$ and $\delta^{15}N$ values.

This study shows that there is no strong effect of seasonal variation detectable in the $\delta^{15}N$ values of nitrogen isotopes in the enamel of equids in temperate environments. This suggests that, in order to measure an accurate average $\delta^{15}N$ value, bulk samples of tooth enamel from equids – and likely other large herbivores – in temperature environments do not need to cover an entire year of growth. In addition, the correlation observed between $\delta^{13}C$ and $\delta^{15}N$ enamel values seems to indicate that, in such environments, the mechanisms controlling carbon and nitrogen isotope fractionation are positively related. Lastly, this study improves the time-resolution of the Neumark-Nord 2 isotopic dataset, allowing for a better reconstruction of the past ecosystem by providing seasonal data.

Bibliography

Abraham, M. (2014, March 12). *The birth of a foal: What we look for and what we do.* University of Pennsylvenia. https://www.vet.upenn.edu/about/press-room/bellwether/penn-vet-extra/penn-vet-extra-march-2014/the-birth-of-a-foal-what-we-look-for-and-what-we-do

Adams, T. S., & Sterner, R. W. (2000). The effect of dietary nitrogen content on trophic level ^{15}N enrichment. *Limnology and Oceanography, 45*(3), 601-607. https://doi.org/10.4319/lo.2000.45.3.0601

Aichner, B., Dubbert, D., Kiel, C., Kohnert, K., Ogashawara, I., Jechow, A., Harpenslager, S.-F., Hölker, F., Nejstgaard, J. C., Grossart, H.-P., Singer, G., Wollrab, S., & Berger, S. A (2022). Spatial and seasonal patterns of water isotopes in northeastern German lakes. *Earth System Science Data, 14*, 1857–1867, https://doi.org/10.5194/essd-14-1857-2022

Ambrose, S. H. (1991). Effects of diet, climate, and physiology on nitrogen isotope abundances in terrestrial foodwebs. *Journal of Archaeological Science, 18*, 293-317. https://doi.org/10.1016/0305-4403(91)90067-Y

Ambrose, S. H., & DeNiro, M. J. (1986). The Isotopic ecology of East African mammals. *Oecologia, 69*, 395-406. https://doi.org/10.1007/BF00377062

Amundson, R., Austin, A. T., Schuur, E. A. G., Yoo, K., Matzek, V., Kendall, C., Uebersax, A., Brenner, D., & Baisden, W. T. (2003). Global patterns of the isotopic composition of soil and plant nitrogen. *Global Biogeochemical Cycles, 17*(1), 1031. https://doi.org/10.1029/2002gb001903

Bakels, C. (2012). Non-pollen palynomorphs from the Eemian pool Neumark-Nord 2: Determining water quality and the source of high pollen-percentages of herbaceous taxa. *Review of Palaeobotany and Palynology, 186*, 58-61. https://doi.org/10.1016/j.revpalbo.2012.06.003

Balasse, M., Bocherens, H., & Mariotti, A. (1999). Intra-bone variability of collagen and apatite isotopic composition used as evidence of a change of diet. *Journal of Archaeological Science, 26*, 593-598. https://doi.org/10.1006/jasc.1998.0376

Balter, V., Bocherens, H., Person, A., Labourdette, N., Renard, M., & Vandermeersch, B. (2002). Ecological and physiological variability of Sr/Ca and Ba/Ca in mammals of West European mid-Würmian food webs. *Palaeogeography, Palaeoclimatology, Palaeoecology, 186*(1-2), 127-143. https://doi.org/10.1016/s0031-0182(02)00448-0

Beaumont, J., & Montgomery, J. (2016). The great Irish famine: Identifying starvation in the tissues of victims using stable isotope analysis of bone and incremental dentine collagen. *PLoS One, 11*(8), e0160065. https://doi.org/10.1371/journal.pone.0160065

Bender, M. M. (1971). Variations in the $^{13}C/^{12}C$ ratios of plants in relation to the pathway of photosynthetic carbon dioxide fixation. *Phytochemistry, 10*, 1239-1244. https://doi.org/10.1016/S0031-9422(00)84324-1

Bendrey, R., Vella, D., Zazzo, A., Balasse, M., & Lepetz, S. (2015). Exponentially decreasing tooth growth rate in horse teeth: implications for isotopic analyses. *Archaeometry, 57*(6), 1104-1124. https://doi.org/10.1111/arcm.12151

Bershaw, J., Garzione, C. N., Higgins, P., MacFadden, B. J., Anaya, F., & Alvarenga, H. (2010). Spatial–temporal changes in Andean plateau climate and elevation from stable isotopes of mammal teeth. *Earth and Planetary Science Letters, 289*(3-4), 530-538. https://doi.org/10.1016/j.epsl.2009.11.047

Bocherens, H., & Drucker, D. (2003). Trophic level isotopic enrichment of carbon and nitrogen in bone collagen: Case studies from recent and ancient terrestrial ecosystems. *International Journal of Osteoarchaeology, 13*(1-2), 46-53. https://doi.org/10.1002/oa.662

Boddey, R. M., & Dobereiner, J. (1995). Nitrogen fixation associated with grasses and cereals: Recent progress and perspectives for the future. *Fertilizer Research, 42*, 241-250. https://doi.org/10.1007/BF00750518

Bonafini, M., Pellegrini, M., Ditchfield, P., & Pollard, A. M. (2013). Investigation of the 'canopy effect' in the isotope ecology of temperate woodlands. *Journal of Archaeological Science, 40*(11), 3926-3935. https://doi.org/10.1016/j.jas.2013.03.028

Bradshaw, R., & Mitchell, F. J. G. (1999). The palaeoecological approach to reconstructing former grazing-vegetation interactions. *Forest Ecology and Management, 120*, 3-12. https://doi.org/10.1016/S0378-1127(98)00538-6

Braman, R. S., & Hendrix, S. A. (1989). Nanogram nitrite and nitrate determination in environmental and biological materials by Vanadium(III) reduction with chemiluminescence detection. *Analytical Chemistry, 61*(24), 2715-2718. https://doi.org/10.1021/ac00199a007

Brand, W. A., Coplen, T. B., Vogl, J., Rosner, M., & Prohaska, T. (2014). Assessment of international reference materials for isotope-ratio analysis (IUPAC Technical Report). *Pure and Applied Chemistry, 86*(3), 425-467. https://doi.org/10.1515/pac-2013-1023

Britton, K., Gaudzinski-Windheuser, S., Roebroeks, W., Kindler, L., & Richards, M. P. (2012). Stable isotope analysis of well-preserved 120,000-year-old herbivore bone collagen from the Middle Palaeolithic site of Neumark-Nord 2, Germany reveals niche separation between bovids and equids. *Palaeogeography, Palaeoclimatology, Palaeoecology, 333-334*, 168-177. https://doi.org/10.1016/j.palaeo.2012.03.028

Britton, K., Pederzani, S., Kindler, L., Roebroeks, W., Gaudzinski-Windheuser, S., Richards, M. P., & Tütken, T. (2019). Oxygen isotope analysis of Equus teeth evidences early Eemian and early Weichselian palaeotemperatures at the Middle Palaeolithic site of Neumark-Nord 2, Saxony-Anhalt, Germany. *Quaternary Science Reviews, 226*. https://doi.org/10.1016/j.quascirev.2019.106029

Broadmeadow, M. S. J., Griffiths, H., Maxwell, C., & Borland, A. M. (1992). The carbon isotope ratio of plant organic material reflects temporal and spatial variations in CO_2 within tropical forest formations in Trinidad. *Oecologia, 89*, 435-441. https://doi.org/10.1007/BF00317423

Bryant, J. D., & Froelich, P. N. (1995). A model of oxygen isotope fractionation in body water of large mammals. *Geochimica et Cosmochimica Acta, 59*(21), 4523-4537. https://doi.org/10.1016/0016-7037(95)00250-4

Bryant, J. D., Koch, P. L., Froelich, P. N., Showers, W. J., & Genna, B. J. (1996). Oxygen isotope partitioning between phosphate and carbonate in mammalian apatite. *Geochimica et Cosmochimica Acta, 60*(24), 5145-5148. https://doi.org/10.1016/S0016-7037(96)00308-0

Cantalapiedra-Hijar, G., Ortigues-Marty, I., Sepchat, B., Agabriel, J., Huneau, J. F., & Fouillet, H. (2015). Diet-animal fractionation of nitrogen stable isotopes reflects the efficiency of nitrogen assimilation in ruminants. *British Journal of Nutrition, 113*(7), 1158-1169. https://doi.org/10.1017/S0007114514004449

Casciotti, K. L., Sigman, D. M., Galanter, H., M., Bohike, J. K., & Hilkert, A. (2002). Measurement of the oxygen isotopic composition of nitrate in seawater and freshwater using the denitrifier method *Analytical Chemistry, 74*, 4905-4912. https://doi.org/https://doi.org/10.1021/ac020113w

Castiblanco, G. A., Rutishauser, D., Ilag, L. L., Martignon, S., Castellanos, J. E., & Mejia, W. (2015). Identification of proteins from human permanent erupted enamel. *European Journal of Oral Sciences, 123*(6), 390-395. https://doi.org/10.1111/eos.12214

Caut, S., Angulo, E., & Courchamp, F. (2009). Variation in discrimination factors ($\Delta^{15}N$ and $\Delta^{13}C$): the effect of diet isotopic values and applications for diet reconstruction. *Journal of Applied Ecology, 46*(2), 443-453. https://doi.org/10.1111/j.1365-2664.2009.01620.x

Cerling, T., Harris, J. M., & Passey, B. H. (2003). Diets of East African bovidae based on stable isotope analysis *Journal of Mammalogy, 84*(2), 456-470. https://doi.org/10.1644/1545-1542(2003)084<0456:DOEABB>2.0.CO;2

Cerling, T. E., Bernasconi, S. M., Hofstetter, L. S., Jaggi, M., Wyss, F., Rudolf von Rohr, C., & Clauss, M. (2021). CH_4/CO_2 ratios and carbon isotope enrichment between diet and breath in herbivorous mammals. *Frontiers in Ecology and Evolution, 9*. https://doi.org/10.3389/fevo.2021.638568

Cerling, T. E., & Harris, J. M. (1999). Carbon isotope fractionation between diet and bioapetite in ungulate mammals and implications for ecological and paleoecological studies. *Oecologia, 120*, 347-363. https://doi.org/10.1007/s004420050868

Chenery, C., Müldner, G., Evans, J., Eckardt, H., & Lewis, M. (2010). Strontium and stable isotope evidence for diet and mobility in Roman Gloucester, UK. *Journal of Archaeological Science, 37*(1), 150-163. https://doi.org/10.1016/j.jas.2009.09.025

Chinique de Armas, Y., Mavridou, A. M., Garcell Dominguez, J., Hanson, K., & Laffoon, J. (2022). Tracking breastfeeding and weaning practices in ancient populations by combining carbon, nitrogen and oxygen stable isotopes from multiple non-adult tissues. *PLoS One, 17*(2), e0262435. https://doi.org/10.1371/journal.pone.0262435

Clementz, M. T. (2012). New insight from old bones: Stable isotope analysis of fossil mammals. *Journal of Mammalogy, 93*(2), 368-380. https://doi.org/10.1644/11-mamm-s-179.1

Codron, J., Codron, D., Lee-Thorp, J. A., Sponheimer, M., Bond, W. J., de Ruiter, D., & Grant, R. (2005). Taxonomic, anatomical, and spatio-temporal variations in the stable carbon and nitrogen isotopic compositions of plants from an African savanna. *Journal of Archaeological Science, 32*(12), 1757-1772. https://doi.org/10.1016/j.jas.2005.06.006

Coplen, T. B., Kendall, C., & Hopple, J. (1983). Comparison of stable isotope reference samples. *Nature, 302*, 236-238. https://doi.org/10.1038/302236a0

Craine, J. M., Ballantyne, F., Peel, M., Zambatis, N., Morrow, C., & Stock, W. D. (2009). Grazing and landscape controls on nitrogen availability across 330 South African savanna sites. *Austral Ecology, 34*(7), 731-740. https://doi.org/10.1111/j.1442-9993.2009.01978.x

Craine, J. M., Elmore, A. J., Aidar, M. P. M., Bustamante, M., Dawson, T. E., Hobbie, E. A., Kahmen, A., Mack, M. C., McLauchlan, K. K., Michelsen, A., Nardoto, G. B., Pardo, L. H., Penuelas, J., Reich, P. B., Schuur, E. A. G.,

Stock, W. D., Templer, P. H., Virginia, R. A., Welker, J. M., & Wright, I. J. (2009). Global patterns of foliar nitrogen isotopes and their relationships with climate, mycorrhizal fungi, foliar nutrient concentrations, and nitrogen availability. *New Phytologist, 183*(4), 980-992. https://doi.org/10.1111/j.1469-8137.2009.02917.x

Craine, J. M., Lee, W. G., Bond, W. J., Williams, R. J., & Johnson, L. C. (2005). Environmental constraints on a global relationship among leaf and root traits of grasses. *Ecology, 86*(1), 12-19. https://doi.org/10.1890/04-1075

Dailey-Chwalibog, T., Huneau, J. F., Mathe, V., Kolsteren, P., Mariotti, F., Mostak, M. R., Alim, M. A., Khan, M., Khan, M. A. H., Guesdon, B., & Fouillet, H. (2020). Weaning and stunting affect nitrogen and carbon stable isotope natural abundances in the hair of young children. *Scientific Reports, 10*(1), 2522. https://doi.org/10.1038/s41598-020-59402-8

de Winter, N. J., Snoeck, C., & Claeys, P. (2016). Seasonal cyclicity in trace elements and stable isotopes of modern horse enamel. *PLoS One, 11*(11), e0166678. https://doi.org/10.1371/journal.pone.0166678

Delgado Huertas, A., Iacumin, P., Stenni, B., Sanchez, C., B., & Longinelli, A. (1995). Oxygen isotope variations of phosphate in mammalian bone and tooth enamel. *Geochimica et Cosmochimica Acta, 59*, 4299-4305. https://doi.org/10.1016/0016-7037(95)00286-9

DeNiro, M. J. (1985). Postmortem preservation and alteration of in vivo bone collagen isotope ratios in relation to palaeodietary reconstruction. *Nature, 317*, 806-809. https://doi.org/10.1038/317806a0

DeNiro, M. J., & Epstein, S. (1981). Influence of diet on the distribution of nitrogen isotopes in animals. *Geochimica et Cosmochimica Acta, 45*, 341-351. https://doi.org/10.1016/0016-7037(81)90244-1

Dijkstra, P., Williamson, C., Menyailo, O., Doucett, R., Koch, G., & Hungate, B. A. (2003). Nitrogen stable isotope composition of leaves and roots of plants growing in a forest and a meadow. *Isotopes in Environmental and Health Studies, 39*(1), 29-39. https://doi.org/10.1080/1025601031000102189

Döbereiner, J. (1977). Biological nitrogen fixation in tropical grasses: Possibilities for partial replacement of mineral N fertilizers. *Ambio, 6*, 174-177.

Doi, H., Akamatsu, F., & Gonzalez, A. L. (2017). Starvation effects on nitrogen and carbon stable isotopes of animals: an insight from meta-analysis of fasting experiments. *Royal Society Open Science, 4*(8), 170633. https://doi.org/10.1098/rsos.170633

Dombrosky, J. (2019). A ~1000-year ^{13}C Suess correction model for the study of past ecosystems. *The Holocene, 30*(3), 474-478. https://doi.org/10.1177/0959683619887416

Drucker, D. G., Bridault, A., Hobson, K. A., Szuma, E., & Bocherens, H. (2008). Can carbon-13 in large herbivores reflect the canopy effect in temperate and boreal ecosystems? Evidence from modern and ancient ungulates. *Palaeogeography, Palaeoclimatology, Palaeoecology, 266*(1-2), 69-82. https://doi.org/10.1016/j.palaeo.2008.03.020

Ehleringer, J., & Cerling, T. (2002). C3 and C4 Photosynthesis. In H. A. Mooney & J. G. Canadell (Eds.), *Volume 2, The Earth system: biological and ecological dimensions of global environmental change* (Vol. 2, pp. 186-190). John Wiley & Sons.

Elliott, J. C. (2002). Calcium Phosphate Biominerals. *Reviews in Mineralogy and Geochemistry, 48*(1), 427-453. https://doi.org/10.2138/rmg.2002.48.11

Evans, R. D. (2001). Physiological mechanisms influencing plant nitrogen isotope composition. *TRENDS in Plant Science, 6*(3), 121-126. https://doi.org/10.1016/S1360-1385(01)01889-1

Evans, R. D., Bloom, A. J., Sukrapanna, S. S., & Ehleringer, J. R. (1996). Nitrogen isotope composition of tomato (Lycopersicon esculentum Mill. cv. T-5) grown under ammonium or nitrate nutrition. *Plant, Cell and Environment, 19*(11), 1317-1323. https://doi.org/10.1111/j.1365-3040.1996.tb00010.x

Farquhar, G. D., Ehleringer, J. R., & Hubick, K. T. (1989). Carbon isotope discrimination and photosynthesis. *Annual Review of Plant Physiology and Plant Molecular Biology, 40*, 503-537. https://doi.org/https://doi.org/10.1146/annurev.pp.40.060189.002443

Fox-Dobbs, K., Bump, J. K., Peterson, R. O., Fox, D. L., & Koch, P. L. (2007). Carnivore-specific stable isotope variables and variation in the foraging ecology of modern and ancient wolf populations: case studies from Isle Royale, Minnesota, and La Brea. *Canadian Journal of Zoology, 85*(4), 458-471. https://doi.org/10.1139/z07-018

Fox-Dobbs, K., Leonard, J. A., & Koch, P. L. (2008). Pleistocene megafauna from eastern Beringia: Paleoecological and paleoenvironmental interpretations of stable carbon and nitrogen isotope and radiocarbon records. *Palaeogeography, Palaeoclimatology, Palaeoecology, 261*(1-2), 30-46. https://doi.org/10.1016/j.palaeo.2007.12.011

Fry, B. (2006). *Stable Isotope Ecology*. Springer.

Fuller, B. T., Fuller, J. L., Harris, D. A., & Hedges, R. E. (2006). Detection of breastfeeding and weaning in modern human infants with carbon and nitrogen stable isotope ratios. *American Journal of Physical Anthropology, 129*(2), 279-293. https://doi.org/10.1002/ajpa.20249

Gaebler, O. H., Vitti, T. G., & Vukmirovich, R. (1966). Isotope effects in metabolism of 14N and 15N from unlabeled dietary proteins. *Canadian Journal of Biochemistry, 44*(9), 1249-1257. https://doi.org/https://doi.org/10.1139/o66-142

Gannes, L. Z., del Rio, C. M., & Koch, P. (1998). Natural abundance variations in stable isotopes and their potential uses in animal physiological ecology. *Comparative Biochemistry and Physiology, 119*(3), 725-737. https://doi.org/https://doi.org/10.1016/S1095-6433(98)01016-2

Garcia-Moreno, A., Smith, G., Kindler, L., Gaudzinski-Windheuser, S., & Roebroeks, W. (2015). *Modelling the spatiality of seasonality. Integrating seasonal data into the spatial analysis of Neumark-Nord 2/2B (Germany).* European society for the Study of Human Evolution (ESHE), London.

García-Moreno, A., Smith, G. M., Kindler, L., Pop, E., Roebroeks, W., Gaudzinski-Windheuser, S., & Klinkenberg, V. (2016). Evaluating the incidence of hydrological processes during site formation through orientation analysis. A case study of the middle Palaeolithic Lakeland site of Neumark-Nord 2 (Germany). *Journal of Archaeological Science: Reports, 6*, 82-93. https://doi.org/10.1016/j.jasrep.2016.01.023

Gaudzinski-Windheuser, S., Kindler, L., Pop, E., Roebroeks, W., & Smith, G. (2014). The Eemian Interglacial lake-landscape at Neumark-Nord (Germany) and its potential for our knowledge of hominin subsistence strategies. *Quaternary International, 331*, 31-38. https://doi.org/10.1016/j.quaint.2013.07.023

Gaudzinski-Windheuser, S., & Roebroeks, W. (2014). Multidisciplinary studies of the Middle Palaeolithic record from Neumark-Nord (Germany): An introduction. In S. Gaudzinski-Windheuser, W. Roebroeks, & H. Meller (Eds.), *Multidisciplinary Studies of the Middle Palaeolithic record from Neumark-Nord (Germany)* (Vol. 1, pp. 9-12). Landesmuseum fur Vorgeschichte.

Gebauer, G., & Schulze, E. D. (1991). Carbon and nitrogen isotope ratios in different compartments of a healthy and a declining Picea abies forest in the Fichtelgebirge, NE Bavaria. *Oecologia, 87*, 198-207. https://doi.org/10.1007/BF00325257

Gehler, A., Gingerich, P. D., & Pack, A. (2016). Temperature and atmospheric CO2 concentration estimates through the PETM using triple oxygen isotope analysis of mammalian bioapatite. *PNAS, 113*(28), 7739-7744. https://doi.org/10.1073/pnas.1518116113

Gil-Bona, A., & Bidlack, F. B. (2020). Tooth enamel and its dynamic protein matrix. *International Journal of Molecular Sciences, 21*(12). https://doi.org/10.3390/ijms21124458

Gordon Betts, J., Young, K. A., Wise, J. A., Johnson, E., Poe, B., Kruse, D. H., Korol, O., Johnson, J. E., Womble, M., & DeSaix, P. (2013). *Anatomy and Physiology*. OpenStax. https://openstax.org/books/anatomy-and-physiology

Guiry, E., Noël, S., & Fowler, J. (2021). Archaeological herbivore δ13C and δ34S provide a marker for saltmarsh use and new insights into the process of 15N-enrichment in coastal plants. *Journal of Archaeological Science, 125*. https://doi.org/10.1016/j.jas.2020.105295

Handley, L. L., Austin, A. T., Stewart, G. R., Robinson, D., Scrimgeour, C. M., Raven, J. A., Heaton, T. H. E., & Schmidt, S. (1999). The ^{15}N natural abundance ($\delta^{15}N$) of ecosystem samples reflects measures of water availability. *Functional Plant Biology, 26*(2), 185-199. https://doi.org/10.1071/pp98146

Handley, L. L., & Raven, J. A. (1992). The use of natural abundance of nitrogen isotopes in plant physiology and ecology. *Plant, Cell and Environment, 15*(9), 965-985. https://doi.org/10.1111/j.1365-3040.1992.tb01650.x

Hare, V. J., Loftus, E., Jeffrey, A., & Ramsey, C. B. (2018). Atmospheric CO_2 effect on stable carbon isotope composition of terrestrial fossil archives. *Nature Communications, 9*(1), 252. https://doi.org/10.1038/s41467-017-02691-x

Hartman, G. (2010). Are elevated δ15N values in herbivores in hot and arid environments caused by diet or animal physiology? *Functional Ecology, 25*(1), 122-131. https://doi.org/10.1111/j.1365-2435.2010.01782.x

Hartman, G., & Danin, A. (2010). Isotopic values of plants in relation to water availability in the Eastern Mediterranean region. *Oecologia, 162*(4), 837-852. https://doi.org/10.1007/s00442-009-1514-7

Heaton, T. H. E. (1987). The $^{15}N/^{14}N$ ratios of plants in South Africa and Namibia: relationship to climate and coastal/saline environments. *Oecologia, 74*, 236-246. https://doi.org/https://doi.org/10.1007/BF00379365

Heaton, T. H. E. (1999). Spatial, species, and temporal variations in the ^{13}C /^{12}C ratios of C_3 plants: implications for palaeodiet studies. *Journal of Archaeological Science, 26*, 637-649. https://doi.org/10.1006/jasc.1998.0381

Hennig, J. D., Beck, J. L., Scasta, J. D. (2018). Spatial ecology observations from feral horses equipped with global positioning system transmitters. *Human-Wildlife Interactions, 12*(1), 75-84. https://doi.org/10.26077/z9cn-4h37

Hobbie, E. A., & Werner, R. A. (2004). Intramolecular, compound-specific, and bulk carbon isotope patterns in C_3 and C_4 plants: a review and synthesis. *New Phytologist, 161*, 371-385. https://doi.org/10.1046/j.1469-8137.2004.00970.x

Hoppe, K. (2006). Correlation between the oxygen isotope ratio of North American bison teeth and local waters: Implication for paleoclimatic reconstructions. *Earth and Planetary Science Letters, 244*(1-2), 408-417. https://doi.org/10.1016/j.epsl.2006.01.062

Hoppe, K. A., Amundson, R., Vavra, M., McClaran, M. P., & Anderson, D. L. (2004). Isotopic analysis of tooth enamel carbonate from modern North American feral horses: Implications for paleoenvironmental reconstructions. *Palaeogeography, Palaeoclimatology, Palaeoecology, 203*(3-4), 299-311. https://doi.org/10.1016/s0031-0182(03)00688-6

Hoppe, K. A., Stover, S. M., Pascoe, J. R., & Amundson, R. (2004). Tooth enamel biomineralization in extant horses: implications for isotopic microsampling. *Palaeogeography, Palaeoclimatology, Palaeoecology, 206*(3-4), 355-365. https://doi.org/10.1016/j.palaeo.2004.01.012

Iacumin, P., Bocherens, H., Mariotti, A., & Longinelli, A. (1996). Oxygen isotope analyses of co-existing carbonate in biogenic apatite: a way to monitor diagenetic bone phosphate? *Earth and Planetary Science Letters, 142*, 1-6. https://doi.org/10.1016/0012-821X(96)00093-3

Iacumin, P., Rossi, M., Selmo, E., & Venturelli, G. (2022). Oxygen isotopes in carbonate and phosphate of modern mammal bioapatite: New data and critical revision after about 25 Years from the first recognitions. *Minerals, 12*(10). https://doi.org/10.3390/min12101204

Jaouen, K., & Pons, M.-L. (2016). Potential of non-traditional isotope studies for bioarchaeology. *Archaeological and Anthropological Sciences, 9*(7), 1389-1404. https://doi.org/10.1007/s12520-016-0426-9

Jaouen, K., Richards, M. P., Le Cabec, A., Welker, F., Rendu, W., Hublin, J. J., Soressi, M., & Talamo, S. (2019). Exceptionally high $\delta^{15}N$ values in collagen single amino acids confirm Neandertals as high-trophic level carnivores. *PNAS, 116*(11), 4928-4933. https://doi.org/10.1073/pnas.1814087116

Kalcsits, L. A., Buschhaus, H. A., & Guy, R. D. (2014). Nitrogen isotope discrimination as an integrated measure of nitrogen fluxes, assimilation and allocation in plants. *Physiologia Plantarum, 151*(3), 293-304. https://doi.org/10.1111/ppl.12167

Keenan, S. W. (2016). From bone to fossil: A review of the diagenesis of bioapatite. *American Mineralogist, 101*(9), 1943-1951. https://doi.org/10.2138/am-2016-5737

King, S. R. B. (2002). Home range and habitat use of free-ranging Przewalski horses at Hustai National Park, Mongolia. *Applied Animal Behaviour Science, 78*(2-4), 103-113. https://doi.org/10.1016/S0168-1591(02)00087-4

Kim, S.-T., Coplen, T. B., & Horita, J. (2015). Normalization of stable isotope data for carbonate minerals: Implementation of IUPAC guidelines. *Geochimica et Cosmochimica Acta, 158*, 276-289. https://doi.org/10.1016/j.gca.2015.02.011

Kindler, L., Smith, G., Garcia-Moreno, A., Gaudzinski-Windheuser, S., Pop, E., & Roebroeks, W. (2020). The last interglacial (Eemian) lakeland of Neumark-Nord (Saxony-Anhalt, Germany). Sequencing Neanderthal occupations, assessing subsistence opportunities and prey selection based on estimations of ungulate carrying capacities, biomass production and energey values. In A. Garcia-Moreno, J. M. Hutson, G. Smith, L. Kindler, E. Turner, A. Villaluenga, & S. Gaudzinski-Windheuser (Eds.), *Human behavioural adaptations to interglacial lakeshore environments* (pp. 67-104). https://doi.org/https://doi.org/10.11588/propylaeum.647

Kindler, L., Smith, G., & Wagner, M. (2014). Introduction to faunal analysis at Neumark-Nord 2. In S. Gaudzinski-Windheuser, W. Roebroeks, & H. Meller (Eds.), *Multidisciplinary studies of the Middle Paleolithic record from Neumark-Nord (Germany)* (Vol. 1, pp. 197-210). Landesmuseum fur Vorgeschichte.

Kindler, L., Smith, G. M., Garcia-Moreno, A., & Gaudzinski-Windheuser, S. (2015). *The Eemian Zoo of Neumark-Nord 2 (Germany): Neanderthal adaptations to interglacial environments on the European Plain*. European society for the Study of Human Evolution (ESHE), London.

Koch, P. L., Tuross, N., & Fogel, M. L. (1997). The effects of sample treatment and diagenesis on the isotopic integrity of carbonate in biogenic hydroxylapatite. *Journal of Archaeological Science, 24*, 417-429. https://doi.org/10.1006/jasc.1996.0126

Kohn, M. J. (1996). Predicting animal $\delta^{18}O$: Accounting for diet and physiological adaptation. *Geochimica et Cosmochimica Acta, 60*(23), 4811-4829. https://doi.org/10.1016/S0016-7037(96)00240-2

Kohn, M. J. (2010). Carbon isotope compositions of terrestrial C_3 plants as indicators of (paleo)ecology and (paleo)climate. *Proceedings of the National Academy of Sciences, 107*(46), 19691-19695. https://doi.org/10.1073/pnas.1004933107

Kohn, M. J., & Cerling, T. E. (2002). Stable isotope compositions of biological apatite. *Reviews in Mineralogy and Geochemistry, 48*(1), 455-488. https://doi.org/10.2138/rmg.2002.48.12

Kohn, M. J., Schoeninger, M. J., & Barker, W. W. (1999). Altered states: Effects of diagenesis on fossil tooth chemistry. *Geochimica et Cosmochimica Acta, 63*(18), 2737-2747. https://doi.org/10.1016/S0016-7037(99)00208-2

Krajcarz, M. T., Krajcarz, M., & Bocherens, H. (2018). Collagen-to-collagen prey-predator isotopic enrichment ($\Delta^{13}C$, $\Delta^{15}N$) in terrestrial mammals - a case study of a subfossil red fox den. *Palaeogeography, Palaeoclimatology, Palaeoecology, 490*, 563-570. https://doi.org/10.1016/j.palaeo.2017.11.044

Lacruz, R. S., Habelitz, S., Wright, J. T., & Paine, M. L. (2017). Dental enamel formation and implications for oral health and disease. *Physiological Reviews, 97*(3), 939-993. https://doi.org/10.1152/physrev.00030.2016

Lazzerini, N., Coulon, A., Simon, L., Marchina, C., Noost, B., Lepetz, S., & Zazzo, A. (2019). Grazing high and low: Can we detect horse altitudinal mobility using high-resolution isotope ($\delta^{13}C$ and $\delta^{15}N$ values) time series in tail hair? A case study in the Mongolian Altai. *Rapid Communications in Mass Spectrometry, 33*(19), 1512-1526. https://doi.org/10.1002/rcm.8496

Lee-Thorp, J., & Merwe, v. d., N. J. (1991). Aspects of the chemistry of modern and fossil biological apatites. *Journal of Archaeological Science, 18*, 343-354. https://doi.org/10.1016/0305-4403(91)90070-6

Leichliter, J., Lüdecke, T., Foreman, A., Bourgon, N., Duprey, N., Vonhof, H., Souksavatdy, V., Bacon, A.-M., Sigman, D., Tütken, T., & Martinez-Garcia, A. (2023). Tooth enamel nitrogen isotope composition records trophic position: A tool for reconstructng food webs. *Communications Biology, 6*, article 373, 8 pages https://doi.org/10.1038/s42003-023-04744-y

Leichliter, J. N., Lüdecke, T., Foreman, A. D., Duprey, N. N., Winkler, D. E., Kast, E. R., Vonhof, H., Sigman, D. M., Haug, G. H., Clauss, M., Tütken, T., & Martínez-García, A. (2021). Nitrogen isotopes in tooth enamel record diet and trophic level enrichment: Results from a controlled feeding experiment. *Chemical Geology, 563*, 120047. https://doi.org/10.1016/j.chemgeo.2020.120047

Lüdecke, T., Leichliter, J. N., Aldeias, V., Bamford, M. K., Biro, D., Braun, D. R., Capelli, C., Cybulski, J. D., Duprey, N. N., Ferreira da Silva, M. J., Foreman, A. D., Habermann, J. M., Haug, G. H., Martínez, F. I., Mathe, J., Mulch, A., Sigman, D. M., Vonhof, H., Bobe, R., Carvalho, S., & Martínez-García, A. (2022). Carbon, nitrogen, and oxygen stable isotopes in modern tooth enamel: A case study from Gorongosa National Park, central Mozambique. *Frontiers in Ecology and Evolution, 10*. https://doi.org/10.3389/fevo.2022.958032

Marino, B. D., & McElroy, M. B. (1991). Isotopic composition of atmospheric CO_2 inferred from carbon in C_4 plant cellulose. *Nature, 349*, 127-131. https://doi.org/https://doi.org/10.1038/349127a0

Marshall, J. D., Brooks, J. R., & Lajtha, K. (2007). Sources of variation in the stable isotopic composition of plants. In R. Michener & K. Lajtha (Eds.), *Stable Isotopes in Ecology and Environmental Science* (2nd ed., pp. 22-60). Blackwell.

Martin, J. E., Tacail, T., Balter, V., & Smith, A. (2017). Non-traditional isotope perspectives in vertebrate palaeobiology. *Palaeontology, 60*(4), 485-502. https://doi.org/10.1111/pala.12300

Martinez-Garcia, A., Sigman, D. M., Ren, H., Anderson, R. F., Straub, M., Hodell, D. A., Jaccard, S. L., Eglinton, T. I., & Haug, G. H. (2014). Iron fertilization of the subantarctic ocean during the last ice age. *Science, 343*, 1347-1350. https://doi.org/10.1126/science.1246848

Martínez-García, A., Jung, J., Ai, X. E., Sigman, D. M., Auderset, A., Duprey, N. N., Foreman, A., Fripiat, F., Leichliter, J., Lüdecke, T., Moretti, S., & Wald, T. (2022). Laboratory assessment of the impact of chemical oxidation, mineral dissolution, and heating on the nitrogen isotopic composition of fossil-bound organic matter. *Geochemistry, Geophysics, Geosystems, 23*(8). https://doi.org/10.1029/2022gc010396

McIlvin, M. R., & Casciotti, K. L. (2011). Technical updates to the bacterial method for nitrate isotopic analyses. *Analytical Chemistry, 83*(5), 1850-1856. https://doi.org/10.1021/ac1028984.

Medina, E., & Minchin, P. (1980). Stratification of $\delta^{13}C$ values of leaves in Amazonian Rain Forests. *Oecologia, 45*, 377-378. https://doi.org/10.1007/BF00540209

Medina, E., Montes, G., Cuevas, E., & Rokzandic, Z. (1986). Profiles of CO_2 concentration and $\delta^{13}C$ values in tropical rain forests of the upper Rio Negro Basin, Venezuela. *Journal of Tropical Ecology, 2*(3), 207-217. https://doi.org/10.1017/s0266467400000821

Mehra, O. P., & Jackson, M. L. (1958). Iron oxide removal from soils and clays by a dithionite-citrate system buffered with sodium bicarbonate. *Clays and Clay minerals, 7*, 317-327. https://doi.org/https://doi.org/10.1346/ccmn.1958.0070122

Merwe, v. d., N. J., & Medina, E. (1989). Photosynthesis and ^{13}C /^{12}C ratios in Amazonian rain forests. *Geochimica et Cosmochimica Acta, 53*, 1091-1094. https://doi.org/10.1016/0016-7037(89)90213-5

Merwe, v. d., N. J., & Medina, E. (1991). The canopy effect, carbon isotope ratios in foodwebs in Amazonia. *Journal of Archaeological Science, 18*, 249-259. https://doi.org/10.1016/0305-4403(91)90064-V

Milano, S., Pop, E., Kuijper, W., Roebroeks, W., Gaudzinski-Windheuser, S., Penkman, K., Kindler, L., & Britton, K. (2020). Environmental conditions at the Last Interglacial (Eemian) site Neumark-Nord 2, Germany inferred

from stable isotope analysis of freshwater mollusc opercula. *Boreas, 49*(3), 477-487. https://doi.org/10.1111/bor.12437

Miller, H., Chenery, C., Lamb, A. L., Sloane, H., Carden, R. F., Atici, L., & Sykes, N. (2019). The relationship between the phosphate and structural carbonate fractionation of fallow deer bioapatite in tooth enamel. *Rapid Communications in Mass Spectrometry, 33*(2), 151-164. https://doi.org/10.1002/rcm.8324

Mitchell, F. J. G. (2005). How open were European primeval forests? Hypothesis testing using palaeoecological data. *Journal of Ecology, 93*(1), 168-177. https://doi.org/10.1111/j.1365-2745.2004.00964.x

Muzuka, A. N. N. (1999). Isotopic compositions of tropical East African flora and their potential as source indicators of organic matter in coastal marine sediments. *Journal of African Earth Sciences, 28*, 757-766. https://doi.org/10.1016/S0899-5362(99)00044-5

Nacarino-Meneses, C., Jordana, X., Orlandi-Oliveras, G., & Kohler, M. (2017). Reconstructing molar growth from enamel histology in extant and extinct Equus. *Sci Rep, 7*(1), 15965. https://doi.org/10.1038/s41598-017-16227-2

Nelson, S. V. (2005). Paleoseasonality inferred from equid teeth and intra-tooth isotopic variability. *Palaeogeography, Palaeoclimatology, Palaeoecology, 222*(1-2), 122-144. https://doi.org/10.1016/j.palaeo.2005.03.012

Nier, A. O. (1950). A redetermination of the relative abundances of the isotopes of carbon, nitrogen, oxygen, argon, and potassium. *Physical Review, 77*(6), 789-793. https://doi.org/10.1103/PhysRev.77.789

O'Leary, M. H. (1981). Carbon isotope fractionation in plants. *Phytochemistry, 20*(4), 553-567. https://doi.org/10.1016/0031-9422(81)85134-5

Ostrom, N. E., & Ostrom, P. H. (1998). Nitrogen isotopes. In *Geochemistry. Encyclopedia of Earth Science*. Springer. https://doi.org/https://doi.org/10.1007/1-4020-4496-8_215

Parker, R. B., & Toots, H. (1970). Minor elements in fossil bone. *Geological Society of America Bulletin, 81*, 925-932. https://doi.org/10.1130/0016-7606(1970)81[925:MEIFB]2.0.CO;2

Passey, B., & Cerling, T. (2002). Tooth enamel mineralization in ungulates: Implications for recovering a primary isotopic time-series. *Geochimica et Cosmochimica Acta, 66*(18), 3225-3234. https://doi.org/10.1016/S0016-7037(02)00933-X

Passey, B. H., Robinson, T. F., Ayliffe, L. K., Cerling, T. E., Sponheimer, M., Dearing, M. D., Roeder, B. L., & Ehleringer, J. R. (2005). Carbon isotope fractionation between diet, breath CO_2, and bioapatite in different mammals. *Journal of Archaeological Science, 32*(10), 1459-1470. https://doi.org/10.1016/j.jas.2005.03.015

Pederzani, S., & Britton, K. (2019). Oxygen isotopes in bioarchaeology: Principles and applications, challenges and opportunities. *Earth-Science Reviews, 188*, 77-107. https://doi.org/10.1016/j.earscirev.2018.11.005

Pellegrini, M., Lee-Thorp, J., & Donahue, R. E. (2011). Exploring the variation of the $\delta^{18}O_p$ and $\delta^{18}O_c$ relationship in enamel increments. *Palaeogeography, Palaeoclimatology, Palaeoecology, 310*, 71-83. https://doi.org/10.1016/j.palaeo.2011.02.023

Pop, E. (2014). Analysis of the Neumark-Nord 2/2 lithic assemblage: Results and interpretations. In S. Gaudzinski-Windheuser & W. Roebroeks (Eds.), *Multidisciplinary studies of the Middle Paleolithic record from Neumark-Nord (Germany)* (Vol. 1, pp. 143-196). Landesmuseum für Vorgeschichte.

Pop, E., & Bakels, C. (2015). Semi-open environmental conditions during phases of hominin occupation at the Eemian Interglacial basin site Neumark-Nord 2 and its wider environment. *Quaternary Science Reviews, 117*, 72-81. https://doi.org/10.1016/j.quascirev.2015.03.020

Pop, E., Bakels, C., Kuijper, W., Mücher, H., & van Dijk, M. (2015). The dynamics of small postglacial lake basins and the nature of their archaeological record: A case study of the Middle Palaeolithic site Neumark-Nord 2, Germany. *Geoarchaeology, 30*(5), 393-413. https://doi.org/10.1002/gea.21526

Pop, E., Kuijper, W., van Hees, E., Smith, G., García-Moreno, A., Kindler, L., Gaudzinski-Windheuser, S., & Roebroeks, W. (2016). Fires at Neumark-Nord 2, Germany: An analysis of fire proxies from a Last Interglacial Middle Palaeolithic basin site. *Journal of Field Archaeology, 41*(5), 603-617. https://doi.org/10.1080/00934690.2016.1208518

Poupin, N., Bos, C., Mariotti, F., Huneau, J. F., Tome, D., & Fouillet, H. (2011). The nature of the dietary protein impacts the tissue-to-diet ^{15}N discrimination factors in laboratory rats. *PLoS One, 6*(11), e28046. https://doi.org/10.1371/journal.pone.0028046

Pryor, A. J. E., Stevens, R. E., O'Connell, T. C., & Lister, J. R. (2014). Quantification and propagation of errors when converting vertebrate biomineral oxygen isotope data to temperature for palaeoclimate reconstruction. *Palaeogeography, Palaeoclimatology, Palaeoecology, 412*, 99-107. https://doi.org/10.1016/j.palaeo.2014.07.003

Rao, Z., Guo, W., Cao, J., Shi, F., Jiang, H., & Li, C. (2017). Relationship between the stable carbon isotopic composition of modern plants and surface soils and climate: A global review. *Earth-Science Reviews, 165*, 110-119. https://doi.org/10.1016/j.earscirev.2016.12.007

Ren, H., Sigman, D. M., Thunell, R. C., & Prokopenko, M. G. (2012). Nitrogen isotopic composition of planktonic foraminifera from the modern ocean and recent sediments. *Limnology and Oceanography, 57*(4), 1011-1024. https://doi.org/10.4319/lo.2012.57.4.1011

Reynard, B., & Balter, V. (2014). Trace elements and their isotopes in bones and teeth: Diet, environments, diagenesis, and dating of archeological and paleontological samples. *Palaeogeography, Palaeoclimatology, Palaeoecology, 416*, 4-16. https://doi.org/10.1016/j.palaeo.2014.07.038

Robinson, C. (2014). Enamel maturation: A brief background with implications for some enamel dysplasias. *Frontiers in Physiology, 5*, 388. https://doi.org/10.3389/fphys.2014.00388

Robinson, C., Kirkham, J., Brookes, S. J., Bonass, W. A., & Shore, R. C. (1995). The chemistry of enamel development. *International Journal of Developmental Biology, 39*, 145-152. https://doi.org/10.1387/ijdb.7626401

Robinson, D. (2001). $\delta^{15}N$ as an integrator of the nitrogen cycle. *TRENDS in Plant Science, 16*(3), 153-162. https://doi.org/10.1016/S0169-5347(00)02098-X

Robinson, R. S., Brunelle, B. G., & Sigman, D. M. (2004). Revisiting nutrient utilization in the glacial Antarctic: Evidence from a new method for diatom-bound N isotopic analysis. *Paleoceanography, 19*(3), PA3001. https://doi.org/10.1029/2003pa000996

Roebroeks, W., & Bakels, C. C. (2015). 'Forest Furniture' or 'Forest Managers'? On Neanderthal presence in Last Interglacial environments. In *Settlement, Society and Cognition in Human Evolution* (pp. 174-188). Cambridge University Press https://doi.org/10.1017/cbo9781139208697.011

Roebroeks, W., MacDonald, K., Scherjon, F., Bakels, C., Kindler, L., Nikulina, A., Pop, E., & Gaudzinski-Windheuser, S. (2021). Landscape modification by Last Interglacial Neanderthals. *Science Advances, 7*(51), eabj5567. https://doi.org/10.1126/sciadv.abj5567

Sakae, T., Suzuki, K., & Kozawa, Y. (1994). A short review of studies on chemical and physical properties of enmael crystallites. Tooth enamel microstructure: Proceedings of the enamel microstructure wrokshop, University of Bonn, Andernach, Germany.

Sandom, C. J., Ejrnaes, R., Hansen, M. D., & Svenning, J. C. (2014). High herbivore density associated with vegetation diversity in interglacial ecosystems. *PNAS, 111*(11), 4162-4167. https://doi.org/10.1073/pnas.1311014111

Savory, A., & Brudevold, F. (1959). The distribution of nitrogen in human enamel. *Journal of Dental Research, 38*(3), 436-442. https://doi.org/10.1177/00220345590380030301

Schmidt, S., & Stewart, G. R. (2003). $\delta^{15}N$ values of tropical savanna and monsoon forest species reflect root specialisations and soil nitrogen status. *Oecologia, 134*(4), 569-577. https://doi.org/10.1007/s00442-002-1150-y

Schoeninger, M. J. (2014). Stable isotope analyses and the evolution of human diets. *Annual Review of Anthropology, 43*(1), 413-430. https://doi.org/10.1146/annurev-anthro-102313-025935

Schoeninger, M. J., & DeNiro, M. J. (1984). Stable nitrogen isotope ratios of bone collagen reflect marine and terrestrial components of prehistoric human diet. *Science, 220*, 1381-1383. https://doi.org/10.1126/science.6344217

Sealy, J. C., Merwe, v. d., N. J., Lee-Thorp, J. A., & Lanham, J. L. (1987). Nitrogen isotopic ecology in southern Africa: Implication for environmental and dietary tracing. *Geochimica et Cosmochimica Acta, 51*, 2707-2717. https://doi.org/10.1016/0016-7037(87)90151-7

Sier, M. J., Roebroeks, W., Bakels, C. C., Dekkers, M. J., Bruhl, E., De Loecker, D., Gaudzinski-Windheuser, S., Hesse, N., Jagich, A., Kindler, L., Kuijper, W. J., Laurat, T., Mucher, H. J., Penkman, K. E., Richter, D., & van Hinsbergen, D. J. (2011). Direct terrestrial-marine correlation demonstrates surprisingly late onset of the last interglacial in central Europe. *Quaternary Research, 75*(1), 213-218. https://doi.org/10.1016/j.yqres.2010.11.003

Sigman, D., Casciotti, K. L., Andreani, M., Barford, C., Galanter, M., & Bohike, J. K. (2001). A bacterial method for the nitrogen isotopic analysis of nitrate in seawater and freshwater. *Analytical Chemistry, 73*(17), 4145-4153. https://doi.org/10.1021/ac010088e

Silfer, J. A., Engel, M. H., & Macko, S. A. (1992). Kinetic fractionation of stable carbon and nitrogen isotopes during peptide bond hydrolysis: Experimental evidence and geochemical implications. *Chemical Geology: Isotope Geoscience Section, 101*, 211-221. https://doi.org/10.1016/0009-2541(92)90003-N

Smedley, M. P., Dawson, T. E., Comstock, J. P., Donovan, L. A., Sherrill, D. E., Cook, C. S., & Ehleringer, J. R. (1991). Seasonal carbon isotope discrimination in a grassland community. *Oecologia, 85*(3), 314-320. https://doi.org/10.1007/BF00320605

Sponheimer, M., & Lee-Thorp, J. A. (2006). Enamel diagenesis at South African Australopith sites: Implications for paleoecological reconstruction with trace elements. *Geochimica et Cosmochimica Acta, 70*(7), 1644-1654. https://doi.org/10.1016/j.gca.2005.12.022

Sponheimer, M., Robinson, T., Ayliffe, L., Roeder, B., Hammer, J., Passey, B., West, A., Cerling, T., Dearing, D., & Ehleringer, J. (2003). Nitrogen isotopes in mammalian herbivores: Hair $\delta^{15}N$ values from a controlled feeding study. *International Journal of Osteoarchaeology, 13*(1-2), 80-87. https://doi.org/10.1002/oa.655

Staszyk, C., Suske, A., & Poschke, A. (2015). Equine dental and periodontal anatomy: A tutorial review. *Equine Veterinary Education, 27*(9), 474-481. https://doi.org/10.1111/eve.12

Stewart, W. D. P. (1977). Present-day nitrogen-fixing plants. *Ambio, 6*, 166-173. https://www.jstor.org/stable/4312269

Strahl, J., Krbetschek, M. R., Luckert, J., Machalett, B., Meng, S., Oches, E. A., Rappsilber, I., Wansa, S., & Zöller, L. (2010). Geologie, Paläontologie und Geochronologie des Eem-Beckens Neumark-Nord 2 und Vergleich mit dem Becken Neumark-Nord 1 (Geiseltal, Sachsen-Anhalt). *E&G Quaternary Science Journal, 59*(1/2), 120-167. https://doi.org/10.3285/eg.59.1-2.09

Studer, A. S., Sigman, D. M., Martínez-García, A., Thöle, L. M., Michel, E., Jaccard, S. L., Lippold, J. A., Mazaud, A., Wang, X. T., Robinson, L. F., Adkins, J. F., & Haug, G. H. (2018). Increased nutrient supply to the Southern Ocean during the Holocene and its implications for the pre-industrial atmospheric CO_2 rise. *Nature Geoscience, 11*(10), 756-760. https://doi.org/10.1038/s41561-018-0191-8

Svenning, J. C. (2002). A review of natural vegetation openness in north-western Europe. *Biological Conversation, 104*, 133-148. https://doi.org/10.1016/S0006-3207(01)00162-8

Szpak, P. (2014). Complexities of nitrogen isotope biogeochemistry in plant-soil systems: Implications for the study of ancient agricultural and animal management practices. *Frontiers in Plant Science, 5*, 288. https://doi.org/10.3389/fpls.2014.00288

Tacail, T., Kovacikova, L., Bruzek, J., & Balter, V. (2017). Spatial distribution of trace element Ca-normalized ratios in primary and permanent human tooth enamel. *Science of the Total Environment, 603-604*, 308-318. https://doi.org/10.1016/j.scitotenv.2017.06.021

Tejada-Lara, J. V., MacFadden, B. J., Bermudez, L., Rojas, G., Salas-Gismondi, R., & Flynn, J. J. (2018). Body mass predicts isotope enrichment in herbivorous mammals. *Proceedings: Biological Science, 285*(1881). https://doi.org/10.1098/rspb.2018.1020

Teruel J. de, D., Alcolea, A., Hernandez, A., & Ruiz, A. J. (2015). Comparison of chemical composition of enamel and dentine in human, bovine, porcine and ovine teeth. *Archives of Oral Biology, 60*(5), 768-775. https://doi.org/10.1016/j.archoralbio.2015.01.014

Trundell, D. A. (2020). Equine reproduction: Seasonality, endometritis, and twinning in the mare. In C. Rutland & A. Rizvanov (Eds.), *Equine Science* (18 pages). IntechOpen. https://doi.org/10.5772/intechopen.92999

Tsutaya, T., & Yoneda, M. (2015). Reconstruction of breastfeeding and weaning practices using stable isotope and trace element analyses: A review. *American Journal of Physical Anthropology, 156 Suppl 59*, 2-21. https://doi.org/10.1002/ajpa.22657

Turner, C. (2000). The Eemian interglacial in the North European plain and adjacent areas. *Netherlands Journal of Geosciences, 79*(2-3), 217-231. https://doi.org/10.1017/s0016774600023660

Ungar, P. S. (2015). Primate teeth and plant fracture properties. *Nature Education Knowledge, 6*(7), 3.

Ungar, P. S., & Lucas, P. W. (2010). Tooth form and function in biological anthropology. In C. S. Larsen (Ed.), *A Companion to Biological Anthropology* (pp. 516-529). Wiley-Blackwell.

Uno, K. T., Rivals, F., Bibi, F., Pante, M., Njau, J., & de la Torre, I. (2018). Large mammal diets and paleoecology across the Oldowan-Acheulean transition at Olduvai Gorge, Tanzania from stable isotope and tooth wear analyses. *Journal of Human Evolution, 120*, 76-91. https://doi.org/10.1016/j.jhevol.2018.01.002

Vander Zanden, M. J., Clayton, M. K., Moody, E. K., Solomon, C. T., & Weidel, B. C. (2015). Stable isotope turnover and half-life in animal tissues: a literature synthesis. *PLoS One, 10*(1), e0116182. https://doi.org/10.1371/journal.pone.0116182

Vera, F. W. M. (1997). *Metaforen voor de wildernis: Eik, hazelaar, rund, en paard.* [Landbouwuniversiteit te Wageningen].

Vera, F. W. M. (2000). *Grazing Ecology and Forest History*. CABI publishing.

Vonhof, H. B., de Graaf, S., Spero, H. J., Schiebel, R., Verdegaal, S. J. A., Metcalfe, B., & Haug, G. H. (2020). High-precision stable isotope analysis of <5 μg $CaCO_3$ samples by continuous-flow mass spectrometry. *Rapid Commun Mass Spectrom, 34*(19), e8878. https://doi.org/10.1002/rcm.8878

Vonhof, H. B., Tutken, T., Leichliter, J. N., Ludecke, T., & Haug, G. H. (2020). *High-precision stable isotope analysis of structural carbonate in < 100 μg tooth enamel samples by continuous-flow mass spectrometry*. The Society of Vertebrate Paleontology 80th Annual Meeting, https://vertpaleo.org/wp-content/uploads/2021/03/SVP_2020_ProgramAbstracts-Volume-FINAL-for-Publishing-1.27.2021.pdf

Wacker, U., Rutz, T., Löffler, N., Conrad, A. C., Tütken, T., Böttcher, M. E., & Fiebig, J. (2016). Clumped isotope thermometry of carbonate-bearing apatite: Revised sample pre-treatment, acid digestion, and temperature calibration. *Chemical Geology, 443*, 97-110. https://doi.org/10.1016/j.chemgeo.2016.09.009

Wang, Y., & Cerling, T. (1994). A model of fossil tooth and bone diagenesis: Implications for paleodiet reconstruction from stable isotopes. *Palaeogeography, Palaeoclimatology, Palaeoecology, 107*, 281-289. https://doi.org/10.1016/0031-0182(94)90100-7

Weigand, M. A., Foriel, J., Barnett, B., Oleynik, S., & Sigman, D. M. (2016). Updates to instrumentation and protocols for isotopic analysis of nitrate by the denitrifier method. *Rapid Communications in Mass Spectrometry, 30*(12), 1365-1383. https://doi.org/10.1002/rcm.7570

Welker, F., Ramos-Madrigal, J., Gutenbrunner, P., Mackie, M., Tiwary, S., Rakownikow Jersie-Christensen, R., Chiva, C., Dickinson, M. R., Kuhlwilm, M., de Manuel, M., Gelabert, P., Martinon-Torres, M., Margvelashvili, A., Arsuaga, J. L., Carbonell, E., Marques-Bonet, T., Penkman, K., Sabido, E., Cox, J., Olsen, J. V., Lordkipanidze, D., Racimo, F., Lalueza-Fox, C., Bermudez de Castro, J. M., Willerslev, E., & Cappellini, E. (2020). The dental proteome of *Homo antecessor*. *Nature, 580*(7802), 235-238. https://doi.org/10.1038/s41586-020-2153-8

White, T. D., & Folkens, P. A. (2005). *The Human Bone Manual*. Elsevier Academic Press.

Wolf, N., Carleton, S. A., & Martínez del Rio, C. (2009). Ten years of experimental animal isotopic ecology. *Functional Ecology, 23*(1), 17-26. https://doi.org/10.1111/j.1365-2435.2009.01529.x

Zazzo, A., Lécuyer, C., Sheppard, S. M. F., Grandjean, P., & Mariotti, A. (2004). Diagenesis and the reconstruction of paleoenvironments: A method to restore original $\delta^{18}O$ values of carbonate and phosphate from fossil tooth enamel. *Geochimica et Cosmochimica Acta, 68*(10), 2245-2258. https://doi.org/10.1016/j.gca.2003.11.009

Standard reference list

AG-Lox: Leichliter, J. N., Lüdecke, T., Foreman, A. D., Duprey, N. N., Winkler, D. E., Kast, E. R., Vonhof, H., Sigman, D. M., Haug, G. H., Clauss, M., Tütken, T., & Martínez-García, A. (2021). Nitrogen isotopes in tooth enamel record diet and trophic level enrichment: Results from a controlled feeding experiment. *Chemical Geology, 563*, 120047. https://doi.org/10.1016/j.chemgeo.2020.120047

AG-Lox and VICS: Vonhof, H. B., de Graaf, S., Spero, H. J., Schiebel, R., Verdegaal, S. J. A., Metcalfe, B., & Haug, G. H. (2020). High-precision stable isotope analysis of <5 mug CaCO3 samples by continuous-flow mass spectrometry. *Rapid Communications in Mass Spectrometry, 34*(19), e8878. https://doi.org/10.1002/rcm.8878

IAEA-603: Reference Product for Environment and Trade (n.d). *IAEA-603*. International Atomic Energy Agency. Retrieved Ocotber 9, 2022, from https://nucleus.iaea.org/sites/ReferenceMaterials/Pages/IAEA-603.aspx

IAEA-NO-3: Reference Product for Environment and Trade (n.d). *IAEA-NO-3*. International Atomic Energy Agency. Retrieved Ocotber 9, 2022, from https://nucleus.iaea.org/sites/ReferenceMaterials/Pages/IAEA-NO-3.aspx

NBS18: Reference Product for Environment and Trade (n.d). *NBS18*. International Atomic Energy Agency. Retrieved Ocotber 9, 2022, from https://nucleus.iaea.org/sites/ReferenceMaterials/Pages/NBS18.aspx

NBS120c: Chenery, C., Müldner, G., Evans, J., Eckardt, H., & Lewis, M. (2010). Strontium and stable isotope evidence for diet and mobility in Roman Gloucester, UK. *Journal of Archaeological Science, 37*(1), 150-163. https://doi.org/10.1016/j.jas.2009.09.025

USGS34: Reference Materials and Calibration Services (July 10, 2018). *RSIL: Report of Stable Isotopic Composition for reference materials USGS32 USGS34 and USGS35*. United States Geological Survey. https://www.usgs.gov/media/files/rsil-report-stable-isotopic-composition-reference-materials-usgs32-usgs34-and-usgs35

USGS40: Reference Materials and Calibration Services (July 10, 2018). *RSIL: Report of Stable Isotopic Composition for reference materials USGS40*. United States Geological Survey. https://www.usgs.gov/media/files/rsil-report-stable-isotopic-composition-reference-material-usgs40

USGS65: Reference Materials and Calibration Services (February 27, 2020). *RSIL: Report of Stable Isotopic Composition for reference materials USGS64 USGS65 and USGS66*. United States Geological Survey. https://www.usgs.gov/media/files/rsil-report-stable-isotopic-composition-reference-materials-usgs64-usgs65-and-usgs66

Appendix A

Identified plant species present in unit 8 of NMN2.

Table A.1: All identified plant species present in unit 8 of NMN2 based on pollen analysis. The analysis was performed by C. C. Bakels (Sier et al, 2011). The species in bold are from figure S5. The other species are from table S1.

Tree, shrubs, lianas	Herbs, open space	Waterside and lake vegetation
Betula	***Artemisia***	***Monoletae psilatae***
Carpinus	***Asteraceae liguliflorae***	***Ranunculus aquatilis* group**
Corylus	***Asteraceae tubuliflorae***	***Spirogyra***
Fraxinus	***Caryophyllaceae***	*Sparganium erectum type*
Picea	***Chenopodiaceae***	*Typha latifolia*
Pinus	***Cyperaceae***	*Myriophyllum spicatum*
Quercus	***Poaceae***	
Ulmus	***Polygonum aviculare***	
Alnus	*Galium* type	
Tilia	*Filipendula*	
Salix	*Ranunculus acris* type	
Rosacae	Ericales	
Ilex	Apiaceae	
Acer	Brassicaceae	
Cornus sanguinea	*Rumex acetosa* type	
Humulus/Cannabis	*Caltha*	
Hedera	*Triglochin*	
Myrica	*Plantago coronopus*	
Frangula	*Trifolium* type	
Prunus	*Campanula*	
	Thalictrum	
	Plantago major/media	
	Spergularia	
	Veronica	
	Stachys type	

	Mentha type	
	Papaver rhoeas type	
	Helianthemum nummularium type	
	Lysimachia vulgaris type	
	Saxifraga aizoides type	
	Onobrychis	
	Parietaria	

Appendix B

All $\delta^{13}C_{enamel}$, $\delta^{18}O_{enamel}$, and $\delta^{15}N_{enamel}$ measurements per sample.

Table B.1: All $\delta^{13}C_{enamel}$ cold trap measurements (in ‰ vs VPDB), the average, and standard deviation per sample corrected against the AG-Lox standard, as explained in section 5.4. All samples were measured in duplicate. As a quality control, samples were measured in triplicate, or more, if the standard deviation of either the $\delta^{13}C$ or the $\delta^{18}O$ value was above 0.5. The last row contains the average $\delta^{13}C$ value and the average standard deviation of all 259 samples together.

Sample ID	First $\delta^{13}C$	Duplicate $\delta^{13}C$	Triplicate $\delta^{13}C$	Quadruplicate $\delta^{13}C$	Average $\delta^{13}C$	Standard deviation $\delta^{13}C$
NMN-120a	-12.0	-11.9	-11.9		-11.9	0.0
NMN-120b	-11.8	-11.8	-11.6		-11.7	0.1
NMN-120c	-11.0	-11.2	-11.4		-11.2	0.1
NMN-120d	-11.5	-11.3	-11.3		-11.4	0.1
NMN-120e	-11.9	-11.8			-11.9	0.0
NMN-120f	-11.6	-11.6	-12.0		-11.7	0.2
NMN-120g	-11.2	-11.4			-11.3	0.1
NMN-120h	-11.0	-11.1			-11.0	0.0
NMN-120i	-11.8	-11.7			-11.7	0.1
NMN-120j	-11.9	-12.0			-12.0	0.1
NMN-120k	-11.7	-11.4			-11.5	0.1
NMN-120l	-11.8	-11.9			-11.9	0.1
NMN-120m	-11.9	-11.9			-11.9	0.0
NMN-121a	-10.3	-11.0			-10.6	0.3
NMN-121b	-11.8	-11.8			-11.8	0.0
NMN-121c	-12.1	-11.6			-11.8	0.3
NMN-121d	-11.9	-11.8			-11.9	0.0
NMN-121e	-11.8	-11.6			-11.7	0.1
NMN-121f	-11.5	-11.6			-11.5	0.0
NMN-121g	-11.3	-11.6			-11.4	0.1
NMN-121h	-11.6	-11.8			-11.7	0.1
NMN-121i	-11.9	-11.7			-11.8	0.1

NMN-121j	-12.1	-12.1			-12.1	0.0
NMN-121k	-12.2	-12.5			-12.4	0.1
NMN-121l	-12.4	-12.6			-12.5	0.1
NMN-121m	-12.1	-12.2	-11.6		-12.0	0.3
NMN-121n	-12.2	-12.2	-12.2		-12.2	0.0
NMN-121o	-11.9	-12.2	-11.9		-12.0	0.1
NMN-121p	-12.2	-12.3	-12.1		-12.2	0.1
NMN-121q	-12.2	-12.1	-12.0		-12.1	0.1
NMN-122a	-11.7	-11.3	-11.3		-11.5	0.2
NMN-122b	-11.5	-11.4	-11.5		-11.5	0.0
NMN-122c	-11.8	-11.7	-11.8		-11.8	0.1
NMN-122d	-11.6	-11.3	-11.5		-11.4	0.1
NMN-122e	-11.4	-11.5	-11.6		-11.5	0.1
NMN-122f	-11.8	-11.5			-11.7	0.1
NMN-122g	-11.8	-11.5			-11.7	0.1
NMN-122h	-11.8	-11.7			-11.7	0.0
NMN-122i	-12.0	-11.9			-11.9	0.1
NMN-122j	-12.3	-11.8			-12.0	0.2
NMN-122k	-12.4	-12.4			-12.4	0.0
NMN-122l	-12.6	-12.6			-12.6	0.0
NMN-122m	-12.8	-12.6			-12.7	0.1
NMN-122n	-12.7	-12.6			-12.6	0.0
NMN-122o	-12.7	-12.6			-12.6	0.1
NMN-122p	-12.7	-12.6			-12.6	0.1
NMN-122q	-12.4	-12.3			-12.4	0.1
NMN-123a	-10.8	-11.4	-10.9		-11.0	0.2
NMN-123b	-12.6	-12.3			-12.4	0.2
NMN-123c	-12.6	-12.3			-12.5	0.1
NMN-123d	-12.3	-12.5			-12.4	0.1
NMN-123e	-12.3	-12.5			-12.4	0.1

NMN-123f	-12.8	-12.4			-12.6	0.2
NMN-123g	-12.4	-12.3			-12.3	0.0
NMN-123h	-12.5	-12.3			-12.4	0.1
NMN-123i	-12.5	-12.5			-12.5	0.0
NMN-123j	-12.3	-12.2			-12.2	0.1
NMN-123k	-12.1	-11.8	-11.7	-11.7	-11.8	0.2
NMN-123l	-11.7	-11.9			-11.8	0.1
NMN-123m	-11.9	-12.1			-12.0	0.1
NMN-123n	-12.0	-12.0			-12.0	0.0
NMN-123o	-12.4	-12.5			-12.4	0.0
NMN-123p	-12.3	-12.7			-12.5	0.2
NMN-124a	-12.0	-12.0			-12.0	0.0
NMN-124b	-12.2	-12.2			-12.2	0.0
NMN-124c	-11.8	-12.4			-12.1	0.3
NMN-124d	-12.1	-12.3			-12.2	0.1
NMN-124e	-12.1	-12.6			-12.4	0.2
NMN-124f	-12.2	-12.5			-12.3	0.1
NMN-124g	-12.4	-12.5			-12.5	0.0
NMN-124h	-12.0	-12.4			-12.2	0.2
NMN-124i	-12.0	-12.0			-12.0	0.0
NMN-124j	-12.5	-11.6			-12.0	0.4
NMN-124k	-11.2	-12.1			-11.6	0.4
NMN-124l	-11.6	-11.8			-11.7	0.1
NMN-124m	-11.8	-11.5			-11.6	0.2
NMN-124n	-11.1	-11.7			-11.4	0.3
NMN-124o	-12.0	-12.0			-12.0	0.0
NMN-124p	-12.0	-12.2			-12.1	0.1
NMN-124q	-11.3	-11.5			-11.4	0.1
NMN-125a	-12.1	-12.3			-12.2	0.1
NMN-125b	-12.3	-12.4			-12.3	0.0

NMN-125c	-12.5	-12.4			-12.4	0.0
NMN-125d	-12.3	-12.4			-12.4	0.0
NMN-125e	-12.2	-12.4			-12.3	0.1
NMN-125f	-12.4	-12.3			-12.3	0.1
NMN-125g	-12.5	-12.4			-12.4	0.0
NMN-125h	-12.6	-12.6			-12.6	0.0
NMN-125i	-12.8	-12.7			-12.8	0.1
NMN-125j	-12.7	-12.6			-12.7	0.0
NMN-125k	-12.8	-12.8			-12.8	0.0
NMN-125l	-12.6	-12.7			-12.7	0.0
NMN-125m	-12.8	-12.7			-12.7	0.0
NMN-125n	-12.9	-13.1			-13.0	0.1
NMN-125o	-13.1	-13.0			-13.1	0.0
NMN-125p	-13.2	-12.7			-13.0	0.2
NMN-125q	-13.1	-13.0			-13.1	0.1
NMN-125r	-12.6	-12.9			-12.7	0.1
NMN-125s	-12.8	-12.7			-12.8	0.0
NMN-126a	-12.0	-11.6			-11.8	0.2
NMN-126b	-12.3	-12.5			-12.4	0.1
NMN-126c	-12.2	-12.3			-12.2	0.0
NMN-126d	-12.5	-12.6			-12.5	0.1
NMN-126e	-12.7	-12.7			-12.7	0.0
NMN-126f	-12.9	-12.8			-12.9	0.0
NMN-126g	-13.0	-12.4			-12.7	0.3
NMN-126h	-12.0	-12.6			-12.3	0.3
NMN-126i	-12.5	-12.5			-12.5	0.0
NMN-126j	-12.6	-12.7			-12.7	0.1
NMN-126k	-12.2	-12.3			-12.2	0.0
NMN-126l	-12.2	-12.1			-12.1	0.0
NMN-126m	-12.2	-12.4			-12.3	0.1

NMN-126n	-12.5	-12.5			-12.5	0.0
NMN-126o	-12.4	-12.2			-12.3	0.1
NMN-126p	-12.6	-12.5			-12.5	0.1
NMN-126q	-12.3	-12.6			-12.4	0.1
NMN-126r	-12.3	-12.2	-12.4		-12.3	0.1
NMN-126s	-12.2	-12.2	-12.2		-12.2	0.0
NMN-127a	-11.4	-11.4	-11.3		-11.4	0.1
NMN-127b	-11.8	-11.8	-11.4		-11.7	0.2
NMN-127c	-11.8	-11.9	-12.1		-11.9	0.1
NMN-127d	-11.8	-11.4	-11.9		-11.7	0.2
NMN-127e	-12.0	-12.1	-11.9		-12.0	0.1
NMN-127f	-11.8	-11.9			-11.8	0.0
NMN-127g	-12.0	-11.9			-12.0	0.0
NMN-127h	-11.7	-11.8			-11.8	0.1
NMN-127i	-11.8	-11.8			-11.8	0.0
NMN-127j	-11.5	-11.6			-11.6	0.0
NMN-127k	-11.5	-11.7			-11.6	0.1
NMN-127l	-12.0	-11.5			-11.8	0.2
NMN-127m	-12.0	-12.1			-12.1	0.0
NMN-127n	-11.9	-12.2			-12.0	0.1
NMN-128a	-12.7	-12.6			-12.6	0.1
NMN-128b	-12.8	-12.5			-12.6	0.1
NMN-128c	-12.5	-12.9			-12.7	0.2
NMN-128d	-12.3	-12.3			-12.3	0.0
NMN-128e	-12.5	-12.4			-12.5	0.0
NMN-128f	-12.2	-12.1			-12.1	0.0
NMN-128g	-12.5	-12.7			-12.6	0.1
NMN-128h	-12.7	-12.8			-12.7	0.0
NMN-128i	-12.7	-12.7			-12.7	0.0
NMN-128j	-12.4	-12.4			-12.4	0.0

NMN-128k	-12.4	-12.5			-12.5	0.0
NMN-128l	-12.6	-12.6			-12.6	0.0
NMN-128m	-12.6	-12.6			-12.6	0.0
NMN-128n	-12.5	-12.5			-12.5	0.0
NMN-128o	-12.5	-12.5			-12.5	0.0
NMN-128p	-12.3	-12.4			-12.3	0.0
NMN-128q	-12.2	-12.3			-12.2	0.1
NMN-128r	-12.3	-12.3			-12.3	0.0
NMN-128s	-12.2	-12.3			-12.3	0.0
NMN-128t	-12.4	-12.3			-12.4	0.1
NMN-129a	-10.8	-10.9			-10.8	0.1
NMN-129b	-11.9	-11.9			-11.9	0.0
NMN-129c	-12.4	-12.4			-12.4	0.0
NMN-129d	-12.5	-12.6			-12.5	0.0
NMN-129e	-12.6	-12.4			-12.5	0.1
NMN-129f	-12.9	-12.8			-12.9	0.0
NMN-129g	-12.6	-12.7			-12.7	0.0
NMN-129h	-12.8	-12.8			-12.8	0.0
NMN-129i	-12.6	-12.7			-12.7	0.0
NMN-129j	-12.6	-12.7			-12.6	0.0
NMN-129k	-12.6	-12.5			-12.6	0.0
NMN-129l	-12.5	-12.6			-12.5	0.1
NMN-129m	-12.7	-12.7			-12.7	0.0
NMN-129n	-12.6	-12.7			-12.6	0.0
NMN-129o	-12.5	-12.5			-12.5	0.0
NMN-129p	-12.5	-12.5			-12.5	0.0
NMN-129q	-12.7	-12.6			-12.6	0.1
NMN-129r	-12.5	-12.6			-12.5	0.1
NMN-129s	-12.4	-12.5			-12.4	0.0
NMN-129t	-12.1	-12.4			-12.3	0.1

NMN-129u	-12.4	-12.3			-12.4	0.0
NMN-129v	-12.2	-12.3			-12.3	0.0
NMN-129w	-12.2	-12.2			-12.2	0.0
NMN-130a	-12.3	-12.2			-12.3	0.1
NMN-130b	-12.5	-12.2			-12.4	0.1
NMN-130c	-12.7	-12.6			-12.6	0.0
NMN-130d	-12.7	-12.3			-12.5	0.2
NMN-130e	-12.6	-12.7			-12.7	0.0
NMN-130f	-12.4	-12.5			-12.5	0.0
NMN-130g	-12.6	-12.5			-12.5	0.1
NMN-130h	-12.3	-12.4			-12.3	0.0
NMN-130i	-12.5	-12.3			-12.4	0.1
NMN-130j	-12.5	-12.4			-12.5	0.1
NMN-130k	-12.4	-12.5			-12.4	0.0
NMN-130l	-12.7	-12.6			-12.6	0.0
NMN-130m	-12.6	-12.1			-12.3	0.2
NMN-130n	-12.3	-12.5			-12.4	0.1
NMN-130o	-12.4	-12.4			-12.4	0.0
NMN-130p	-12.6	-12.5			-12.5	0.1
NMN-130q	-12.6	-12.4			-12.5	0.1
NMN-130r	-12.4	-12.0			-12.2	0.2
NMN-130s	-12.3	-12.2			-12.3	0.1
NMN-130t	-12.4	-12.2			-12.3	0.1
NMN-130u	-12.1	-12.1			-12.1	0.0
NMN-130v	-12.4	-12.3			-12.3	0.0
NMN-130w	-12.6	-12.2			-12.4	0.2
NMN-130x	-12.4	-12.3			-12.3	0.0
NMN-130y	-12.6	-12.5			-12.5	0.0
NMN-130z	-12.8	-12.6			-12.7	0.1
NMN-131a	-11.8	-11.9			-11.8	0.1

NMN-131b	-12.5	-12.7			-12.6	0.1
NMN-131c	-12.6	-12.6			-12.6	0.0
NMN-131d	-12.5	-12.2			-12.4	0.2
NMN-131e	-12.2	-12.4			-12.3	0.1
NMN-131f	-12.5	-12.6			-12.5	0.1
NMN-131g	-12.9	-12.4			-12.6	0.2
NMN-131h	-12.5	-12.4			-12.5	0.1
NMN-131i	-12.5	-12.4			-12.4	0.1
NMN-131j	-12.1	-12.0			-12.0	0.1
NMN-131k	-12.3	-12.2			-12.2	0.0
NMN-131l	-12.4	-12.5			-12.4	0.0
NMN-131m	-12.5	-12.4			-12.5	0.1
NMN-131n	-12.6	-12.4			-12.5	0.1
NMN-131o	-12.5	-12.6			-12.6	0.1
NMN-131p	-12.5	-13.0			-12.8	0.2
NMN-131q	-12.7	-12.5			-12.6	0.1
NMN-131r	-12.3	-12.3			-12.3	0.0
NMN-131s	-12.6	-12.7			-12.7	0.0
NMN-132a	-12.4	-12.1			-12.3	0.1
NMN-132b	-12.5	-12.4			-12.5	0.0
NMN-132c	-12.3	-12.4			-12.4	0.0
NMN-132d	-11.8	-12.3			-12.1	0.3
NMN-132e	-12.2	-12.2			-12.2	0.0
NMN-132f	-12.2	-12.1			-12.1	0.0
NMN-132g	-12.2	-12.2			-12.2	0.0
NMN-132h	-12.3	-12.1			-12.2	0.1
NMN-132i	-12.4	-12.4			-12.4	0.0
NMN-132j	-12.5	-12.5			-12.5	0.0
NMN-132k	-12.4	-12.1			-12.3	0.1
NMN-132l	-12.5	-12.5			-12.5	0.0

NMN-132m	-12.7	-12.7			-12.7	0.0
NMN-132n	-12.7	-12.7			-12.7	0.0
NMN-132o	-12.7	-12.7			-12.7	0.0
NMN-132p	-12.7	-12.8			-12.8	0.0
NMN-132q	-12.8	-12.7			-12.8	0.1
NMN-132r	-12.9	-12.9			-12.9	0.0
NMN-132s	-12.9	-12.9			-12.9	0.0
NMN-132t	-12.9	-12.9			-12.9	0.0
NMN-132u	-12.9	-12.9			-12.9	0.0
NMN-133a	-11.4	-11.5			-11.5	0.0
NMN-133b	-11.6	-11.5			-11.6	0.1
NMN-133c	-11.6	-11.6			-11.6	0.0
NMN-133d	-11.8	-11.6			-11.7	0.1
NMN-133e	-11.7	-11.5			-11.6	0.1
NMN-133f	-12.3	-12.2			-12.2	0.0
NMN-133g	-12.6	-12.5			-12.5	0.1
NMN-133h	-12.6	-12.4			-12.5	0.1
NMN-133i	-12.3	-12.3			-12.3	0.0
NMN-133j	-12.5	-12.3			-12.4	0.1
NMN-133k	-12.3	-12.3			-12.3	0.0
NMN-133l	-12.2	-12.2			-12.2	0.0
NMN-133m	-12.1	-12.1			-12.1	0.0
NMN-133n	-12.1	-12.0			-12.0	0.1
NMN-133o	-11.9	-11.7			-11.8	0.1
NMN-133p	-12.1	-12.1			-12.1	0.0
NMN-133q	-12.2	-12.3			-12.3	0.0
NMN-133r	-12.3	-12.4			-12.4	0.0
Total average					-12.3	0.1

Table B.2: All $\delta^{18}O_{enamel}$ cold trap measurements (in ‰ vs VPDB), the average, and standard deviation per sample corrected against the AG-Lox standard, as explained in section 5.4. All samples were measured in duplicate. As a quality control, samples were measured in triplicate, or more, if the standard deviation of either the $\delta^{13}C$ or the $\delta^{18}O$ value was above 0.5. The last row contains the average $\delta^{18}O$ value and the average standard deviation of all 259 samples together.

Sample ID	First $\delta^{18}O$	Duplicate $\delta^{18}O$	Triplicate $\delta^{18}O$	Quadruplicate $\delta^{18}O$	Average $\delta^{18}O$	Standard deviation $\delta^{18}O$
NMN-120a	-7.1	-7.2	-7.1		-7.2	0.0
NMN-120b	-5.9	-6.2	-6.3		-6.1	0.2
NMN-120c	-5.0	-5.1	-5.2		-5.1	0.1
NMN-120d	-5.7	-6.2	-5.6		-5.8	0.3
NMN-120e	-6.7	-6.6			-6.7	0.0
NMN-120f	-7.0	-6.9	-7.2		-7.0	0.1
NMN-120g	-6.5	-6.3			-6.4	0.1
NMN-120h	-5.9	-5.5			-5.7	0.2
NMN-120i	-6.2	-6.0			-6.1	0.1
NMN-120j	-5.0	-5.0			-5.0	0.0
NMN-120k	-5.2	-4.8			-5.0	0.2
NMN-120l	-5.2	-5.0			-5.1	0.1
NMN-120m	-5.5	-5.4			-5.4	0.1
NMN-121a	-6.4	-6.0			-6.2	0.2
NMN-121b	-7.3	-7.3			-7.3	0.0
NMN-121c	-5.6	-5.7			-5.6	0.0
NMN-121d	-6.6	-6.5			-6.5	0.1
NMN-121e	-6.0	-5.7			-5.8	0.1
NMN-121f	-5.6	-5.3			-5.4	0.1
NMN-121g	-5.0	-5.0			-5.0	0.0
NMN-121h	-5.1	-4.8			-5.0	0.1
NMN-121i	-5.4	-5.3			-5.3	0.0
NMN-121j	-6.0	-6.1			-6.0	0.1
NMN-121k	-6.8	-6.4			-6.6	0.2
NMN-121l	-7.5	-7.4			-7.5	0.1

NMN-121m	-7.1	-7.2	-6.7		-7.0	0.2
NMN-121n	-7.1	-7.0	-7.1		-7.1	0.1
NMN-121o	-6.9	-6.8	-6.7		-6.8	0.1
NMN-121p	-6.7	-6.6	-6.8		-6.7	0.1
NMN-121q	-6.5	-6.3	-6.3		-6.4	0.1
NMN-122a	-6.5	-6.4	-6.7		-6.5	0.1
NMN-122b	-7.1	-7.2	-7.1		-7.2	0.0
NMN-122c	-5.3	-5.2	-5.4		-5.3	0.1
NMN-122d	-6.2	-5.8	-5.9		-6.0	0.2
NMN-122e	-6.7	-6.6	-6.6		-6.6	0.0
NMN-122f	-6.9	-6.7			-6.8	0.1
NMN-122g	-6.5	-6.0			-6.2	0.3
NMN-122h	-5.7	-5.6			-5.6	0.1
NMN-122i	-5.4	-5.4			-5.4	0.0
NMN-122j	-5.4	-5.4			-5.4	0.0
NMN-122k	-6.1	-6.1			-6.1	0.0
NMN-122l	-7.0	-7.2			-7.1	0.1
NMN-122m	-7.6	-7.8			-7.7	0.1
NMN-122n	-9.1	-8.4			-8.7	0.3
NMN-122o	-7.5	-7.3			-7.4	0.1
NMN-122p	-7.5	-7.3			-7.4	0.1
NMN-122q	-7.6	-7.3			-7.5	0.2
NMN-123a	-6.5	-6.5	-6.7		-6.5	0.1
NMN-123b	-6.1	-6.4			-6.2	0.2
NMN-123c	-5.7	-5.6			-5.6	0.0
NMN-123d	-5.3	-5.5			-5.4	0.1
NMN-123e	-5.4	-6.1			-5.8	0.3
NMN-123f	-6.4	-6.4			-6.4	0.0
NMN-123g	-6.9	-6.7			-6.8	0.1
NMN-123h	-7.1	-7.0			-7.0	0.1

NMN-123i	-7.3	-7.1			-7.2	0.1
NMN-123j	-6.8	-6.9			-6.9	0.0
NMN-123k	-6.0	-6.0	-5.9	-5.8	-5.9	0.1
NMN-123l	-5.2	-5.3			-5.2	0.0
NMN-123m	-4.8	-4.9			-4.9	0.1
NMN-123n	-5.1	-5.1			-5.1	0.0
NMN-123o	-5.0	-4.9			-4.9	0.1
NMN-123p	-5.1	-5.3			-5.2	0.1
NMN-124a	-7.0	-7.0			-7.0	0.0
NMN-124b	-6.8	-6.7			-6.7	0.0
NMN-124c	-6.9	-6.5			-6.7	0.2
NMN-124d	-5.7	-6.0			-5.8	0.1
NMN-124e	-5.9	-5.9			-5.9	0.0
NMN-124f	-6.4	-6.8			-6.6	0.2
NMN-124g	-6.7	-7.1			-6.9	0.2
NMN-124h	-6.9	-6.9			-6.9	0.0
NMN-124i	-6.6	-6.4			-6.5	0.1
NMN-124j	-5.8	-5.7			-5.7	0.1
NMN-124k	-5.0	-5.5			-5.2	0.3
NMN-124l	-5.1	-5.2			-5.2	0.0
NMN-124m	-5.2	-4.8			-5.0	0.2
NMN-124n	-4.6	-4.9			-4.8	0.1
NMN-124o	-5.1	-4.9			-5.0	0.1
NMN-124p	-5.6	-5.7			-5.7	0.0
NMN-124q	-6.2	-6.1			-6.1	0.0
NMN-125a	-6.1	-6.3			-6.2	0.1
NMN-125b	-6.5	-6.5			-6.5	0.0
NMN-125c	-6.3	-6.4			-6.4	0.1
NMN-125d	-6.4	-6.3			-6.3	0.0
NMN-125e	-5.6	-5.7			-5.6	0.0

NMN-125f	-4.8	-4.8			-4.8	0.0
NMN-125g	-4.7	-4.5			-4.6	0.1
NMN-125h	-5.0	-4.8			-4.9	0.1
NMN-125i	-5.6	-5.6			-5.6	0.0
NMN-125j	-6.0	-6.1			-6.0	0.0
NMN-125k	-6.5	-6.2			-6.4	0.1
NMN-125l	-6.6	-6.7			-6.7	0.0
NMN-125m	-6.9	-6.9			-6.9	0.0
NMN-125n	-7.0	-6.8			-6.9	0.1
NMN-125o	-6.4	-6.5			-6.4	0.0
NMN-125p	-6.4	-6.3			-6.3	0.1
NMN-125q	-6.5	-6.2			-6.3	0.1
NMN-125r	-6.1	-6.2			-6.1	0.1
NMN-125s	-6.3	-6.1			-6.2	0.1
NMN-126a	-6.9	-6.6			-6.7	0.1
NMN-126b	-7.5	-7.6			-7.6	0.0
NMN-126c	-5.3	-5.4			-5.3	0.0
NMN-126d	-5.7	-5.7			-5.7	0.0
NMN-126e	-6.7	-6.5			-6.6	0.1
NMN-126f	-6.9	-6.8			-6.9	0.0
NMN-126g	-6.7	-6.5			-6.6	0.1
NMN-126h	-6.0	-6.3			-6.2	0.1
NMN-126i	-5.8	-5.6			-5.7	0.1
NMN-126j	-5.5	-5.1			-5.3	0.2
NMN-126k	-4.6	-4.8			-4.7	0.1
NMN-126l	-5.5	-5.4			-5.5	0.0
NMN-126m	-6.4	-6.6			-6.5	0.1
NMN-126n	-7.2	-7.2			-7.2	0.0
NMN-126o	-7.3	-7.3			-7.3	0.0
NMN-126p	-7.5	-7.7			-7.6	0.1

NMN-126q	-7.6	-8.0			-7.8	0.2
NMN-126r	-6.9	-7.0	-7.1		-7.0	0.1
NMN-126s	-6.5	-6.6	-6.6		-6.6	0.0
NMN-127a	-6.7	-6.8	-6.6		-6.7	0.1
NMN-127b	-8.0	-8.1	-7.9		-8.0	0.1
NMN-127c	-7.0	-7.1	-7.4		-7.1	0.2
NMN-127d	-5.8	-6.0	-6.2		-6.0	0.1
NMN-127e	-6.6	-6.5	-6.4		-6.5	0.1
NMN-127f	-7.3	-7.5			-7.4	0.1
NMN-127g	-7.3	-7.8			-7.5	0.2
NMN-127h	-7.5	-7.2			-7.3	0.1
NMN-127i	-6.5	-6.7			-6.6	0.1
NMN-127j	-6.2	-6.6			-6.4	0.2
NMN-127k	-6.0	-6.2			-6.1	0.1
NMN-127l	-5.9	-5.8			-5.9	0.0
NMN-127m	-6.5	-6.3			-6.4	0.1
NMN-127n	-6.9	-7.5			-7.2	0.3
NMN-128a	-6.8	-6.6			-6.7	0.1
NMN-128b	-6.3	-6.0			-6.1	0.1
NMN-128c	-4.7	-5.2			-4.9	0.3
NMN-128d	-4.8	-4.9			-4.8	0.0
NMN-128e	-5.5	-6.0			-5.7	0.3
NMN-128f	-6.3	-6.5			-6.4	0.1
NMN-128g	-6.4	-6.7			-6.5	0.1
NMN-128h	-6.5	-6.5			-6.5	0.0
NMN-128i	-6.0	-6.2			-6.1	0.1
NMN-128j	-5.5	-5.8			-5.7	0.1
NMN-128k	-5.1	-5.3			-5.2	0.1
NMN-128l	-4.7	-5.0			-4.8	0.1
NMN-128m	-4.9	-4.9			-4.9	0.0

NMN-128n	-4.9	-4.8			-4.8	0.0
NMN-128o	-5.8	-5.7			-5.8	0.0
NMN-128p	-6.6	-6.7			-6.6	0.0
NMN-128q	-7.0	-7.1			-7.1	0.0
NMN-128r	-6.9	-6.8			-6.9	0.0
NMN-128s	-6.6	-6.6			-6.6	0.0
NMN-128t	-6.1	-6.2			-6.2	0.1
NMN-129a	-5.3	-5.1			-5.2	0.1
NMN-129b	-6.2	-6.6			-6.4	0.2
NMN-129c	-6.5	-6.3			-6.4	0.1
NMN-129d	-5.2	-5.5			-5.3	0.2
NMN-129e	-5.0	-4.9			-5.0	0.1
NMN-129f	-6.2	-6.0			-6.1	0.1
NMN-129g	-6.6	-6.6			-6.6	0.0
NMN-129h	-6.7	-6.4			-6.5	0.2
NMN-129i	-6.2	-6.2			-6.2	0.0
NMN-129j	-6.0	-6.4			-6.2	0.2
NMN-129k	-5.5	-5.4			-5.4	0.0
NMN-129l	-5.1	-5.4			-5.2	0.1
NMN-129m	-4.9	-4.8			-4.8	0.0
NMN-129n	-4.7	-4.7			-4.7	0.0
NMN-129o	-5.1	-5.0			-5.0	0.0
NMN-129p	-6.1	-5.9			-6.0	0.1
NMN-129q	-6.8	-6.4			-6.6	0.2
NMN-129r	-6.8	-7.0			-6.9	0.1
NMN-129s	-7.1	-7.1			-7.1	0.0
NMN-129t	-6.8	-6.9			-6.8	0.0
NMN-129u	-6.9	-6.6			-6.7	0.1
NMN-129v	-6.0	-6.1			-6.1	0.1
NMN-129w	-5.7	-5.5			-5.6	0.1

NMN-130a	-6.5	-6.4			-6.5	0.1
NMN-130b	-6.8	-6.9			-6.9	0.1
NMN-130c	-7.8	-7.6			-7.7	0.1
NMN-130d	-7.5	-7.2			-7.3	0.1
NMN-130e	-7.1	-6.9			-7.0	0.1
NMN-130f	-6.6	-6.2			-6.4	0.2
NMN-130g	-6.0	-5.7			-5.9	0.1
NMN-130h	-5.4	-5.2			-5.3	0.1
NMN-130i	-5.5	-4.9			-5.2	0.3
NMN-130j	-5.5	-5.4			-5.4	0.0
NMN-130k	-5.7	-5.8			-5.7	0.0
NMN-130l	-6.2	-6.3			-6.2	0.0
NMN-130m	-6.8	-6.3			-6.5	0.2
NMN-130n	-6.6	-6.7			-6.6	0.0
NMN-130o	-7.1	-7.0			-7.0	0.0
NMN-130p	-7.3	-6.9			-7.1	0.2
NMN-130q	-6.6	-6.5			-6.6	0.1
NMN-130r	-6.2	-5.9			-6.1	0.1
NMN-130s	-5.7	-5.7			-5.7	0.0
NMN-130t	-5.4	-5.1			-5.2	0.2
NMN-130u	-5.2	-4.7			-5.0	0.2
NMN-130v	-5.1	-4.9			-5.0	0.1
NMN-130w	-5.4	-4.8			-5.1	0.3
NMN-130x	-5.0	-5.0			-5.0	0.0
NMN-130y	-4.9	-5.0			-5.0	0.0
NMN-130z	-5.5	-5.2			-5.3	0.2
NMN-131a	-6.7	-6.6			-6.7	0.0
NMN-131b	-7.7	-7.4			-7.5	0.1
NMN-131c	-7.5	-7.2			-7.3	0.2
NMN-131d	-7.3	-6.7			-7.0	0.3

NMN-131e	-6.4	-6.1			-6.3	0.1
NMN-131f	-6.1	-6.0			-6.1	0.1
NMN-131g	-6.2	-6.6			-6.4	0.2
NMN-131h	-6.3	-6.1			-6.2	0.1
NMN-131i	-6.5	-6.4			-6.5	0.0
NMN-131j	-6.5	-6.3			-6.4	0.1
NMN-131k	-6.0	-6.0			-6.0	0.0
NMN-131l	-5.9	-5.9			-5.9	0.0
NMN-131m	-5.9	-5.7			-5.8	0.1
NMN-131n	-5.7	-5.6			-5.6	0.1
NMN-131o	-5.5	-5.3			-5.4	0.1
NMN-131p	-6.0	-6.5			-6.3	0.3
NMN-131q	-6.0	-5.9			-6.0	0.1
NMN-131r	-6.1	-6.0			-6.0	0.0
NMN-131s	-6.5	-6.7			-6.6	0.1
NMN-132a	-5.5	-5.4			-5.4	0.0
NMN-132b	-5.6	-5.3			-5.5	0.1
NMN-132c	-6.7	-6.7			-6.7	0.0
NMN-132d	-6.4	-6.8			-6.6	0.2
NMN-132e	-6.2	-6.4			-6.3	0.1
NMN-132f	-5.5	-5.4			-5.5	0.1
NMN-132g	-5.2	-5.1			-5.1	0.0
NMN-132h	-5.2	-5.0			-5.1	0.1
NMN-132i	-5.2	-5.5			-5.4	0.2
NMN-132j	-5.4	-5.6			-5.5	0.1
NMN-132k	-5.9	-5.7			-5.8	0.1
NMN-132l	-6.2	-6.2			-6.2	0.0
NMN-132m	-6.7	-6.9			-6.8	0.1
NMN-132n	-7.0	-7.1			-7.1	0.1
NMN-132o	-6.9	-7.0			-7.0	0.0

NMN-132p	-7.2	-6.9			-7.1	0.2
NMN-132q	-6.7	-7.5			-7.1	0.4
NMN-132r	-6.9	-7.2			-7.0	0.1
NMN-132s	-6.9	-6.7			-6.8	0.1
NMN-132t	-6.3	-6.4			-6.3	0.0
NMN-132u	-5.8	-5.9			-5.9	0.0
NMN-133a	-7.1	-7.2			-7.2	0.0
NMN-133b	-6.6	-6.4			-6.5	0.1
NMN-133c	-5.7	-5.9			-5.8	0.1
NMN-133d	-5.5	-5.3			-5.4	0.1
NMN-133e	-5.3	-5.1			-5.2	0.1
NMN-133f	-5.5	-5.2			-5.3	0.2
NMN-133g	-6.4	-6.1			-6.3	0.1
NMN-133h	-6.9	-6.4			-6.6	0.2
NMN-133i	-6.6	-6.4			-6.5	0.1
NMN-133j	-7.2	-6.9			-7.0	0.2
NMN-133k	-6.9	-7.1			-7.0	0.1
NMN-133l	-6.8	-6.5			-6.7	0.1
NMN-133m	-6.3	-5.8			-6.1	0.2
NMN-133n	-5.8	-5.3			-5.5	0.2
NMN-133o	-5.2	-4.8			-5.0	0.2
NMN-133p	-5.2	-5.0			-5.1	0.1
NMN-133q	-5.3	-5.0			-5.1	0.1
NMN-133r	-5.3	-5.6			-5.4	0.1
Total Average					-6.2	0.1

Table B.3: All $\delta^{15}N_{enamel}$ oxidation-denitrification measurements (in ‰ vs Air), the average, and standard deviation per selected sample normalized to atmospheric nitrogen using IAEA-NO-3 and USGS34 and corrected for blank contribution, as explained in section 5.5. All samples were measured in duplicate. As a quality control, samples were measured in triplicate if the standard deviation was above 0.5. The last row contains the average $\delta^{15}N$ value and the average standard deviation of all 72 samples together.

Sample ID	First $\delta^{15}N$	Duplicate $\delta^{15}N$	Triplicate $\delta^{15}N$	Average $\delta^{15}N$	Standard deviation $\delta^{15}N$
NMN-120e	3.6	4.0		3.8	0.2
NMN-120h	3.3	3.4		3.4	0.0
NMN-122c	3.0	3.4		3.2	0.2
NMN-122n	2.7	3.3		3.0	0.3
NMN-126a	4.1	5.4	3.2	4.2	0.9
NMN-126b	3.1	3.6		3.3	0.3
NMN-126c	2.3	3.1		2.7	0.4
NMN-126d	2.5	3.6		3.0	0.5
NMN-126e	2.6	2.7		2.6	0.1
NMN-126f	2.3	3.3		2.8	0.5
NMN-126g	1.7	3.1	2.6	2.5	0.5
NMN-126h	2.5	3.3		2.9	0.4
NMN-126i	2.1	2.8		2.4	0.4
NMN-126j	2.1	3.2		2.6	0.6
NMN-126k	2.2	3.2		2.7	0.5
NMN-126l	2.5	3.5		3.0	0.5
NMN-126m	2.5	3.4		3.0	0.4
NMN-126n	2.1	3.2	3.0	2.8	0.5
NMN-126o	2.3	3.4	2.4	2.7	0.5
NMN-126p	1.9	3.5	2.6	2.7	0.6
NMN-126q	2.1	3.9	2.8	2.9	0.7
NMN-126r	2.3	3.5		2.9	0.6
NMN-126s	3.3	3.6		3.5	0.2
NMN-127b	2.6	3.2		2.9	0.3
NMN-127d	2.2	2.6		2.4	0.2
NMN-129a	4.6	4.9		4.7	0.2

NMN-129n	3.0	3.3		3.1	0.2
NMN-129s	3.4	3.5		3.4	0.1
NMN-130a	3.8	4.4		4.1	0.3
NMN-130b	3.8	4.7		4.3	0.5
NMN-130c	3.4	3.9		3.7	0.2
NMN-130d	3.7	4.4		4.1	0.3
NMN-130e	3.5	4.2		3.9	0.4
NMN-130f	3.8	4.1		3.9	0.1
NMN-130g	4.5	3.5		4.0	0.5
NMN-130h	4.2	4.0		4.1	0.1
NMN-130i	2.9	3.7		3.3	0.4
NMN-130j	4.6	4.2		4.4	0.2
NMN-130k	3.7	4.0		3.8	0.2
NMN-130l	3.6	4.2		3.9	0.3
NMN-130m	3.7	3.5		3.6	0.1
NMN-130n	3.2	3.5		3.3	0.1
NMN-130o	3.3	3.9		3.6	0.3
NMN-130p	3.5	3.2		3.4	0.1
NMN-130q	3.0	3.9		3.4	0.4
NMN-130r	3.4	3.5		3.4	0.0
NMN-130s	3.4	3.4		3.4	0.0
NMN-130t	3.0	3.6		3.3	0.3
NMN-130u	2.8	3.5		3.1	0.4
NMN-130v	3.0	3.4		3.2	0.2
NMN-130w	2.9	3.6		3.2	0.4
NMN-130x	2.5	3.6	3.2	3.1	0.4
NMN-130y	2.1	3.1		2.6	0.5
NMN-130z	3.1	3.9		3.5	0.4
NMN-133a	4.2	4.2		4.2	0.0
NMN-133b	4.8	4.3		4.6	0.3
NMN-133c	5.2	4.3		4.8	0.5
NMN-133d	4.2	4.2		4.2	0.0
NMN-133e	4.5	4.2		4.3	0.2

NMN-133f	4.0	4.1		4.1	0.1
NMN-133g	4.2	3.7		3.9	0.2
NMN-133h	4.0	3.9		4.0	0.0
NMN-133i	4.0	4.2		4.1	0.1
NMN-133j	4.2	4.0		4.1	0.1
NMN-133k	4.2	3.7		3.9	0.2
NMN-133l	3.9	4.0		3.9	0.1
NMN-133m	3.9	4.0		4.0	0.0
NMN-133n	4.0	3.7		3.8	0.2
NMN-133o	4.0	4.0		4.0	0.0
NMN-133p	3.8	3.8		3.8	0.0
NMN-133q	3.8	3.8		3.8	0.0
NMN-133r	4.4	4.1		4.2	0.2
Total Average				3.5	0.3

Appendix C

Results of the trace element analysis of tooth NMN-126

Table C.1: Results of the trace element analysis of tooth NMN-126, performed by T. Tacail at the Institut für Geowissenschaften at the Johannes Gutenberg-Universität, Mainz, Germany. The results for calcium (Ca; second column) are given in µg per g of tooth enamel. The other elements are given as a ratio compared to calcium, as explained in section 5.6. The red slashes in indicate that the amount of the element in the sample was too low to be detected. The values for phosphor (P) are higher than the rest of the elements, because phosphor occurs naturally in relatively large quantities in tooth enamel. Note the slightly elevated values for samples NMN-126a and/or NMN-126b for aluminium (Al), iron (Fe), magnesium (Mg), natrium (Na), strontium (Sr) and zinc (Zn), discussed in section 7.2.

Sample ID	Ca (µg/g)	Al /Ca	B /Ca	Ba /Ca	Fe /Ca	Mg /Ca	Mn /Ca	Na /Ca	P /Ca	Sr /Ca	Zn /Ca
NMN-126a	$26 * 10^4$	0.0010	0.0004	0.0003	0.008	0.008	0.0013	0.01	0.5	0.0006	0.0014
NMN-126b	$17 * 10^4$	0.0194	0.0004	0.0001	0.003	0.035	0.0005	0.06	0.5	0.0006	0.0002
NMN-126c	$41 * 10^4$	0.0003	0.0001	0.0001	0.002	0.006	0.0003	0.01	0.5	0.0005	0.0001
NMN-126d	$32 * 10^4$	/	0.0001	0.0001	0.002	0.006	0.0002	0.01	0.5	0.0005	0.0001
NMN-126e	$16 * 10^4$	/	0.0001	0.0001	0.001	0.006	0.0003	/	0.5	0.0005	0.0002
NMN-126f	$29 * 10^4$	/	0.0003	0.0001	0.001	0.006	0.0002	0.01	0.5	0.0005	0.0002
NMN-126g	$32 * 10^4$	/	0.0004	0.0001	0.001	0.006	0.0004	0.01	0.5	0.0005	0.0001
NMN-126h	$26 * 10^4$	0.0006	0.0004	0.0001	0.002	0.005	0.0004	0.01	0.5	0.0005	0.0001
NMN-126i	$33 * 10^4$	/	0.0001	0.0001	0.001	0.006	0.0005	0.01	0.5	0.0005	0.0001
NMN-126j	$18 * 10^4$	0.0012	0.0003	0.0001	0.002	0.005	0.0007	/	0.5	0.0005	0.0001
NMN-126k	$30 * 10^4$	/	0.0001	0.0001	0.001	0.006	0.0006	0.02	0.5	0.0005	0.0001
NMN-126l	$26 * 10^4$	/	0.0001	0.0001	0.001	0.005	0.0004	0.01	0.5	0.0005	0.0001
NMN-126m	$30 * 10^4$	/	0.0005	0.0001	0.001	0.005	0.0003	0.01	0.5	0.0005	0.0001
NMN-126n	$35 * 10^4$	/	0.0003	0.0001	0.001	0.005	0.0004	0.01	0.5	0.0005	0.0001

NMN-126o	$47 * 10^4$	0.0002	0.0003	0.0002	0.001	0.005	0.0005	0.01	0.5	0.0005	0.0001
NMN-126p	$40 * 10^4$	/	0.0003	0.0002	0.001	0.005	0.0008	0.01	0.5	0.0005	0.0001
NMN-126q	$39 * 10^4$	0.0002	0.0003	0.0002	0.001	0.005	0.0012	0.01	0.5	0.0005	0.0001
NMN-126r	$32 * 10^4$	/	0.0003	0.0002	0.001	0.005	0.0010	0.01	0.5	0.0005	0.0001
NMN-126s	$34 * 10^4$	0.0004	0.0003	0.0005	0.001	0.005	0.0010	0.01	0.5	0.0005	0.0001

Appendix D

The $\delta^{13}C_{enamel}$, $\delta^{13}C_{diet}$, $\delta^{18}O_{enamel}$, $\delta^{18}O_{VSMOW}$, $\delta^{18}O_{PO4}$, and $\delta^{18}O_{bodywater}$ values per sample.

Table D.1: The average $\delta^{13}C_{enamel}$ value (in ‰ vs VPDB), the average $\delta^{13}C_{diet}$ value (in ‰ vs VPDB), the average $\delta^{18}O_{enamel}$ value (in ‰ vs VPDB), average $\delta^{18}O_{enamel}$ value (in ‰ vs VSMOW), the average $\delta^{18}O_{PO4}$ value (in ‰ vs VSMOW), and the average $\delta^{18}O_{bodywater}$ value (in ‰ vs VSMOW) per sample. The $\delta^{13}C_{diet}$ value was calculated by subtracting the enrichment factor ($\epsilon^* = 13.5$) from the $\delta^{13}C_{enamel}$ value. The $\delta^{18}O_{VSMOW}$ value was calculated following equation 4, the $\delta^{18}O_{PO4}$ following equation 10, and the $\delta^{18}O_{bodywater}$ following equation 3. The last row shows the average value of all 259 samples for each column.

Sample ID	$\delta^{13}C_{enamel}$	$\delta^{13}C_{diet}$	$\delta^{18}O_{enamel}$	$\delta^{18}O_{VSMOW}$	$\delta^{18}O_{PO4}$	$\delta^{18}O_{bodywater}$
NMN-120a	-11.9	-25.4	-7.2	23.5	15.9	-7.8
NMN-120b	-11.7	-25.2	-6.1	24.6	17.0	-6.7
NMN-120c	-11.2	-24.7	-5.1	25.7	18.0	-5.5
NMN-120d	-11.4	-24.9	-5.8	24.9	17.3	-6.4
NMN-120e	-11.9	-25.4	-6.7	24.1	16.4	-7.3
NMN-120f	-11.7	-25.2	-7.0	23.7	16.1	-7.7
NMN-120g	-11.3	-24.8	-6.4	24.3	16.7	-7.0
NMN-120h	-11.0	-24.5	-5.7	25.1	17.4	-6.2
NMN-120i	-11.7	-25.2	-6.1	24.6	17.0	-6.7
NMN-120j	-12.0	-25.5	-5.0	25.8	18.1	-5.4
NMN-120k	-11.5	-25.0	-5.0	25.8	18.1	-5.4
NMN-120l	-11.9	-25.4	-5.1	25.7	18.0	-5.5
NMN-120m	-11.9	-25.4	-5.4	25.3	17.7	-5.9
NMN-121a	-10.6	-24.1	-6.2	24.5	16.9	-6.8
NMN-121b	-11.8	-25.3	-7.3	23.4	15.8	-8.0
NMN-121c	-11.8	-25.3	-5.6	25.1	17.5	-6.1
NMN-121d	-11.9	-25.4	-6.5	24.2	16.6	-7.1
NMN-121e	-11.7	-25.2	-5.8	24.9	17.3	-6.4
NMN-121f	-11.5	-25.0	-5.4	25.3	17.7	-5.9
NMN-121g	-11.4	-24.9	-5.0	25.8	18.1	-5.4
NMN-121h	-11.7	-25.2	-5.0	25.8	18.2	-5.4
NMN-121i	-11.8	-25.3	-5.3	25.4	17.8	-5.8
NMN-121j	-12.1	-25.6	-6.0	24.7	17.1	-6.6
NMN-121k	-12.4	-25.9	-6.6	24.1	16.5	-7.3
NMN-121l	-12.5	-26.0	-7.5	23.2	15.6	-8.2

NMN-121m	-12.0	-25.5	-7.0	23.7	16.1	-7.7
NMN-121n	-12.2	-25.7	-7.1	23.6	16.0	-7.7
NMN-121o	-12.0	-25.5	-6.8	23.9	16.3	-7.5
NMN-121p	-12.2	-25.7	-6.7	24.0	16.4	-7.3
NMN-121q	-12.1	-25.6	-6.4	24.4	16.7	-7.0
NMN-122a	-11.5	-25.0	-6.5	24.2	16.6	-7.2
NMN-122b	-11.5	-25.0	-7.2	23.5	15.9	-7.8
NMN-122c	-11.8	-25.3	-5.3	25.5	17.8	-5.7
NMN-122d	-11.4	-24.9	-6.0	24.8	17.1	-6.5
NMN-122e	-11.5	-25.0	-6.6	24.1	16.5	-7.3
NMN-122f	-11.7	-25.2	-6.8	23.9	16.3	-7.5
NMN-122g	-11.7	-25.2	-6.2	24.5	16.9	-6.8
NMN-122h	-11.7	-25.2	-5.6	25.1	17.5	-6.1
NMN-122i	-11.9	-25.4	-5.4	25.4	17.7	-5.9
NMN-122j	-12.0	-25.5	-5.4	25.3	17.7	-5.9
NMN-122k	-12.4	-25.9	-6.1	24.6	17.0	-6.7
NMN-122l	-12.6	-26.1	-7.1	23.6	16.0	-7.8
NMN-122m	-12.7	-26.2	-7.7	23.0	15.4	-8.4
NMN-122n	-12.6	-26.1	-8.7	21.9	14.4	-9.6
NMN-122o	-12.6	-26.1	-7.4	23.3	15.7	-8.1
NMN-122p	-12.6	-26.1	-7.4	23.3	15.7	-8.1
NMN-122q	-12.4	-25.9	-7.5	23.2	15.6	-8.2
NMN-123a	-11.0	-24.5	-6.5	24.2	16.6	-7.2
NMN-123b	-12.4	-25.9	-6.2	24.5	16.9	-6.8
NMN-123c	-12.5	-26.0	-5.6	25.1	17.5	-6.1
NMN-123d	-12.4	-25.9	-5.4	25.4	17.7	-5.9
NMN-123e	-12.4	-25.9	-5.8	25.0	17.4	-6.3
NMN-123f	-12.6	-26.1	-6.4	24.4	16.7	-7.0
NMN-123g	-12.3	-25.8	-6.8	23.9	16.3	-7.5
NMN-123h	-12.4	-25.9	-7.0	23.7	16.1	-7.7
NMN-123i	-12.5	-26.0	-7.2	23.5	15.9	-7.9
NMN-123j	-12.2	-25.7	-6.9	23.9	16.2	-7.5
NMN-123k	-11.8	-25.3	-5.9	24.8	17.2	-6.4
NMN-123l	-11.8	-25.3	-5.2	25.5	17.9	-5.7

NMN-123m	-12.0	-25.5	-4.9	25.9	18.3	-5.3
NMN-123n	-12.0	-25.5	-5.1	25.7	18.0	-5.5
NMN-123o	-12.4	-25.9	-4.9	25.8	18.2	-5.4
NMN-123p	-12.5	-26.0	-5.2	25.6	17.9	-5.6
NMN-124a	-12.0	-25.5	-7.0	23.7	16.1	-7.7
NMN-124b	-12.2	-25.7	-6.7	24.0	16.4	-7.4
NMN-124c	-12.1	-25.6	-6.7	24.0	16.4	-7.3
NMN-124d	-12.2	-25.7	-5.8	24.9	17.3	-6.4
NMN-124e	-12.4	-25.9	-5.9	24.8	17.2	-6.4
NMN-124f	-12.3	-25.8	-6.6	24.1	16.5	-7.2
NMN-124g	-12.5	-26.0	-6.9	23.8	16.2	-7.6
NMN-124h	-12.2	-25.7	-6.9	23.8	16.2	-7.6
NMN-124i	-12.0	-25.5	-6.5	24.2	16.6	-7.2
NMN-124j	-12.0	-25.5	-5.7	25.0	17.4	-6.3
NMN-124k	-11.6	-25.1	-5.2	25.5	17.9	-5.7
NMN-124l	-11.7	-25.2	-5.2	25.6	18.0	-5.6
NMN-124m	-11.6	-25.1	-5.0	25.8	18.1	-5.4
NMN-124n	-11.4	-24.9	-4.8	26.0	18.4	-5.2
NMN-124o	-12.0	-25.5	-5.0	25.8	18.1	-5.4
NMN-124p	-12.1	-25.6	-5.7	25.1	17.4	-6.2
NMN-124q	-11.4	-24.9	-6.1	24.6	17.0	-6.7
NMN-125a	-12.2	-25.7	-6.2	24.6	16.9	-6.7
NMN-125b	-12.3	-25.8	-6.5	24.2	16.6	-7.1
NMN-125c	-12.4	-25.9	-6.4	24.4	16.7	-7.0
NMN-125d	-12.4	-25.9	-6.3	24.4	16.8	-6.9
NMN-125e	-12.3	-25.8	-5.6	25.1	17.5	-6.1
NMN-125f	-12.3	-25.8	-4.8	26.0	18.3	-5.2
NMN-125g	-12.4	-25.9	-4.6	26.2	18.5	-5.0
NMN-125h	-12.6	-26.1	-4.9	25.8	18.2	-5.3
NMN-125i	-12.8	-26.3	-5.6	25.2	17.5	-6.1
NMN-125j	-12.7	-26.2	-6.0	24.7	17.1	-6.6
NMN-125k	-12.8	-26.3	-6.4	24.3	16.7	-7.0
NMN-125l	-12.7	-26.2	-6.7	24.1	16.4	-7.3
NMN-125m	-12.7	-26.2	-6.9	23.8	16.2	-7.6

NMN-125n	-13.0	-26.5	-6.9	23.8	16.2	-7.6
NMN-125o	-13.1	-26.6	-6.4	24.3	16.7	-7.0
NMN-125p	-13.0	-26.5	-6.3	24.4	16.8	-6.9
NMN-125q	-13.1	-26.6	-6.3	24.4	16.8	-6.9
NMN-125r	-12.7	-26.2	-6.1	24.6	17.0	-6.7
NMN-125s	-12.8	-26.3	-6.2	24.5	16.9	-6.8
NMN-126a	-11.8	-25.3	-6.7	24.0	16.4	-7.4
NMN-126b	-12.4	-25.9	-7.6	23.1	15.5	-8.3
NMN-126c	-12.2	-25.7	-5.3	25.4	17.8	-5.8
NMN-126d	-12.5	-26.0	-5.7	25.1	17.4	-6.2
NMN-126e	-12.7	-26.2	-6.6	24.1	16.5	-7.3
NMN-126f	-12.9	-26.4	-6.9	23.8	16.2	-7.5
NMN-126g	-12.7	-26.2	-6.6	24.1	16.5	-7.2
NMN-126h	-12.3	-25.8	-6.2	24.6	17.0	-6.7
NMN-126i	-12.5	-26.0	-5.7	25.0	17.4	-6.2
NMN-126j	-12.7	-26.2	-5.3	25.4	17.8	-5.8
NMN-126k	-12.2	-25.7	-4.7	26.1	18.4	-5.1
NMN-126l	-12.1	-25.6	-5.5	25.3	17.7	-5.9
NMN-126m	-12.3	-25.8	-6.5	24.2	16.6	-7.1
NMN-126n	-12.5	-26.0	-7.2	23.5	15.9	-7.9
NMN-126o	-12.3	-25.8	-7.3	23.4	15.8	-8.0
NMN-126p	-12.5	-26.0	-7.6	23.0	15.5	-8.4
NMN-126q	-12.4	-25.9	-7.8	22.9	15.3	-8.6
NMN-126r	-12.3	-25.8	-7.0	23.7	16.1	-7.7
NMN-126s	-12.2	-25.7	-6.6	24.1	16.5	-7.2
NMN-127a	-11.4	-24.9	-6.7	24.0	16.4	-7.3
NMN-127b	-11.7	-25.2	-8.0	22.7	15.1	-8.8
NMN-127c	-11.9	-25.4	-7.1	23.6	16.0	-7.8
NMN-127d	-11.7	-25.2	-6.0	24.7	17.1	-6.6
NMN-127e	-12.0	-25.5	-6.5	24.2	16.6	-7.1
NMN-127f	-11.8	-25.3	-7.4	23.3	15.7	-8.1
NMN-127g	-12.0	-25.5	-7.5	23.2	15.6	-8.3
NMN-127h	-11.8	-25.3	-7.3	23.3	15.7	-8.1
NMN-127i	-11.8	-25.3	-6.6	24.1	16.5	-7.2

NMN-127j	-11.6	-25.1	-6.4	24.3	16.7	-7.0
NMN-127k	-11.6	-25.1	-6.1	24.6	17.0	-6.6
NMN-127l	-11.8	-25.3	-5.9	24.9	17.2	-6.4
NMN-127m	-12.1	-25.6	-6.4	24.3	16.7	-7.0
NMN-127n	-12.0	-25.5	-7.2	23.5	15.9	-7.9
NMN-128a	-12.6	-26.1	-6.7	24.0	16.4	-7.3
NMN-128b	-12.6	-26.1	-6.1	24.6	17.0	-6.7
NMN-128c	-12.7	-26.2	-4.9	25.8	18.2	-5.3
NMN-128d	-12.3	-25.8	-4.8	25.9	18.3	-5.2
NMN-128e	-12.5	-26.0	-5.7	25.0	17.4	-6.2
NMN-128f	-12.1	-25.6	-6.4	24.3	16.7	-7.0
NMN-128g	-12.6	-26.1	-6.5	24.2	16.6	-7.1
NMN-128h	-12.7	-26.2	-6.5	24.2	16.6	-7.1
NMN-128i	-12.7	-26.2	-6.1	24.6	17.0	-6.7
NMN-128j	-12.4	-25.9	-5.7	25.1	17.5	-6.2
NMN-128k	-12.5	-26.0	-5.2	25.5	17.9	-5.7
NMN-128l	-12.6	-26.1	-4.8	25.9	18.3	-5.3
NMN-128m	-12.6	-26.1	-4.9	25.9	18.2	-5.3
NMN-128n	-12.5	-26.0	-4.8	25.9	18.3	-5.2
NMN-128o	-12.5	-26.0	-5.8	25.0	17.3	-6.3
NMN-128p	-12.3	-25.8	-6.6	24.1	16.5	-7.3
NMN-128q	-12.2	-25.7	-7.1	23.6	16.0	-7.7
NMN-128r	-12.3	-25.8	-6.9	23.8	16.2	-7.5
NMN-128s	-12.3	-25.8	-6.6	24.1	16.5	-7.2
NMN-128t	-12.4	-25.9	-6.2	24.6	17.0	-6.7
NMN-129a	-10.8	-24.3	-5.2	25.6	17.9	-5.6
NMN-129b	-11.9	-25.4	-6.4	24.3	16.7	-7.0
NMN-129c	-12.4	-25.9	-6.4	24.3	16.7	-7.0
NMN-129d	-12.5	-26.0	-5.3	25.4	17.8	-5.8
NMN-129e	-12.5	-26.0	-5.0	25.8	18.2	-5.4
NMN-129f	-12.9	-26.4	-6.1	24.6	17.0	-6.7
NMN-129g	-12.7	-26.2	-6.6	24.1	16.5	-7.2
NMN-129h	-12.8	-26.3	-6.5	24.2	16.6	-7.1
NMN-129i	-12.7	-26.2	-6.2	24.6	16.9	-6.7

NMN-129j	-12.6	-26.1	-6.2	24.5	16.9	-6.8
NMN-129k	-12.6	-26.1	-5.4	25.3	17.7	-5.9
NMN-129l	-12.5	-26.0	-5.2	25.5	17.9	-5.7
NMN-129m	-12.7	-26.2	-4.8	25.9	18.3	-5.2
NMN-129n	-12.6	-26.1	-4.7	26.1	18.4	-5.1
NMN-129o	-12.5	-26.0	-5.0	25.7	18.1	-5.5
NMN-129p	-12.5	-26.0	-6.0	24.8	17.1	-6.5
NMN-129q	-12.6	-26.1	-6.6	24.1	16.5	-7.2
NMN-129r	-12.5	-26.0	-6.9	23.8	16.2	-7.5
NMN-129s	-12.4	-25.9	-7.1	23.6	16.0	-7.7
NMN-129t	-12.3	-25.8	-6.8	23.9	16.3	-7.5
NMN-129u	-12.4	-25.9	-6.7	24.0	16.4	-7.4
NMN-129v	-12.3	-25.8	-6.1	24.7	17.0	-6.6
NMN-129w	-12.2	-25.7	-5.6	25.1	17.5	-6.1
NMN-130a	-12.3	-25.8	-6.5	24.2	16.6	-7.1
NMN-130b	-12.4	-25.9	-6.9	23.8	16.2	-7.5
NMN-130c	-12.6	-26.1	-7.7	23.0	15.4	-8.5
NMN-130d	-12.5	-26.0	-7.3	23.4	15.8	-8.0
NMN-130e	-12.7	-26.2	-7.0	23.7	16.1	-7.6
NMN-130f	-12.5	-26.0	-6.4	24.3	16.7	-7.0
NMN-130g	-12.5	-26.0	-5.9	24.9	17.2	-6.4
NMN-130h	-12.3	-25.8	-5.3	25.4	17.8	-5.8
NMN-130i	-12.4	-25.9	-5.2	25.5	17.9	-5.7
NMN-130j	-12.5	-26.0	-5.4	25.3	17.7	-5.9
NMN-130k	-12.4	-25.9	-5.7	25.0	17.4	-6.2
NMN-130l	-12.6	-26.1	-6.2	24.5	16.9	-6.8
NMN-130m	-12.3	-25.8	-6.5	24.2	16.6	-7.2
NMN-130n	-12.4	-25.9	-6.6	24.1	16.5	-7.3
NMN-130o	-12.4	-25.9	-7.0	23.7	16.1	-7.7
NMN-130p	-12.5	-26.0	-7.1	23.6	16.0	-7.8
NMN-130q	-12.5	-26.0	-6.6	24.1	16.5	-7.2
NMN-130r	-12.2	-25.7	-6.1	24.7	17.0	-6.6
NMN-130s	-12.3	-25.8	-5.7	25.1	17.4	-6.2
NMN-130t	-12.3	-25.8	-5.2	25.5	17.9	-5.7

NMN-130u	-12.1	-25.6	-5.0	25.8	18.1	-5.4
NMN-130v	-12.3	-25.8	-5.0	25.7	18.1	-5.5
NMN-130w	-12.4	-25.9	-5.1	25.7	18.0	-5.5
NMN-130x	-12.3	-25.8	-5.0	25.7	18.1	-5.5
NMN-130y	-12.5	-26.0	-5.0	25.8	18.2	-5.4
NMN-130z	-12.7	-26.2	-5.3	25.4	17.8	-5.8
NMN-131a	-11.8	-25.3	-6.7	24.1	16.4	-7.3
NMN-131b	-12.6	-26.1	-7.5	23.1	15.5	-8.3
NMN-131c	-12.6	-26.1	-7.3	23.4	15.8	-8.0
NMN-131d	-12.4	-25.9	-7.0	23.7	16.1	-7.7
NMN-131e	-12.3	-25.8	-6.3	24.5	16.8	-6.8
NMN-131f	-12.5	-26.0	-6.1	24.7	17.0	-6.6
NMN-131g	-12.6	-26.1	-6.4	24.3	16.7	-7.0
NMN-131h	-12.5	-26.0	-6.2	24.5	16.9	-6.7
NMN-131i	-12.4	-25.9	-6.5	24.3	16.7	-7.1
NMN-131j	-12.0	-25.5	-6.4	24.3	16.7	-7.0
NMN-131k	-12.2	-25.7	-6.0	24.7	17.1	-6.5
NMN-131l	-12.4	-25.9	-5.9	24.9	17.2	-6.4
NMN-131m	-12.5	-26.0	-5.8	24.9	17.3	-6.3
NMN-131n	-12.5	-26.0	-5.6	25.1	17.5	-6.1
NMN-131o	-12.6	-26.1	-5.4	25.3	17.7	-5.9
NMN-131p	-12.8	-26.3	-6.3	24.5	16.8	-6.8
NMN-131q	-12.6	-26.1	-6.0	24.8	17.1	-6.5
NMN-131r	-12.3	-25.8	-6.0	24.7	17.1	-6.6
NMN-131s	-12.7	-26.2	-6.6	24.1	16.5	-7.2
NMN-132a	-12.3	-25.8	-5.4	25.3	17.7	-5.9
NMN-132b	-12.5	-26.0	-5.5	25.3	17.6	-6.0
NMN-132c	-12.4	-25.9	-6.7	24.0	16.4	-7.4
NMN-132d	-12.1	-25.6	-6.6	24.1	16.5	-7.2
NMN-132e	-12.2	-25.7	-6.3	24.4	16.8	-6.9
NMN-132f	-12.1	-25.6	-5.5	25.3	17.6	-6.0
NMN-132g	-12.2	-25.7	-5.1	25.6	18.0	-5.6
NMN-132h	-12.2	-25.7	-5.1	25.7	18.0	-5.5
NMN-132i	-12.4	-25.9	-5.4	25.4	17.7	-5.8

NMN-132j	-12.5	-26.0	-5.5	25.3	17.6	-6.0
NMN-132k	-12.3	-25.8	-5.8	25.0	17.3	-6.3
NMN-132l	-12.5	-26.0	-6.2	24.5	16.9	-6.8
NMN-132m	-12.7	-26.2	-6.8	23.9	16.3	-7.5
NMN-132n	-12.7	-26.2	-7.1	23.6	16.0	-7.7
NMN-132o	-12.7	-26.2	-7.0	23.7	16.1	-7.7
NMN-132p	-12.8	-26.3	-7.1	23.6	16.0	-7.7
NMN-132q	-12.8	-26.3	-7.1	23.6	16.0	-7.8
NMN-132r	-12.9	-26.4	-7.0	23.7	16.1	-7.7
NMN-132s	-12.9	-26.4	-6.8	23.9	16.3	-7.4
NMN-132t	-12.9	-26.4	-6.3	24.4	16.8	-6.9
NMN-132u	-12.9	-26.4	-5.9	24.9	17.2	-6.4
NMN-133a	-11.5	-25.0	-7.2	23.5	15.9	-7.8
NMN-133b	-11.6	-25.1	-6.5	24.2	16.6	-7.1
NMN-133c	-11.6	-25.1	-5.8	24.9	17.3	-6.3
NMN-133d	-11.7	-25.2	-5.4	25.4	17.7	-5.9
NMN-133e	-11.6	-25.1	-5.2	25.6	17.9	-5.6
NMN-133f	-12.2	-25.7	-5.3	25.4	17.8	-5.8
NMN-133g	-12.5	-26.0	-6.3	24.5	16.8	-6.8
NMN-133h	-12.5	-26.0	-6.6	24.1	16.5	-7.3
NMN-133i	-12.3	-25.8	-6.5	24.2	16.6	-7.1
NMN-133j	-12.4	-25.9	-7.0	23.7	16.1	-7.7
NMN-133k	-12.3	-25.8	-7.0	23.7	16.1	-7.6
NMN-133l	-12.2	-25.7	-6.7	24.0	16.4	-7.3
NMN-133m	-12.1	-25.6	-6.1	24.7	17.0	-6.6
NMN-133n	-12.0	-25.5	-5.5	25.2	17.6	-6.0
NMN-133o	-11.8	-25.3	-5.0	25.7	18.1	-5.5
NMN-133p	-12.1	-25.6	-5.1	25.7	18.0	-5.5
NMN-133q	-12.3	-25.8	-5.1	25.6	18.0	-5.6
NMN-133r	-12.4	-25.9	-5.4	25.3	17.7	-5.9
Total Average	-12.3	-25.8	-6.2	24.6	16.9	-6.7